

NASA CR-165234  
PWA 5642-21



# TAILORED PLASMA SPRAYED MCrAlY COATINGS FOR AIRCRAFT GAS TURBINE APPLICATIONS

by

F.J. Pennisi

D.K. Gupta

UNITED TECHNOLOGIES CORPORATION  
PRATT & WHITNEY AIRCRAFT  
COMMERCIAL PRODUCTS DIVISION

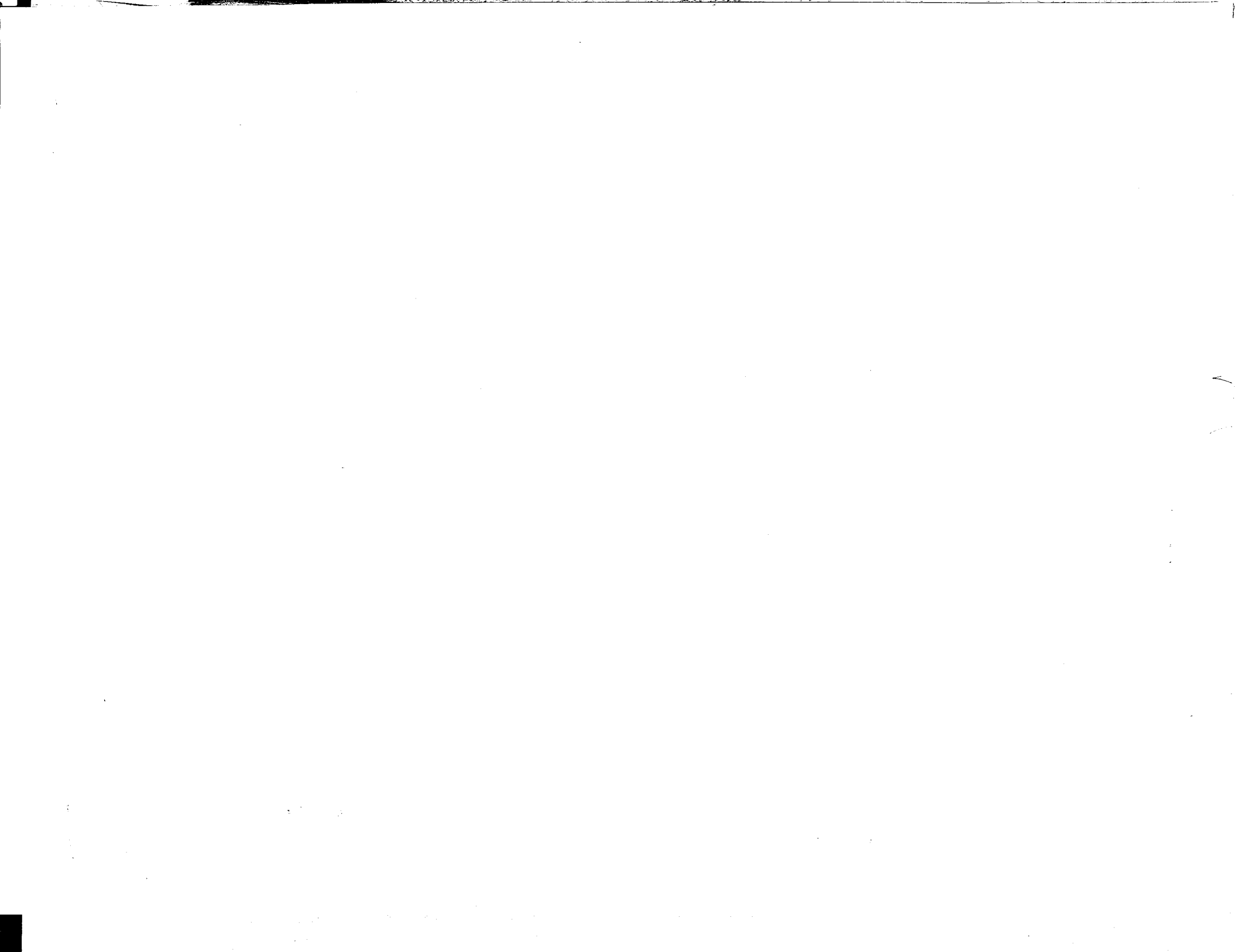
(NASA-CR-165234) TAILORED PLASMA SPRAYED MCrAlY COATINGS FOR AIRCRAFT GAS TURBINE APPLICATIONS (Pratt and Whitney Aircraft) 132 p HC A07/MF A01 CSCL 11F G3/26  
882-19360  
Unclas 13936

Prepared for

NATIONAL AERONAUTICS AND SPACE ADMINISTRATION  
NASA LEWIS RESEARCH CENTER  
CONTRACT NAS3-21730

January 1981

(NASA-CR-165234) TAILORED PLASMA SPRAYED MCrAlY COATINGS FOR AIRCRAFT GAS TURBINE APPLICATIONS (Pratt and Whitney Aircraft) 132 p ~~HC A07/MF A01~~  
X81-10033  
Unclas 41212  
E3/26



1. Report No. NASA CR-165234		2. Government Accession No.		3. Recipient's Catalog No.	
4. Title and Subtitle Tailored Plasma Sprayed MCrAlY Coatings for Aircraft Gas Turbine Applications				5. Report Date January 1981	
				6. Performing Organization Code	
7. Author(s) F.J. Pennisi and D.K. Gupta				8. Performing Organization Report No. PWA 5642-21	
				10. Work Unit No.	
9. Performing Organization Name and Address United Technologies Corporation Pratt & Whitney Aircraft Group - CPD East Hartford, Connecticut 06108				11. Contract or Grant No. NAS3-21730	
				13. Type of Report and Period Covered Contractor Report	
12. Sponsoring Agency Name and Address National Aeronautics and Space Administration Washington, D.C.				14. Sponsoring Agency Code	
15. Supplementary Notes Project Manager: John P. Merutka, NASA Lewis Research Center, Cleveland, Ohio 44135					
16. Abstract Eighteen plasma sprayed coating systems, nine based on the NiCoCrAlY chemistry and nine based on the CoCrAlY composition, were evaluated to identify coating systems which will provide equivalent or superior life to that shown by the electron beam physical vapor deposited NiCoCrAlY and CoCrAlY coatings respectively. NiCoCrAlY-type coatings were examined on a single crystal alloy and the CoCrAlY based coatings were optimized on the B1900+Hf alloy. Cyclic burner rig oxidation and hot corrosion and tensile ductility tests were used to evaluate the various coating candidates. For the single crystal alloy, a low pressure chamber plasma sprayed NiCoCrAlY+Si coating exhibited a 2X oxidation life improvement at 1394 <sup>o</sup> K (2050 <sup>o</sup> F) over the vapor deposited NiCoCrAlY material while showing equivalent tensile ductility. A silicon modified low pressure chamber plasma sprayed CoCrAlY coating was found to be more durable than the baseline vapor deposited CoCrAlY coating on the B1900+Hf alloy.					
17. Key Words (Suggested by Author(s)) Oxidation Resistant Coatings Hot Corrosion Resistant Coatings Plasma Sprayed MCrAlY Coatings Ductility			18. Distribution Statement  Unclassified - Unlimited		
19. Security Classif. (of this report) Unclassified		20. Security Classif. (of this page) Unclassified		21. No. of Pages 120	22. Price*

\* For sale by the National Technical Information Service, Springfield, Virginia 22161





## FOREWORD

This is the final report of the work performed by the Materials Engineering and Research Laboratory of the Pratt & Whitney Aircraft Group of United Technologies Corporation, East Hartford, Connecticut under NASA-Lewis Research Center contract NAS3-21730, entitled Tailored Plasma Sprayed MCrAlY Coatings for Aircraft Gas Turbine Applications.

Mr. John P. Merutka of the NASA-Lewis Research Center served as Project Manager for this program.

The Pratt & Whitney Aircraft Group personnel who contributed to the program are:

Dr. D.K. Gupta, Program Manager

Mr. F.J. Pennisi, Principal Investigator



## TABLE OF CONTENTS

Section	Title	Page
1.0	EXECUTIVE SUMMARY	1
2.0	INTRODUCTION	8
3.0	EXPERIMENTAL PROCEDURE	13
3.1	Materials Fabrication	13
3.1.1	Substrate Alloys	13
3.1.2	Coating Alloy Ingot/Powder	15
3.2	Coating Fabrication	15
3.2.1	Electron Beam Physical Vapor Deposition	15
3.2.2	Plasma Spray Processing	16
3.2.3	Post-Coating Processing	20
3.3	Burner Rig Tests	20
3.3.1	Oxidation Tests	21
3.3.2	Hot Corrosion Tests	23
3.4	Tensile/Ductility Testing	25
3.5	Pre- and Post-Test Coating Evaluations	25
4.0	EXPERIMENTAL RESULTS AND DISCUSSION	26
4.1	Task I Evaluation	26
4.1.1	Candidate Coatings for Initial Screening	26
4.1.2	Results of Initial Screening	31
4.1.3	Pre-Test Microstructures of Burner Rig Specimens	38
4.1.4	Burner Rig Oxidation Tests	43
4.1.5	Burner Rig Hot Corrosion Test Results	67
4.1.6	Coating Ductility Test Results	76
4.2	Summary of Task I Results and Selection of Coatings for Task II	82
4.3	Task II Evaluations	84
4.3.1	Pre-Test Microstructures	85
4.3.2	Burner Rig Oxidation Testing	89
4.3.3	Burner Rig Hot Corrosion Testing	98
4.4	Summary of Task II Results and Selection of Coatings for Task III Engine Testing	106
4.5	Task III Engine Test Evaluations	112
4.6	Discussion	113
5.0	CONCLUSIONS	115
6.0	RECOMMENDATIONS	118
	REFERENCES	119

## LIST OF TABLES

Table	Title	Page
I	Coating Systems Initially Screened in Task I	27
II	Thickness of Coated Specimens Metallographically Evaluated in Task I	33
III	Selected Coating/Process/Alloy Combinations Which Were Burner Rig Tested in Task I	39
IV	Chemical Compositions of Coating Variations Evaluated in Task I	40
V	Particle Size Distribution of Various Powder Materials Evaluated in Task I	40
VI	Visual Conditions of Coated Single Crystal Samples After 350 Hours of Exposure in the Burner Rig Oxidation Test at 1394°K (2050°F)	49
VII	Visual Conditions of Coated Single Crystal Samples After 1000 Hours Test Time in the Burner Rig Oxidation Test at 1394°K (2050°F)	50
VIII	Visual Conditions of Coated B1900 + Hf Samples After 350 Hours of Exposure in the Burner Rig Oxidation Test at 1394°K (2050°F)	66
IX	Visual Conditions of Coated B1900 + Hf Samples After 1000 Hours of Test Time in the Burner Rig Oxidation Test at 1394°K (2050°F)	66
X	Visual Conditions of Samples Evaluated in Burner Rig Hot Corrosion Testing at 1172°K (1650°F)	70
XI	Tensile Ductility of Various Coatings at 588°K (600°F)	77
XII	Beta Phase Concentrations of Various Coatings in the As-Processed Condition	81

LIST OF TABLES (Cont'd)

Table	Title	Page
XIII	Visual Conditions of Task II Single Crystal Specimens After 350 Hours of Exposure in the Burner Rig Oxidation Test at 1394 <sup>o</sup> K (2050 <sup>o</sup> F)	90
XIV	Visual Conditions of Task II Single Crystal Specimens Evaluated in Burner Rig Oxidation Testing at 1394 <sup>o</sup> K (2050 <sup>o</sup> F)	91
XV	Visual Conditions of Task II B1900 + Hf Specimens After 350 Hours of Exposure in the Burner Rig Oxidation Test at 1394 <sup>o</sup> K (2050 <sup>o</sup> F)	97
XVI	Visual Conditions of Coated B1900 + Hf Samples Evaluated in Burner Rig Oxidation Testing at 1394 <sup>o</sup> K (2050 <sup>o</sup> F)	97
XVII	Visual Conditions of Samples Evaluated in the Task II Burner Rig Hot Corrosion Test at 1172 <sup>o</sup> K (1650 <sup>o</sup> F)	104

## LIST OF ILLUSTRATIONS

Figure	Title	Page
1	1394 <sup>o</sup> K (2050 <sup>o</sup> F) Burner Rig Life Results of Various NiCoCrAlY Based Coatings on the Single Crystal Alloy	3
2	1394 <sup>o</sup> K (2050 <sup>o</sup> F) Burner Rig Life Results of Various CoCrAlY Based Coatings on the B1900 + Hf Alloy	4
3	588 <sup>o</sup> K (600 <sup>o</sup> F) Coating Ductility Test Results on Coated B1900 + Hf Alloy Samples	6
4	Overall Program Flow Diagram	12
5	Oxidation-Hot Corrosion Coating Evaluation Test Specimen	14
6	Coating Ductility Test Specimen	14
7	Diagram of Typical EB-PVD Coating Chamber	17
8	P&WA Controlled Atmosphere Plasma Spray System	18
9	Howmet Corporation Pilot-Scale Low Pressure Chamber Plasma Spray Equipment	19
10	Diagram of Burner Rig Oxidation Test Apparatus	22
11	Diagram of Burner Rig Hot Corrosion Test Apparatus With Test Specimens Enclosed to Allow Precise Control of SO <sub>3</sub> and Other Contaminants	24
12	Procedure for Interrupted Tensile Coating Ductility Test. Large coated areas can be evaluated in this test.	25
13	Spalling of the Low Pressure Chamber Plasma Sprayed CoCrAlY+Si Coating on the B1900 + Hf Substrate During Post-Spray Glass Bead Peening	32
14	Comparison of Microstructures Show Low Pressure Chamber Sprayed Coatings (a and b) are Superior in Quality to One-Atmosphere Argon Chamber Sprayed Coatings (c and d)	34
15	Microstructures of Low Pressure Chamber Sprayed NiCoCrAlY Coatings Fabricated Using (a) 1352 <sup>o</sup> K (1975 <sup>o</sup> F) /4 hrs + GBP(17N), (b) 1352 <sup>o</sup> K (1975 <sup>o</sup> F)/1 hr + GBP(17N) + 1352 <sup>o</sup> K (1975 <sup>o</sup> F)/4 hrs, and (c) 1352 <sup>o</sup> K (1975 <sup>o</sup> F)/1 hr + GBP(22N) + 1352 <sup>o</sup> K (1975 <sup>o</sup> F)/4 hrs. GBP = Glass Bead Peening	36

LIST OF ILLUSTRATIONS (Cont'd)

Figure	Title	Page
16	Microstructure of Low Pressure Chamber Sprayed CoCrAlY+HIP Coating After Post-Coating Processing at 1352 <sup>o</sup> K (1975 <sup>o</sup> F)/1 hr + GBP(17N) + HIP 1470 <sup>o</sup> K (2185 <sup>o</sup> F)/3 hrs/103.4 MPa (15 Ksi) + 1352 <sup>o</sup> K (1975 <sup>o</sup> F) 4 hrs. HIP = Hot Isostatic Pressing	37
17	Pre-Test Microstructures of NiCoCrAlY Coatings Made by Electron-Beam Physical Vapor Deposition, Low Pressure Chamber Plasma Spraying, and One Atmosphere Argon Chamber Spraying	41
18	Pre-Test Microstructures of Low Pressure Chamber Sprayed NiCoCrAlY-Type Coatings With Modified Compositions	42
19	Scanning Electron Micrograph of Low Pressure Chamber Sprayed NiCoCrAlY+Ta Coating in the As-Processed Condition Illustrating Presence of a Tantalum Containing Phase in the Coating Microstructure	44
20	Pre-Test Microstructures of CoCrAlY Coatings Made by Various Processes	45
21	Pre-Test Microstructures of Low Pressure Chamber Sprayed CoCrAlY-Type Coatings With Modified Composition/Processes	46
22	Relative Aluminum and Silicon X-Ray Intensities for Low Pressure Chamber Sprayed CoCrAlY+Si Coating on B1900 + Hf Alloy in the Fully Processed Condition	47
23	Post-Test Microstructures of the Test Section of NiCoCrAlY-Type Coatings on the Single Crystal Alloy After 350 Hours of Exposure in an Oxidative Environment at 1394 <sup>o</sup> K (2050 <sup>o</sup> F)	51
24	Post-Test Microstructures of the Test Section of NiCoCrAlY-Type Coatings on the Single Crystal Alloy After 350 Hours of Exposure in an Oxidative Environment at 1394 <sup>o</sup> K (2050 <sup>o</sup> F)	53
25	Surface Condition of Test Bars With NiCoCrAlY-Type Coatings on the Single Crystal Alloy, Exposed in Cyclic Burner Rig Oxidation Test at 1394 <sup>o</sup> K (2050 <sup>o</sup> F)	54

LIST OF ILLUSTRATIONS (Cont'd)

Figure	Title	Page
26	Surface Photographs (10X) of Burner Rig Test Samples After 100 Hours of Oxidation Testing at 1394°K (2050°F). (a) Vapor Deposited NiCoCrAlY on the Single Crystal Alloy; (b) Low Pressure Chamber Sprayed NiCoCrAlY on the Same Alloy.	56
27	Tantalum Diffusion from Single Crystal Alloy into NiCoCrAlY Coatings at 1422°K (2100°F)	57
28	Surface Photographs of Low Pressure Chamber Sprayed Single Crystals Exposed for 198 Hours in a Oxidative Environment at 1394°K (2050°F) in a Cyclic Burner Rig	58
29	Photomicrographs (200X) of NiCoCrAlY and NiCoCrAlY + 1%Si After Oxidation at 1422°K (2100°F). Much more severe degradation of the non-silicon alloy has occurred.	60
30	Post-Test Microstructures of the Test Section of CoCrAlY Coatings on B1900 + Hf Alloy After 350 Hours of Exposure in an Oxidative Environment at 1394°K (2050°F)	62
31	Post-Test Microstructures of the Test Section of Low Pressure Chamber Sprayed CoCrAlY-Type Coatings on B1900 + Hf Alloy After 350 Hours of Exposure in an Oxidative Environment at 1394°K (2050°F)	63
32	Surface Condition of Test Bars With CoCrAlY-Type Plasma Sprayed Coatings on the Single Crystal Alloy Exposed to a Hot Corrosive Environment at 1172°K (1650°F)	65
33	Surface Photographs of Test Samples With NiCoCrAlY-Type Plasma Sprayed Coatings on the Single Crystal Alloy Exposed to a Hot Corrosive Environment at 1172°K (1650°F)	68
34	Surface Photographs of Test Samples With CoCrAlY-Type Plasma Sprayed Coatings on B1900 + Hf Alloy Exposed to a Hot Corrosive Environment at 1172°K (1650°F)	69
35	Post-Test Microstructures of the Test Section of CoCrAlY Coatings on B1900 + Hf Alloy After 350 Hours of Exposure in a Hot Corrosive Environment at 1172°K (1650°F)	72



LIST OF ILLUSTRATIONS (Cont'd)

Figure	Title	Page
36	Post-Test Microstructures of the Test Section of Low Pressure Chamber Sprayed CoCrAlY-Type Coatings on B1900 + Hf Alloy After 350 Hours of Exposure in a Hot Corrosive Environment at 1172 <sup>o</sup> K (1650 <sup>o</sup> F)	73
37	Post-Test Microstructures of the Test Section of NiCoCrAlY Coatings on the Single Crystal Alloy After 350 Hours of Exposure in a Hot Corrosive Environment at 1172 <sup>o</sup> K (1650 <sup>o</sup> F)	74
38	Post-Test Microstructures of the Test Section of Low Pressure Chamber Sprayed NiCoCrAlY-Type Coatings on the Single Crystal Alloy After 350 Hours of Exposure in a Hot Corrosive Environment at 1172 <sup>o</sup> K (1650 <sup>o</sup> F)	75
39	Average Cracking Strains of Coated B1900 + Hf Alloy at 588 <sup>o</sup> K (600 <sup>o</sup> F)	78
40	Post-Test Microstructural Condition of NiCoCrAlY Coated B1900 + Hf Ductility Specimens	79
41	Post-Test Microstructures of Low Pressure Chamber Sprayed CoCrAlY-Type Coatings on B1900 + Hf Alloy After Post-Coating Processing	86
42	Pre-Test Microstructures of Low Pressure Chamber Sprayed CoCrAlY + HIP Coatings on B1900 + Hf Alloy After Post-Coating Processing. Note reduced coating-substrate interdiffusion and lower aluminum loss in case of lower temperature HIP'ed CoCrAlY coating. HIP = Hot Isostatic Pressing	87
43	Pre-Test Microstructures of Low Pressure Chamber Sprayed NiCoCrAlY-Type Coatings on the Single Crystal Alloy After Post-Coating Processing	88
44	Surface Photographs of Test Samples With NiCoCrAlY-Type Coatings on the Single Crystal Alloy Exposed to an Oxidative Environment at 1394 <sup>o</sup> K (2050 <sup>o</sup> F)	92
45	Surface Photographs of Task I Test Samples With NiCoCrAlY-Type Coatings on the Single Crystal Alloy Exposed for 1785 Hours to an Oxidative Environment at 1394 <sup>o</sup> K (2050 <sup>o</sup> F)	93

LIST OF ILLUSTRATIONS (Cont'd)

Figure	Title	Page
46	Post-Test Microstructures of the Test Section of NiCoCrAlY-Type Coatings on the Single Crystal Alloy After 350 Hours of Exposure in an Oxidative Environment at 1394°K (2050°F) during Task II Testing	95
47	Post-Test Microstructures of the Test Section of Low Pressure Chamber Sprayed NiCoCrAlY-Type Coatings on the Single Crystal Alloy After 650 Hours of Exposure in an Oxidative Environment at 1394°K (2050°F)	96
48	Surface Photographs of Test Samples With CoCrAlY-Type Coatings on B1900 + Hf Alloy Exposed to an Oxidative Environment at 1394°K (2050°F)	99
49	Post-Test Microstructures of the Test Section of CoCrAlY-Type Coatings on B1900 + Hf Alloy After 350 Hours of Exposure in an Oxidative Environment at 1394°K (2050°F)	100
50	Surface Photographs of Test Sample With CoCrAlY-Type Coatings on B1900 + Hf Alloy Exposed 500 Hours to a Hot Corrosive Environment at 1172°K (1650°F)	101
51	Surface Photographs of Test Samples With NiCoCrAlY-Type Coatings on the Single Crystal Alloy Exposed 500 Hours to a Hot Corrosive Environment at 1172°K (1650°F)	102
52	Surface Photographs of Test Samples With CoCrAlY-Type Coatings on the Single Crystal Alloy Exposed 1000 Hours to a Hot Corrosive Environment at 1172°K (1650°F)	105
53	Post-Test Microstructures of the Test Section of CoCrAlY-Type Coatings on B1900 + Hf Alloy After 500 Hours of Exposure in a Hot Corrosive Environment at 1172°K (1650°F)	107
54	Post-Test Microstructures of the Test Section of CoCrAlY-Type Coatings on B1900 + Hf Alloy After 500 Hours of Exposure in a Hot Corrosive Environment at 1172°K (1650°F)	108
55	Post-Test Microstructures of the Test Sections of NiCoCrAlY Based Coatings on the Single Crystal Alloy After 500 Hours of Exposure in a Hot Corrosive Environment at 1172°K (1650°F)	109

LIST OF ILLUSTRATIONS (Cont'd)

Figure	Title	Page
56	Post-Test Microstructures of the Test Sections of Both NiCoCrAlY+Si+Ta Modifications on the Single Crystal Alloy After 500 Hours of Exposure in a Hot Corrosive Environment at 1172 <sup>o</sup> K (1650 <sup>o</sup> F)	110



## 1.0 EXECUTIVE SUMMARY

The plasma spray overlay coating process allows greater coating compositional flexibility, better compositional control, and a potential for reduced coating costs in comparison to the electron-beam physical vapor deposition process for fabricating advanced MCrAlY-type coatings for high temperature gas-turbine engine applications. However, in laboratory and engine tests conducted prior to this investigation, plasma sprayed MCrAlY coatings had been consistently less oxidation resistant than similar coatings applied by the electron-beam physical vapor deposition process. The present program was therefore conducted to increase the protectiveness of this type of coating so that, in the future, the benefits of the plasma spray process could be utilized for critical gas turbine applications.

The objectives of the program were: 1) optimization and selection of a plasma sprayed NiCoCrAlY-type coating system and process to provide equivalent or superior performance to the current electron-beam physical vapor deposited NiCoCrAlY in the high temperature oxidation environment of future advanced aircraft gas turbine engines; and 2) optimization and selection of a plasma sprayed CoCrAlY-type coating system and process to provide equivalent or superior performance compared to the current electron-beam physical vapor deposited CoCrAlY in the hot corrosion environment typically encountered by some contemporary aircraft gas turbine engines.

Low pressure chamber plasma spraying and atmospheric pressure argon plasma spraying were employed to produce an initial series of candidate NiCoCrAlY based coating systems for protecting a single crystal nickel-base superalloy and candidate CoCrAlY based coating systems for protecting a conventionally cast B1900+Hf alloy. Burner rig oxidation and hot corrosion tests were used to identify the most promising compositional process candidates. In Task II, the two most promising systems from each group (NiCoCrAlY-type and CoCrAlY-type) were optimized, and, after additional burner rig tests, the best plasma sprayed coating for the single crystal alloy and the best one for the B1900+Hf alloy were selected.

The burner rig cyclic oxidation, hot corrosion tests and ductility tests indicated that low pressure chamber sprayed NiCoCrAlY+Si (Ni-22Co-18Cr-12Al-0.5Y-1.5Si) and CoCrAlY+Si (Co-22Cr-12Al-0.5Y-2.0Si) coatings provided the best high temperature protection for the single crystal and B1900+Hf alloys respectively. Cyclic burner rig testing demonstrated that the useful oxidation lives of these coatings exceeded 1000 hours at 1394<sup>0</sup>K (2050<sup>0</sup>F) whereas the baseline electron-beam physical vapor deposited NiCoCrAlY/single crystal and CoCrAlY/B1900+Hf systems exhibited severe degradation and/or failure during this time interval. The plasma sprayed NiCoCrAlY+Si coatings exhibited a twofold improvement over the baseline electron-beam physical vapor deposited NiCoCrAlY coating on the single crystal alloy.

The tests also indicated that: 1) low pressure chamber plasma sprayed NiCoCrAlY and CoCrAlY coatings are superior to similar coatings produced by the atmospheric pressure argon plasma spray process; and, 2) the low pressure chamber sprayed NiCoCrAlY coatings (without silicon) on the single crystal alloy had durability equivalent to electron-beam physical vapor deposited NiCoCrAlY, whereas the durability of plasma sprayed CoCrAlY on the B1900+Hf substrate was inferior to the baseline vapor deposited coating. These results are summarized in Figures 1 and 2.

Evaluation of plasma sprayed coatings subjected to various post-spray processes revealed that a high intensity (22N level) glass bead peening step followed by normal heat treatment (1352<sup>0</sup>K (1975<sup>0</sup>F)/4 hours/H<sub>2</sub>) provided the most improvement in coating soundness. A post-spray hot isostatic pressing procedure resulted in complete densification of the CoCrAlY coating. However, the CoCrAlY system modified in this manner did not exhibit any improvement in oxidation resistance compared to that shown by the normally processed material.

Cyclic burner rig hot corrosion testing at 1172<sup>0</sup>K (1650<sup>0</sup>F) (30 ppm sea salt; equivalent to 1.3 w/o sulfur in the fuel added via SO<sub>2</sub>) indicated that all plasma sprayed coatings, i.e., NiCoCrAlY, CoCrAlY, NiCoCrAlY+X (where X stands for Si, Ta and Hf additions), CoCrAlY+Si, CoCrAlY+ hot isostatically

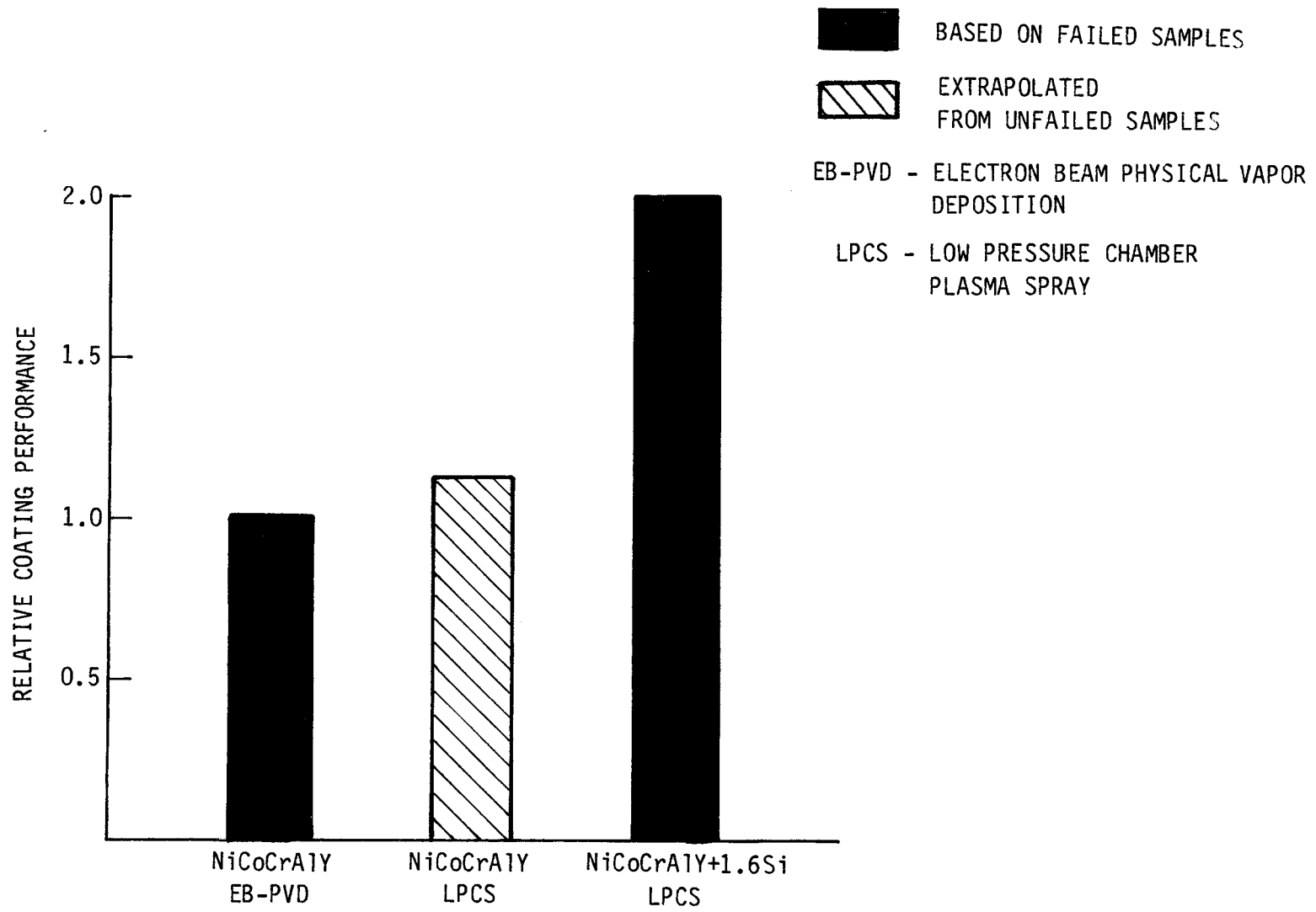


Figure 1 1394<sup>o</sup>K (2050<sup>o</sup>F) Burner Rig Life Results of Various NiCoCrAlY Based Coatings on the Single Crystal Alloy.

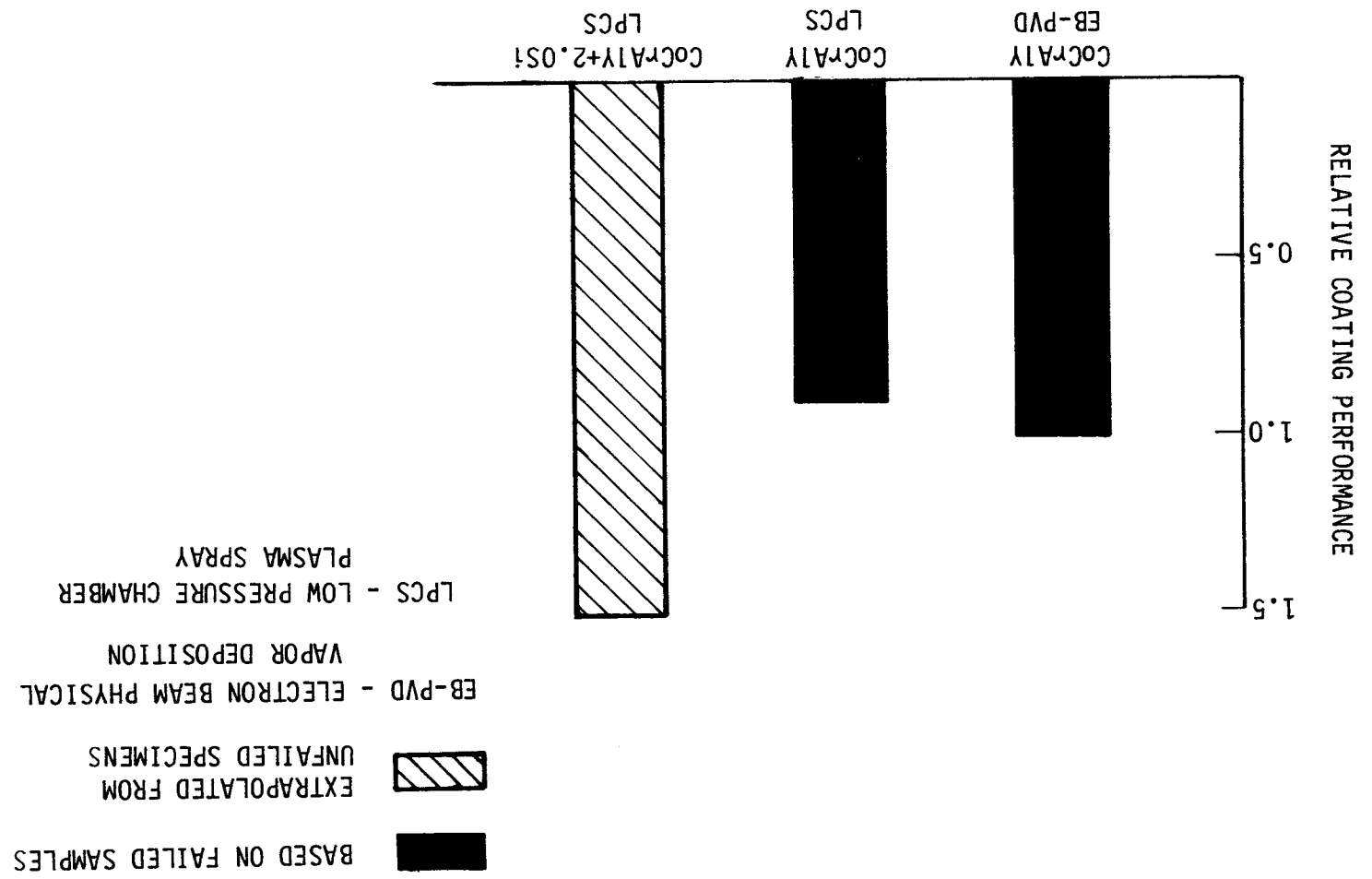


Figure 2 13940K (2050F) Burner Rig Life Results of Various CoCrAlY Based Coatings on the B1900+HF Alloy.



pressed and CoCrAlY (high Cr, low Al) provide a satisfactory degree of protection to the single crystal and the B1900+Hf substrates in a  $\text{Na}_2\text{SO}_4$  contaminated oxidative environment. These coatings, after 500 hours in test, showed no significant surface degradation.

Tensile ductility tests conducted at 588<sup>0</sup>K (600<sup>0</sup>F) indicated that low pressure chamber sprayed NiCoCrAlY and CoCrAlY coatings provide fracture strains superior to those of similar composition vapor deposited coatings. This behavior, which is illustrated in Figure 3, may be related to the difference in structural features such as grain orientation and defect characteristics present in coatings produced by these two processes. Figure 3 also shows the ductility of NiCoCrAlY+Si and CoCrAlY+Si coatings. Test data and coating beta (NiAl,CoAl) phase analysis showed that an increase in the amount of beta present in a coating results in a reduction of ductility. Silicon and tantalum additions to the MCrAlY coatings increase the stability of the beta phase. This increase in beta concentration (for the same value of aluminum present in the coating) reduces coating ductility. However, low pressure chamber plasma sprayed NiCoCrAlY+1.6Si and CoCrAlY+2.0Si coatings exhibited fracture strains which appear equivalent to those of the baseline vapor deposited NiCoCrAlY and CoCrAlY coatings respectively.

The best overall coating selected for the single crystal alloy is NiCoCrAlY+Si (1-2 w/o) and that selected for the B1900+Hf alloy is CoCrAlY+Si (1.5-2.5 w/o). In laboratory testing, both of these coatings exhibited considerable improvement over the performance of baseline vapor deposited NiCoCrAlY and CoCrAlY coatings, thus exceeding the program objectives. Testing in JT8D and JT9D engines will subsequently be conducted to confirm this behavior.

This program has successfully demonstrated the technical capability of plasma sprayed MCrAlY coatings for protecting high temperature turbine airfoil materials in current and advanced engines. However, several additional tasks need to be completed prior to incorporation of the process into full scale airfoil coating production: 1) establishment of production methods, process control techniques, and quality standards for depositing the plasma spray

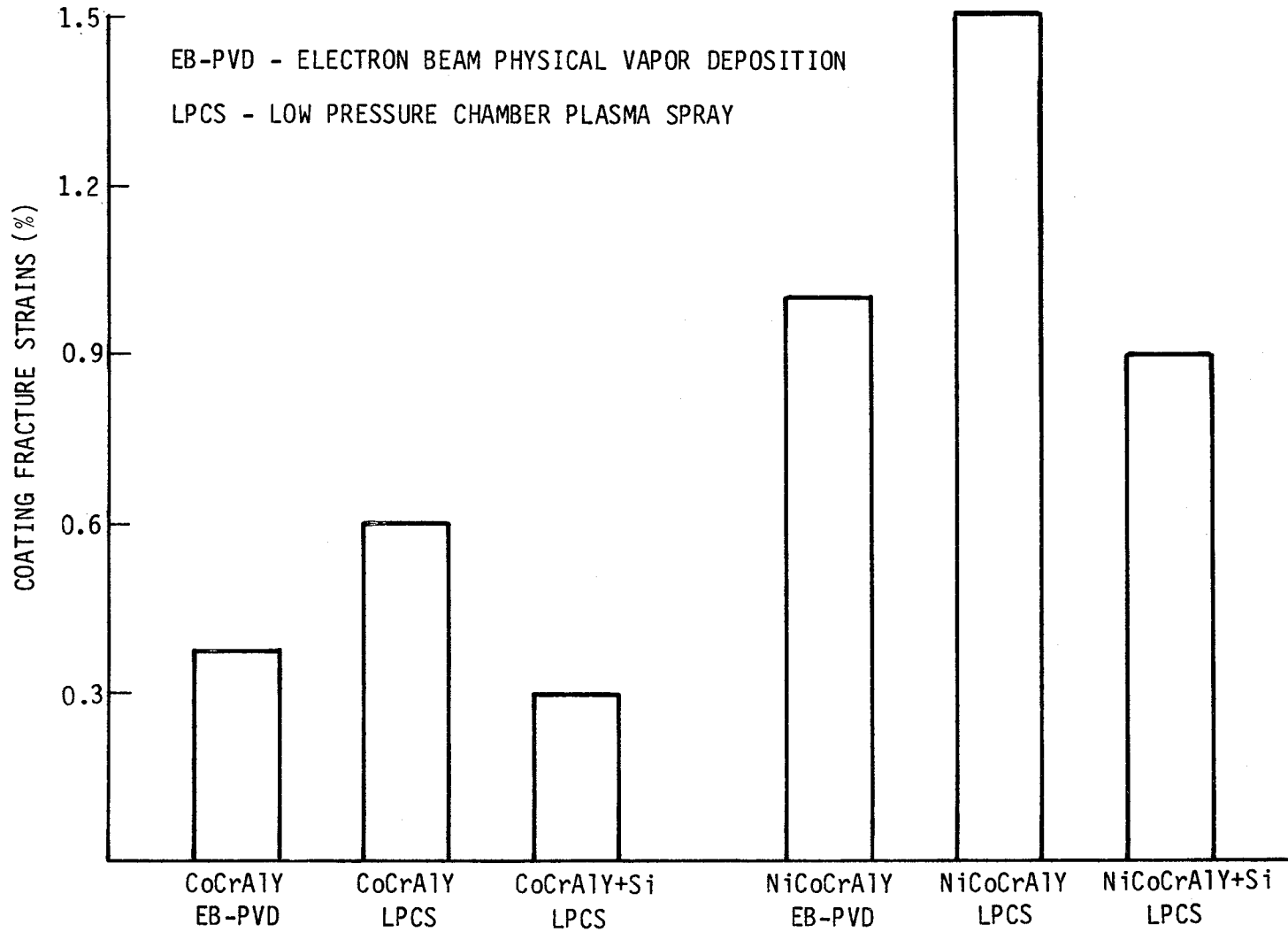


Figure 3 588°K (600°F) Coating Ductility Test Results on Coated B1900+Hf Alloy Samples.

coatings on a high volume basis; and, 2) completion of engine qualification and certification testing for applications in new engines and field service evaluation for applications in existing engines.

The low pressure chamber plasma sprayed NiCoCrAlY+Si coating system, optimized in this program, may provide an improved underlayer for advanced ceramic thermal barrier coating systems. Recent significant progress achieved in increasing the spalling resistance of ceramic thermal barrier coatings has led to oxidation of the underlying air sprayed NiCoCrAlY coating as a life limiting mechanism. Use of the highly oxidation resistant low pressure chamber sprayed NiCoCrAlY+Si as a sublayer is expected to alleviate this problem.

## 2.0 INTRODUCTION

Oxidation and hot corrosion of coatings continue to be major factors limiting the life of turbine airfoils in aircraft gas turbine engines. These problems have led to the widespread use of overlay MCrAlY coatings, typified by CoCrAlY and NiCoCrAlY, in order to provide the best available protection against surface attack. Since their introduction a decade ago, most overlay coatings have been fabricated by the electron-beam physical vapor deposition process. Plasma spraying is a particularly attractive alternative process, however, because of the flexibility in handling a wider range of coating compositions, the capability to maintain tighter compositional control, potential for wide availability of production coating sources, and promise of lower coating cost. Unfortunately, until recently the quality and durability of plasma sprayed MCrAlY coatings was substantially inferior to similar composition coatings fabricated by the electron-beam vapor deposition process.

The density and microstructural quality of plasma sprayed MCrAlY-type overlay coatings have been substantially improved during the past few years by the development of high energy, high velocity plasma processes and refinement in pre- and post-coating treatments. In particular, the low pressure chamber spray process has emerged as a superior method for plasma spraying MCrAlY-type compositions. This process involves high velocity (about Mach 3) spraying in protective atmosphere (e.g. argon) chambers operating at reduced pressures (typically 0.07 atm).

Prior to this investigation, considerable evaluation of the oxidation resistance of NiCoCrAlY coatings produced by the various plasma spray processes, including the low pressure chamber plasma spray process, was performed at Pratt & Whitney Aircraft. Plasma sprayed NiCoCrAlY coatings fabricated in air on D.S. Mar-M200 + Hf exhibited as much as a 50% reduction in high temperature oxidation life compared to electron-beam physical vapor deposited NiCoCrAlY in 1422<sup>0</sup>K (2100<sup>0</sup>F) burner rig oxidation tests. The low pressure chamber plasma sprayed NiCoCrAlY performed substantially better than the air sprayed material but still was inferior to the durability of vapor

deposited NiCoCrAlY. The biggest single difference noted in the behavior of the coatings produced by these two processes was the greater tendency for the protective  $Al_2O_3$  scale to spall from the plasma sprayed coatings. In laboratory hot-corrosion tests at  $1172^{\circ}K$  ( $1650^{\circ}F$ ), while low pressure chamber sprayed CoCrAlY coatings performed somewhat similarly to vapor deposited CoCrAlY, the plasma sprayed coatings were still prone to excessive  $Al_2O_3$  scale spallation which could make the coatings deficient in performance under certain conditions. In addition, it has been repeatedly more difficult to obtain high density plasma sprayed coatings with the CoCrAlY composition compared to that achievable with the softer, more ductile NiCoCrAlY alloy.

During prior Pratt & Whitney Aircraft programs as well as other investigations, several promising approaches were identified to improve the capabilities of plasma sprayed MCrAlY coatings and also achieve coating durability superior to today's vapor deposited NiCoCrAlY and CoCrAlY compositions. Studies indicated that compositional modifications would be more potent than process changes in correcting the oxidation performance deficiencies of plasma sprayed NiCoCrAlY coatings. In particular, additions of hafnium, tantalum, and/or silicon were considered promising ways to improve oxide scale adherence and coating durability. The benefits of Si additions to MCrAl claddings and alloys is well documented in the literature (1, 2, 3). Results obtained in these programs also indicated that both composition and process modifications were required to improve the fabricability and durability of plasma sprayed CoCrAlY coatings.

Data from these initial Pratt & Whitney Aircraft investigations provided the basis for formulating those coating systems which were evaluated in this program on Tailored Plasma Sprayed MCrAlY Coatings for Aircraft Gas Turbine Applications. The objectives of this program were: 1) optimization and selection of a plasma sprayed NiCoCrAlY-type coating system which will provide equivalent or superior performance compared to the current vapor deposited NiCoCrAlY coating in the high temperature environment of advanced aircraft gas turbine engines; and 2) optimization and selection of a plasma sprayed CoCrAlY-type coating system which will provide equivalent or superior performance compared to current vapor deposited CoCrAlY coatings used in

contemporary aircraft gas turbine engines. To accomplish these objectives, an eighteen month technical effort was performed which consisted of the following three tasks.

In Task I - Screening of Composition and Process Variables - a series of experimental nickel and cobalt based MCrAlY-type coating compositions were deposited under various plasma spray process conditions by the argon atmosphere process at Pratt & Whitney Aircraft and by the low pressure chamber process at Howmet Corporation. The coatings were evaluated metallographically to select ten of the most promising combinations for detailed screening evaluation on the current B-1900+Hf turbine blade alloy and on the advanced single crystal turbine alloy. The ten plasma spray candidates were then screened by oxidation and hot corrosion burner rig tests concurrently with Pratt & Whitney Aircraft bill-of-material electron-beam physical vapor deposition NiCoCrAlY and CoCrAlY coatings as baselines. The plasma sprayed coating systems were also tested to measure coating ductility compared to current systems. Pre- and post-burner rig test evaluations were performed on all of the systems using various chemical and metallographic techniques. In addition, studies were conducted to characterize the chemical and microstructural similarities and differences between plasma sprayed and vapor deposited MCrAlY-type coatings using supplemental tests as required.

In Task II - Composition and Process Improvements - four promising plasma spray systems were selected from Task I work and further optimized by composition and process modifications. These modifications to the four systems were evaluated by burner rig oxidation and hot corrosion tests similar to those conducted in Task I. Chemical and metallographic analyses were carried out on the eight Task II systems prior to and after burner rig testing to assist in the evaluation of coating performance. Based on the testing and analysis, the best plasma sprayed coating systems for each of the B-1900+Hf and single crystal alloys were selected for subsequent engine testing in Task III. Turbine blades are being coated with the selected systems and will be evaluated to verify that the desired coating quality and uniformity are achieved. JT8D and JT9D turbine blades and specimens coated with the optimized systems will be supplied to NASA for their evaluation.

In Task III - Engine Testing - additional turbine blades are being coated with the two final plasma spray composition/alloy/process systems and prepared for engine testing. Five (5) B-1900+Hf blades coated with the system optimized for this alloy will be engine tested in a JT8D-17 experimental salted engine test which produces the hot corrosion environment occasionally encountered by this engine during commercial airline service. To provide a baseline, vapor deposited CoCrAlY-coated B-1900+Hf turbine blades will also be tested in the same engine.

A similar number of single crystal turbine blades coated with the plasma spray system optimized for this advanced alloy will be installed and tested in an experimental JT9D-7R4 engine. The test will provide coating exposure to the high temperature oxidation environments in an advanced engine. Vapor deposited NiCoCrAlY-coated single crystal turbine blades will be concurrently tested as the baseline for comparing coating performance. Following testing, the experimentally coated turbine blades from both engines will be metallurgically evaluated to ascertain the degree of improvement in coating performance which was accomplished in this plasma spray coating program.

A flow diagram which summarizes the overall program approach is presented in Figure 4. This report covers the work performed in Tasks I and II.

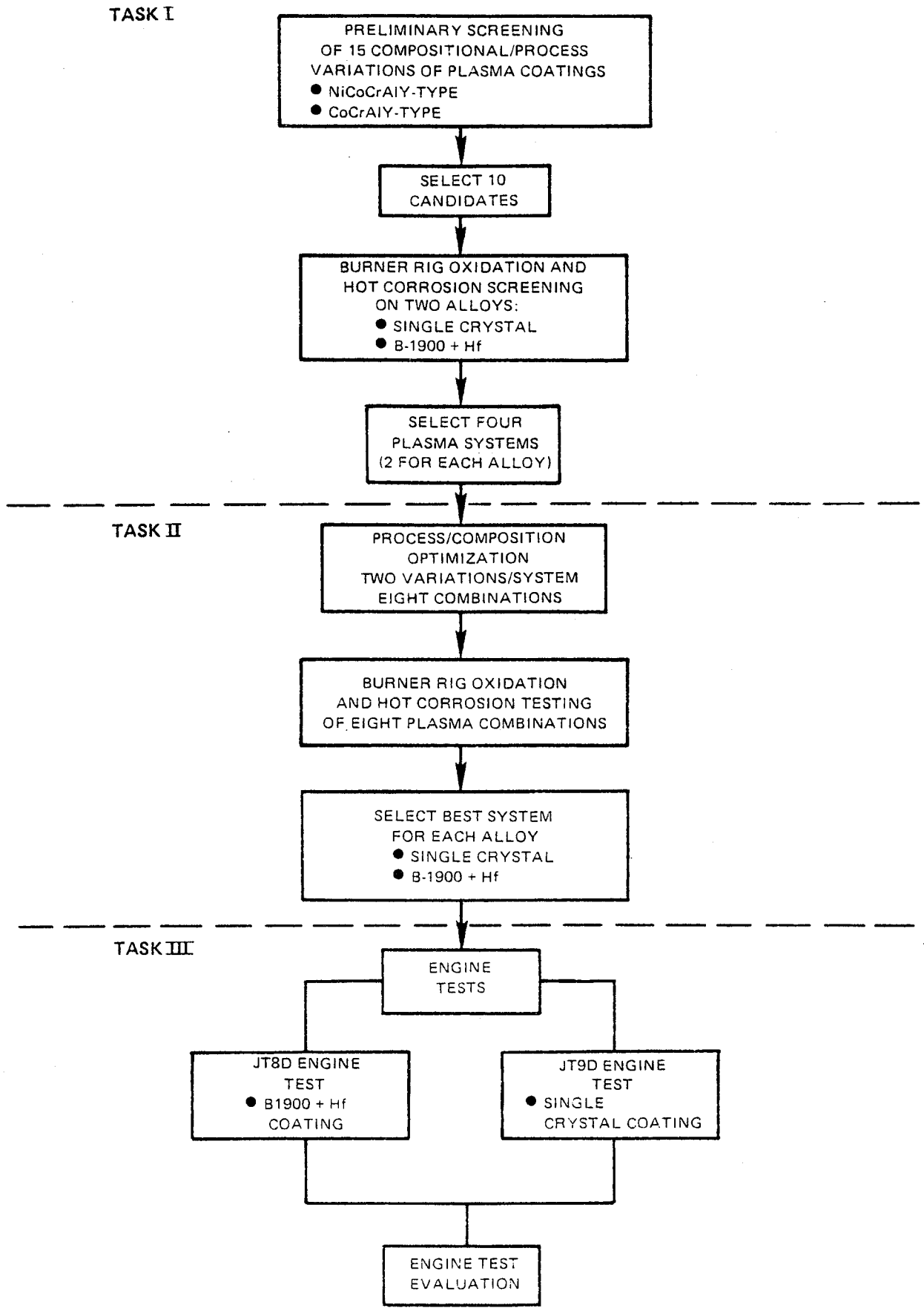


Figure 4 Overall Program Flow Diagram



## 3.0 EXPERIMENTAL PROCEDURE

### 3.1 Materials Fabrication

#### 3.1.1 Substrate Alloys

Plasma sprayed NiCoCrAlY-type coatings were tested on a single crystal alloy representative of an advanced turbine-blade substrate material. Plasma sprayed CoCrAlY-type coatings were tested on the B-1900+Hf alloy representative of a current turbine blade substrate material.

The B-1900+Hf material is a precipitation strengthened nickel-base superalloy and is normally fabricated by conventional investment casting (i.e., equiaxed grain structure). The single crystal nickel-base superalloy is investment cast using a modification of the existing directional solidification process for making columnar grain material. In this modified method, a multiple-turn constriction is placed in the path of the growing columnar grains to select a single (001) oriented grain. This allows a single grain which can grow most rapidly in the direction of the perpendicular growth paths to competitively block out the growth of all the other less favorably oriented grains and fill the mold cavity with material of a single crystal orientation.

Using these two investment casting methods (conventional and modified directional solidification) the burner rig samples of B-1900+Hf and single crystal alloy were fabricated by Pratt & Whitney Aircraft to the configuration shown in Figure 5. The cast samples were appropriately solution heat treated in a protective atmosphere. After cooling to room temperature excess material was removed and the surfaces of the parts lightly grit blasted. Next the samples were polished using 600 grit paper to smooth the surface and round sharp edges in preparation for coating deposition.

Specimens for tensile ductility testing were fabricated from cast B-1900+Hf alloy, 1.25cm (1/2 inch) diameter round bar stock. After the round bar stock had been appropriately heat treated in a protective atmosphere the parts were

machined using conventional methods and the gage length electrochemically ground to the required diameter. Figure 6 shows the ductility specimen dimensions.

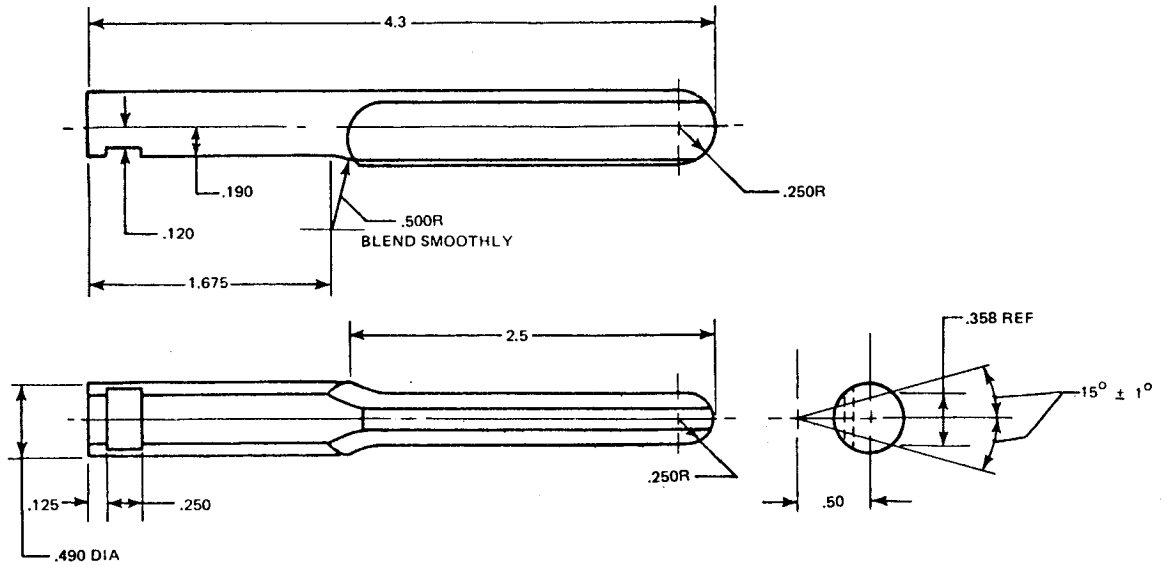


Figure 5 Oxidation-Hot Corrosion Coating Evaluation Test Specimen

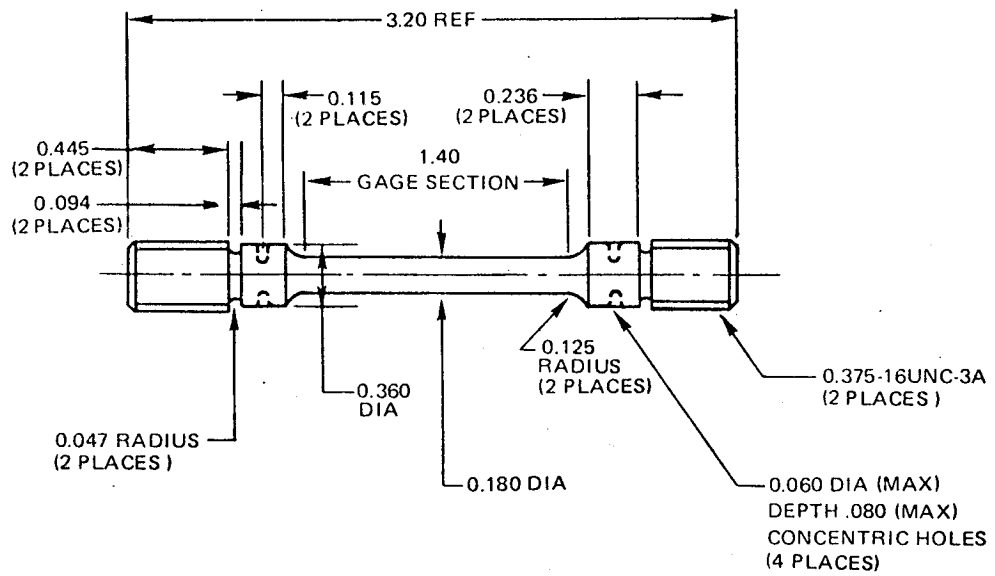


Figure 6 Coating Ductility Test Specimen

### 3.1.2 Coating Alloy Ingot/Powder

Alloy ingots required for electron-beam physical vapor deposition of NiCoCrAlY and CoCrAlY coatings were prepared using conventional casting techniques by Pratt & Whitney Aircraft. All alloy powders used in this program to fabricate plasma spray coatings were manufactured by Alloy Metals Inc. The alloy powders were characterized at Pratt & Whitney Aircraft to establish their elemental composition and particle size distribution. The chemical composition was determined by using conventional wet chemical methods and the particle size distribution was established through the use of a low angle laser scattering technique.

## 3.2 Coating Fabrication

### 3.2.1 Electron Beam Physical Vapor Deposition

Baseline vapor deposited NiCoCrAlY and CoCrAlY coatings were applied to alloy samples at Pratt & Whitney Aircraft using previously well established coating procedures.

In this process an electron-beam is directed on to the surface of material contained in a crucible. The material in the crucible is heated, melted, and evaporated to produce vapor of the coating metals. The parts to be coated are positioned above the molten material in the crucible. The process is conducted in vacuum to permit generation of the electron beam and vaporized species, as well as to avoid contaminating the molten material in the crucible and the vapor phase or the condensate (coating). The vacuum chamber is equipped with load or airlocks, which allow parts for coating to be admitted and withdrawn without interruption of the evaporation process. Since the vapor travels in essentially a line-of-sight manner to the substrate surface, parts are rotated

during coating to achieve complete coverage. Coating alloy ingot is automatically fed through the bottom of the crucible during coating operation. Essential features of the process and equipment are illustrated in Figure 7.

### 3.2.2 Plasma Spray Processing

All plasma spray coating variations which were evaluated in this program were either sprayed in an argon containing chamber at one atmosphere by Pratt and Whitney Aircraft, Manufacturing Division or sprayed in a low pressure inert atmosphere chamber by Howmet Turbine Components Corporation.

For the one atmosphere argon chamber spraying, a Plasmadyne plasma spray system was used. In this system a non-transferred arc plasma gun (SG-100), was used to ionize a mixture of inert gas (argon and helium) at fairly high power input levels (60-70Kw). This results in a high temperature and high velocity (about Mach 2) plasma effluent into which coating powder particles are injected just before its exit from the nozzle. The powder particles are deposited in an inert gas environment (enclosed chamber), therefore, the particles are not adversely affected by oxygen (oxide formation) or by nitrogen (nitride formation) during transport to workpiece. The controlled atmosphere plasma system used in this effort is shown in Figure 8.

For the plasma spray coatings produced in a low pressure chamber, Howmet used its in-house designed and constructed manufacturing scale facility (Figure 9). This facility contains a 120 Kw plasma generator (Electro-Plasma Model No. 03CA) which produces a Mach 3 velocity flame in a chamber maintained at a dynamic partial vacuum. To obtain supersonic plasma stream velocities (Mach 2 to Mach 3) a diverging nozzle and an arc chamber pressure of 7.5 atmospheres is used in the plasma gun. The arc chamber pressure is controlled by controlling the arc power and plasma gas flow rate during operation. The Mach 3 velocity condition is established when the arc chamber-to-ambient pressure ratio of the gas is about 100. To achieve this pressure ratio, the ambient pressure in the spray chamber must be lowered to approximately 0.075 atmospheres. This pressure is maintained through a mechanical vacuum pump or a

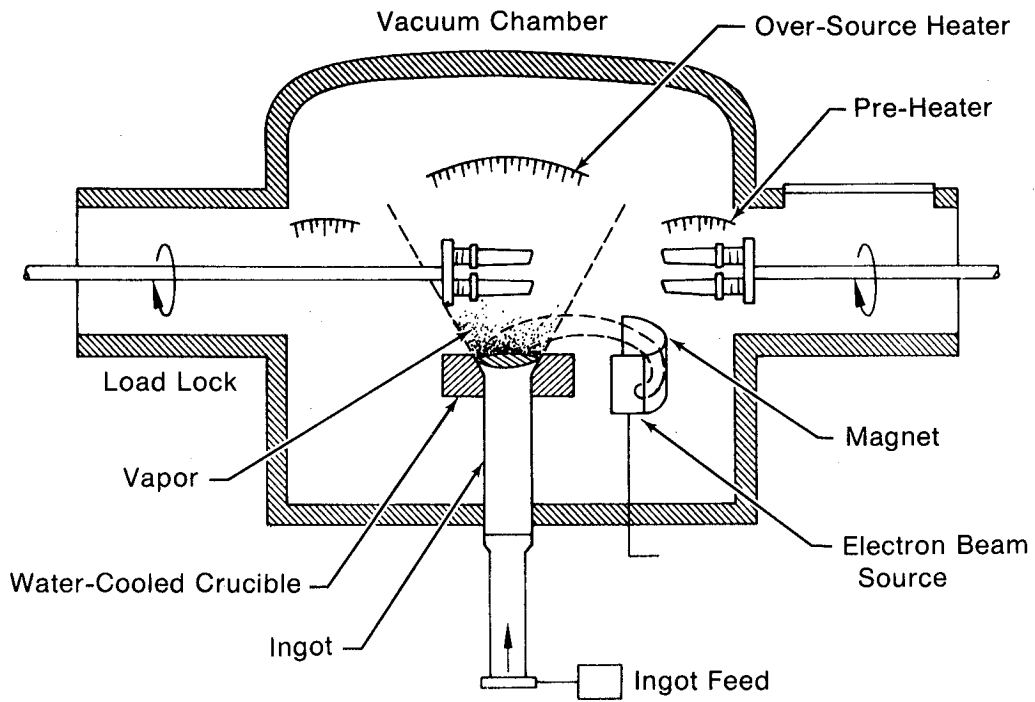


Figure 7 Diagram of Typical EB-PVD Coating Chamber

ORIGINAL PAGE  
BLACK AND WHITE PHOTOGRAPH

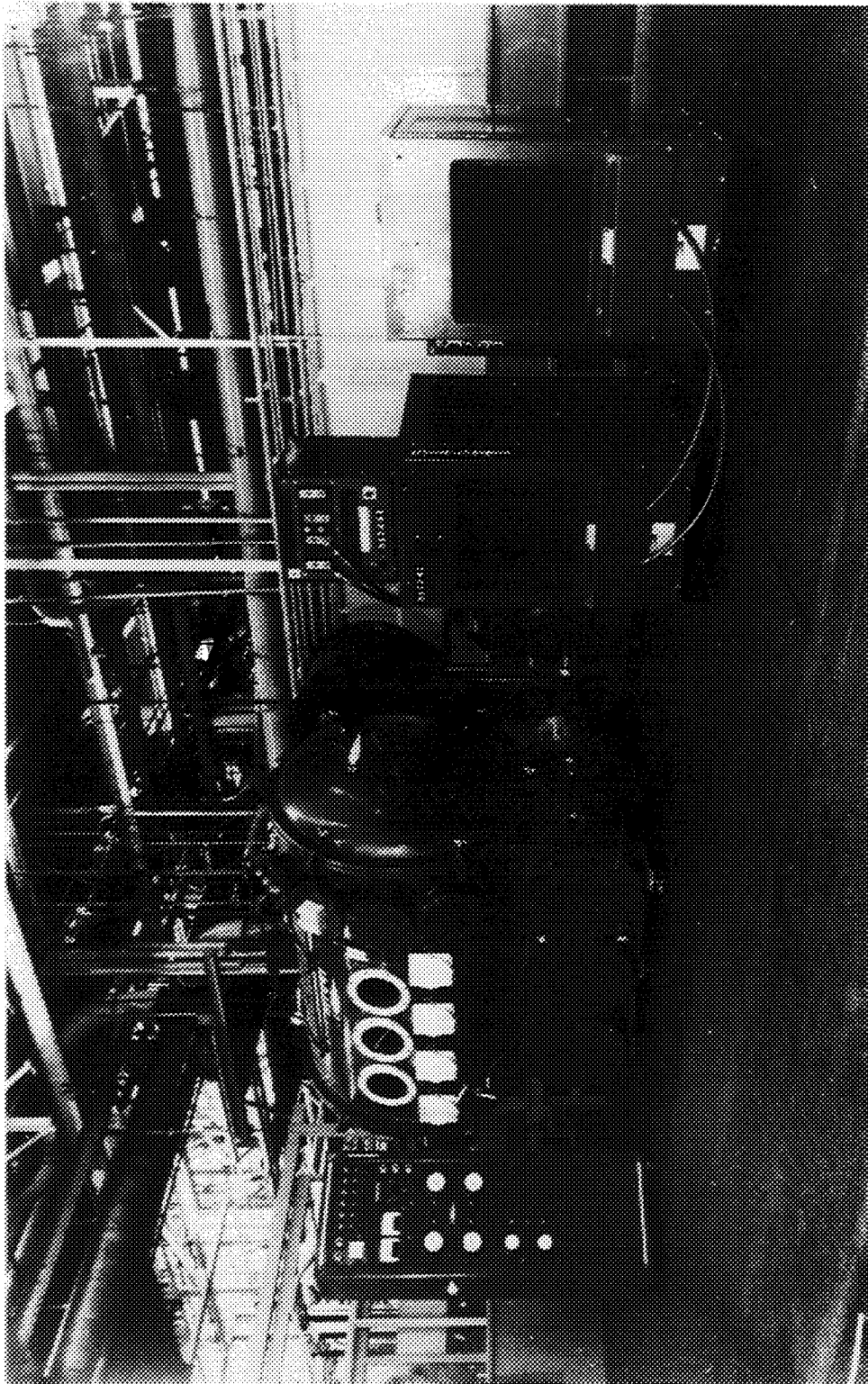


Figure 8 P&WA Controlled Atmosphere Plasma Spray System

ORIGINAL PAGE  
BLACK AND WHITE PHOTOGRAPH

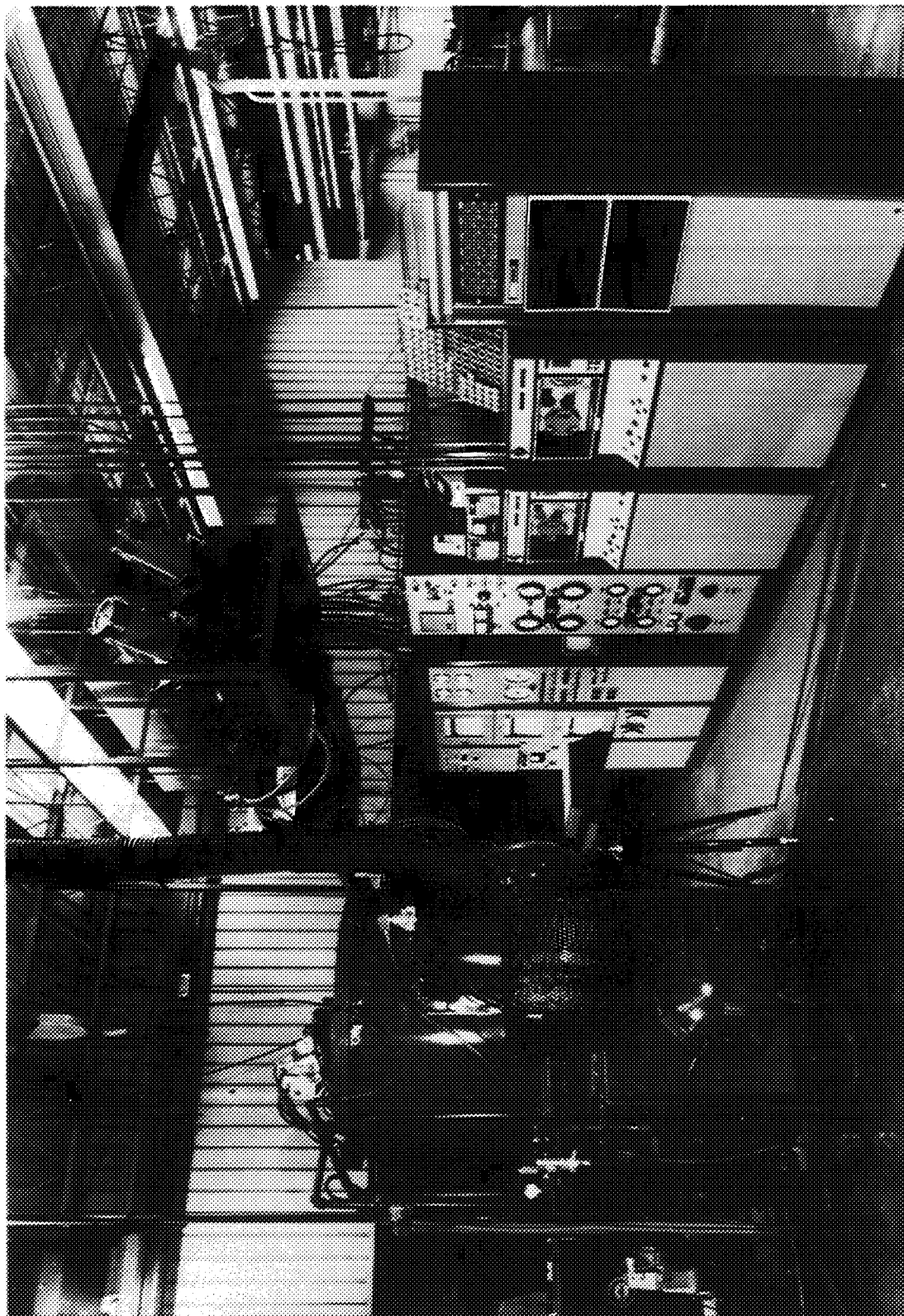


Figure 9 Howmet Corporation Pilot-Scale Low Pressure Chamber Plasma Spray Equipment

combination of pumps during plasma spray operation at the Mach 3 condition. Due to the reduced ambient chamber pressure, the plasma stream is enlarged in volume which results in a lower density plasma flame and a more uniform cross sectional profile of temperature and pressure compared to spraying at one atmosphere pressure.

### 3.2.3 Post-Coating Processing

Following plasma spray coating fabrication, the coated burner rig samples were given a one hour pre-heat treatment at 1352<sup>0</sup>K (1975<sup>0</sup>F) in a hydrogen atmosphere to increase the coating adherence and thus enable high intensity glass bead peening to be utilized without causing coating chipping. Next the samples were glass bead peened at an appropriate intensity level. Finally, the coated samples were given a heat treatment for 3 hrs at 1352<sup>0</sup>K (1975<sup>0</sup>F) in a hydrogen atmosphere. In one coating variation, a CoCrAlY coating was hot isostatically pressed by Howmet at 1470<sup>0</sup>K (2185<sup>0</sup>F) for 3 hrs at 103.4 MPa (15 Ksi) in argon prior to its 4 hrs at 1352<sup>0</sup>K (1975<sup>0</sup>F) in hydrogen heat treatment. In Task II the hot isostatic pressing was conducted at 1352<sup>0</sup>K (1975<sup>0</sup>F)/ 4 hrs/103.4 MPa (15 Ksi) in argon with no subsequent heat treatment. Plasma spray coated B-1900+Hf alloy tensile specimens received similar post-coating processing treatments prior to their appropriate precipitation heat treatments. Following coating deposition of the vapor deposited coatings, the samples given the standard processing consisting of glass bead peening at 17+2N intensity level followed by heat treating at 1352<sup>0</sup>K (1975<sup>0</sup>F) for 4 hours in a hydrogen atmosphere. All post-coating processing steps except for the hot isostatic pressing at 1470<sup>0</sup>K (2185<sup>0</sup>F) were conducted at Pratt & Whitney Aircraft.

### 3.3 Burner Rig Tests

All burner rig testing conducted in this program utilized the appropriately coated solid test bar, shown in Figure 5. This specimen is designed to provide for simulation of the leading edge cross section of typical turbine blades and of discontinuities typical of trailing edges and blade tips. In addition the



specimen length also simulates typical first stage turbine blade dimensions. During burner rig exposure, an approximately 13 mm long region of the specimen is at a uniform ( $\pm 15^{\circ}\text{K}$ ,  $\pm 27^{\circ}\text{F}$ ), maximum temperature, and this region is used as the test section where coating performance is observed.

### 3.3.1 Oxidation Tests

All burner rig oxidation tests performed throughout this program were conducted in Pratt & Whitney Aircraft Mach 0.7 one atmosphere test facilities. The tests were conducted by simultaneous exposure of 12 specimens in a rotating fixture exposed to the unrestricted burner flame. The burner, operating on Jet-A fuel, is controlled through fuel pressure which is automatically adjusted to maintain the required specimen temperature. Specimen temperature is monitored by a radiometric pyrometer. The equipment has the capability of automatic thermal cycling to allow simulation of engine operating cycles. During air cooling of the specimens the burner is pivoted away from the specimen holder by an automatic hydraulic mechanism. Figure 10 shows a schematic of the test apparatus.

Cyclic oxidation testing was conducted at  $1394^{\circ}\text{K}$  ( $2050^{\circ}\text{F}$ ) average metal temperature. Each cycle consisted of a 55 minute exposure to the burner combustion products, followed by 5 minutes of cooling with compressed air at ambient temperature. At 16-20 hour intervals the specimens were optically examined to evaluate the relative surface condition or coating performance of each coating system. The burner rig tests were conducted until specimen failure, or for a maximum of 1000 hours, whichever occurred first. A total of three specimens of each condition were tested. One specimen representing each system (including baselines) was withdrawn after approximately 350 hours of exposure. At this withdrawal interval, a new specimen, coated with the same composition/ process variation as the removed specimen, was added to the test. In this manner, single specimens, representing each system, exposed for 350, 650 and 1000 hours or the failed condition were obtained for performance evaluation.

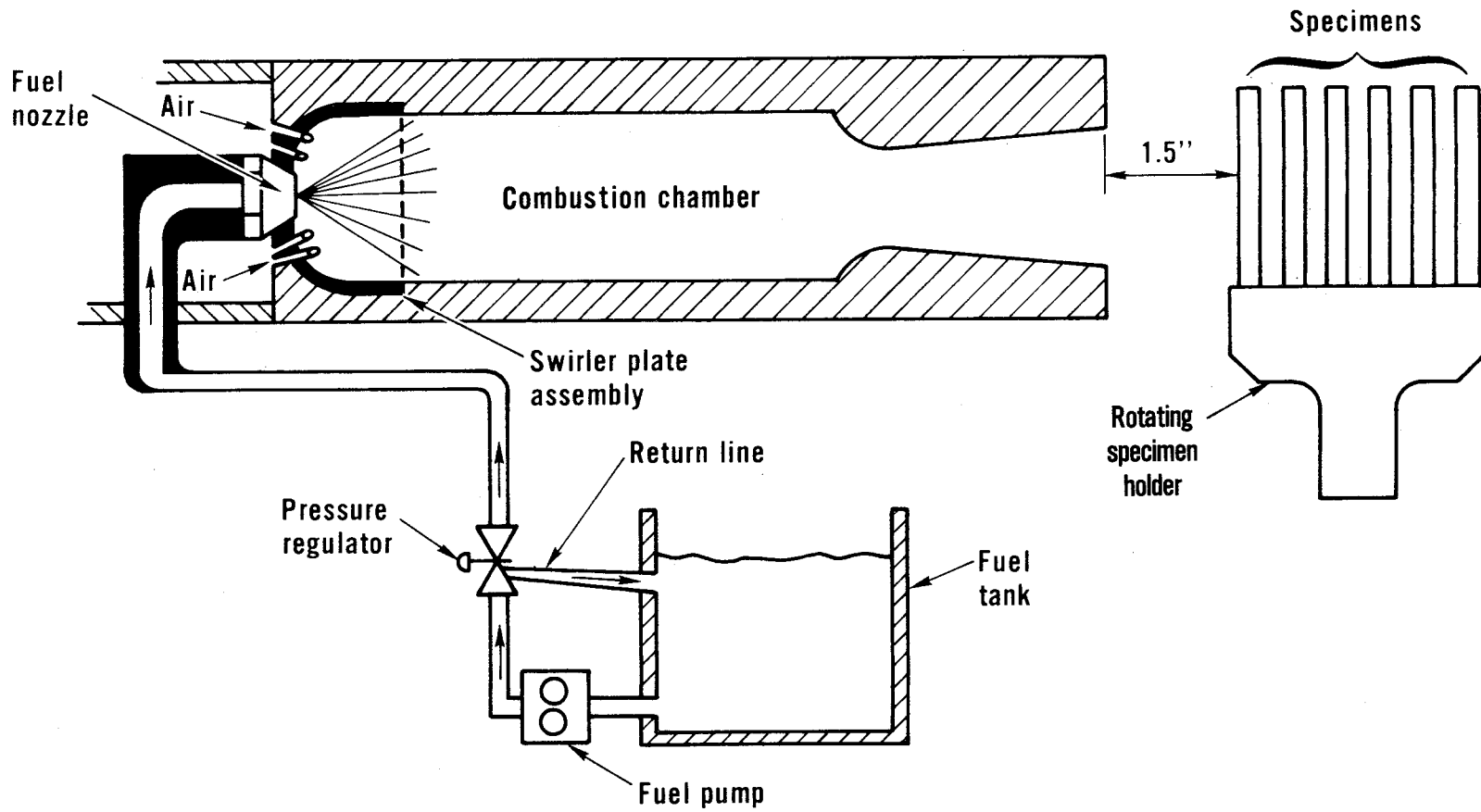


Figure 10 Diagram of Burner Rig Oxidation Test Apparatus

Two events were used as failure criteria to judge coating performance: 1) the time to initial localized oxidation penetration to the coating substrate interface; and, 2) the time when oxidation penetration reached the coating substrate interface over 50 percent of the specimen test section.

### 3.3.2 Hot Corrosion Tests

Hot corrosion testing conducted throughout the program utilized the Pratt & Whitney Aircraft ducted Mach 0.3 burner rig facilities. These rigs utilize an enclosed exhaust flame tube to limit dilution of combustion gases by ambient air during test. This capability allows the concentration of critical gases such as  $\text{SO}_3$  to be maintained at levels characteristic of actual engine operation at the specimen location. The apparatus is shown in Figure 11. During hot corrosion testing in these rigs, continuous metered additions of  $\text{SO}_2$  gas (30.5 liters/hour) were made to the primary combustion air to simulate engine operating environments. During the combustion process, the  $\text{SO}_2$  is partially converted to  $\text{SO}_3$  in the exhaust gas stream. To provide to some extent for engine pressure corrections during one atmosphere laboratory testing, a sulfur addition of 1.3% of the total massflow was applied. An ASTM D-1142-52 artificial sea salt solution was added to the combustor by metered injection at the level of 35 parts per million to provide the primary corrosive medium.

The specimens were exposed at  $1172^{\circ}\text{K}$  ( $1650^{\circ}\text{F}$ ) for 55 minutes in a ducted rig, followed by five minutes of cooling with compressed air. At 16-20 hour intervals, the specimens were optically examined for relative performance evaluation. As in the oxidation testing, a total of three coated specimens representing each of the coating systems were exposed in the hot-corrosion rigs. This exposure was conducted until specimen failure, or for a maximum of 500 hours, whichever occurred first. One specimen from each system was withdrawn after approximately 150 hours of exposure. At this withdrawal interval, a new specimen, coated with the same composition/process variation as for the removed specimen, was added to the test. In this manner, single specimens representing each system, exposed for 150, 350 and 500 hours were obtained for post-test performance evaluation. Failure criteria were the same as for the oxidation testing.

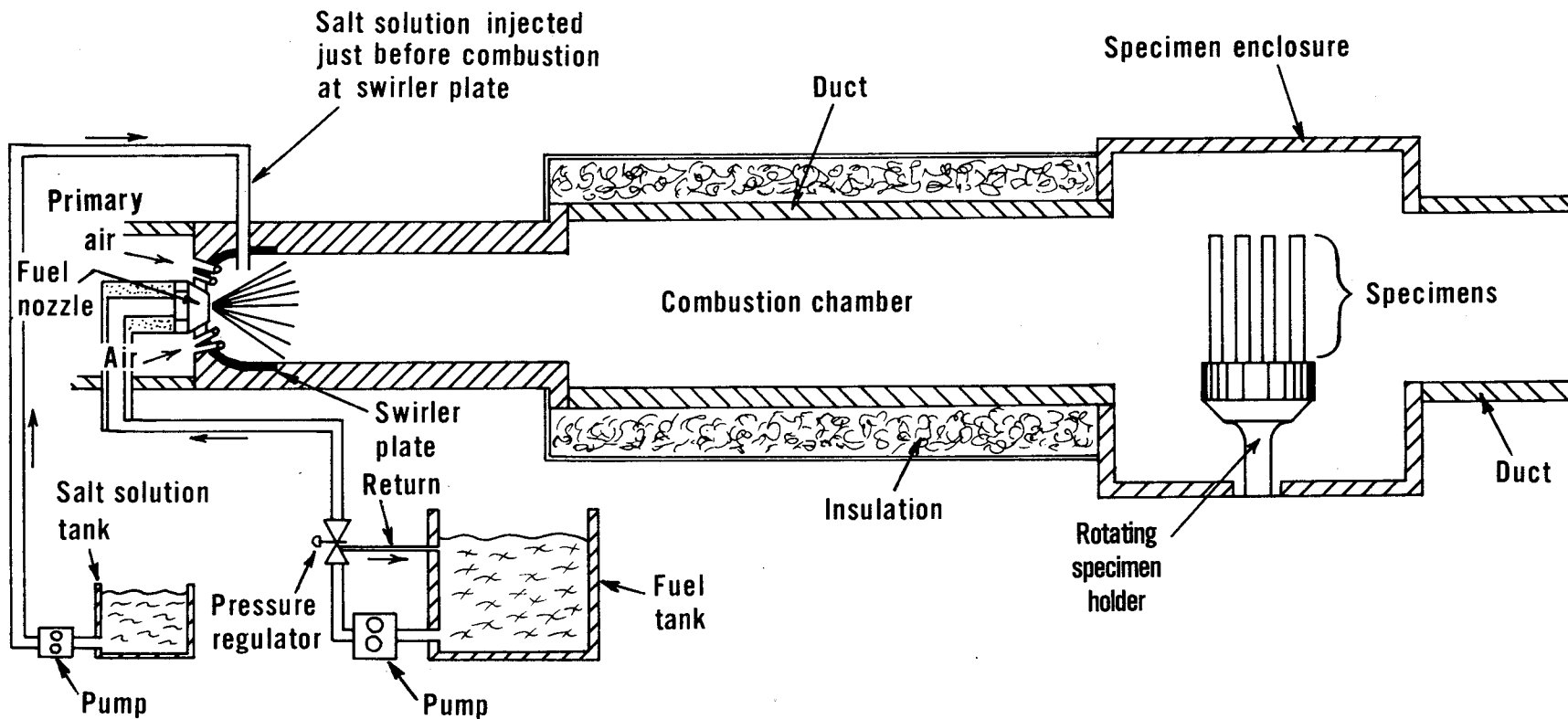


Figure 11 Diagram of Burner Rig Hot Corrosion Test Apparatus With Test Specimens Enclosed to Allow Precise Control of  $\text{SO}_3$  and Other Contaminants

### 3.4 Tensile/Ductility Testing

An interrupted elevated temperature tensile test which is outlined schematically in Figure 12 was used to measure coating ductility. In this test the specimens were monotonically loaded under isothermal conditions to a predetermined finite strain. The specimens were then unloaded and allowed to cool to room temperature at which time plastic surface replicas were taken; with a 0.05% tensile strain applied to the specimen in order to increase crack detectability. This procedure was repeated for increasing strain increments until microscopic examination of the surface replicas indicated that the coating was cracked. In this program all tensile testing was conducted at 588<sup>o</sup>K (600<sup>o</sup>F) based on previous experience that ductility levels at this temperature are indicative of whether MCrAlY coating cracking problems will be encountered during engine exposure.

### 3.5 Pre- and Post-Test Coating Evaluations

The coated specimens prior to testing and after completion of the tests in both tasks were examined by standard analytical techniques. These techniques included use of the light microscope, electron-beam microprobe, scanning electron microscope and x-ray diffraction.

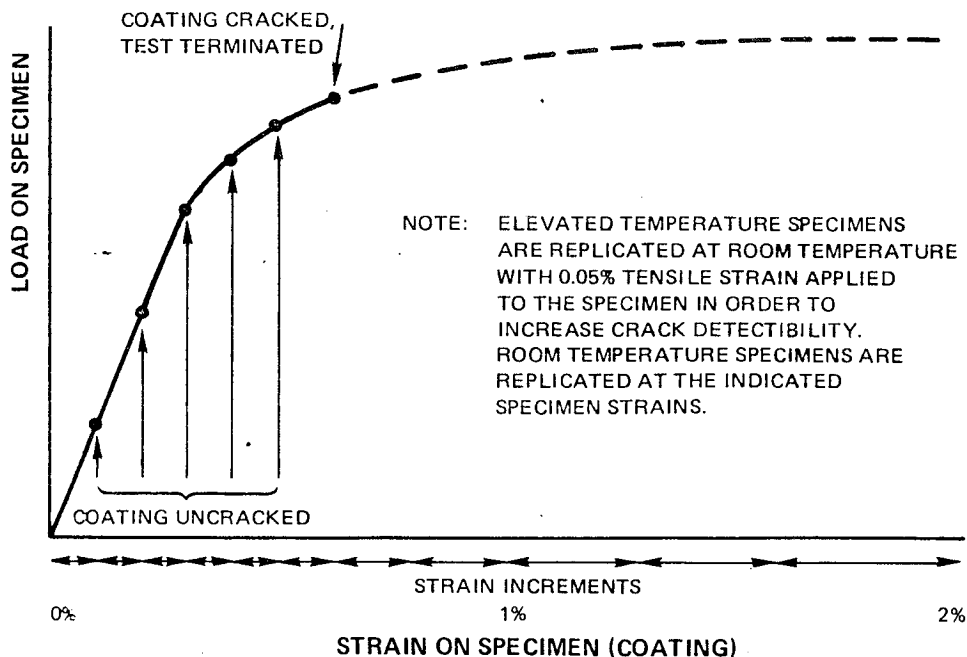


Figure 12 Procedure for Interrupted Tensile Coating Ductility Test. Large coated areas can be evaluated in this test

## 4.0 EXPERIMENTAL RESULTS AND DISCUSSION

### 4.1 Task I Evaluation

Initially in Task I, a series of experimental MCrAlY-type coating compositions were deposited under various plasma spray process conditions and metallographically evaluated to select ten coating/process combinations for detailed burner rig testing. The ten coating candidates were screened by oxidation and hot corrosion burner rig tests concurrently with electron-beam physical vapor deposited NiCoCrAlY and CoCrAlY coatings as baselines. In this task, plasma spray coating systems were also tensile tested to measure ductility compared to baseline coatings.

#### 4.1.1 Candidate Coatings for Initial Screening

The fifteen candidate coating systems used for initial metallographic screening purposes are listed in Table I. The first eight NiCoCrAlY-type coating systems were selected for the single crystal alloy and the remaining seven CoCrAlY-type variations were selected for the B-1900+Hf alloy. A summary of the coating systems chosen and the reasons for the choices follows.

- a) Ni-23Co-18Cr-12.5Al-0.4Y - low pressure chamber plasma spraying followed by glass bead peening at 17N intensity plus final heat treatment at 1352<sup>0</sup>K (1975<sup>0</sup>F) for 4 hours in H<sub>2</sub>.
- b) Ni-23Co-18Cr-12.5Al-0.4Y - low pressure chamber plasma spraying followed by final heat treatment at 1352<sup>0</sup>K (1975<sup>0</sup>F) for 4 hours in H<sub>2</sub> plus glass bead peening at 17N intensity.
- c) Ni-23Co-18Cr-12.5Al-0.4Y - low pressure chamber plasma spraying followed by glass bead peening at 22N intensity plus final heat treatment at 1352<sup>0</sup>K (1975<sup>0</sup>F) for 4 hours in H<sub>2</sub>.

These three post-coating process variations on the low pressure chamber sprayed NiCoCrAlY coating were included in the initial screening to obtain an optimum glass bead peening and heat treatment condition and sequencing of

TABLE I  
COATING SYSTEMS INITIALLY SCREENED IN TASK I

<u>Designation</u>	<u>Coating Type</u>	<u>Coating Composition</u>	<u>Plasma Spray Process</u>	<u>Post Coating Processing</u>
a	NiCoCrAlY	Ni-23Co-18Cr-12.5Al-0.4Y	LPCS	17NGBP+HT
b	NiCoCrAlY	Ni-23Co-18Cr-12.5Al-0.4Y	LPCS	HT+17NGBP
c	NiCoCrAlY	Ni-23Co-18Cr-12.5Al-0.4Y	LPCS	22NGBP+HT
d	NiCoCrAlY+Hf	Ni-23Co-18Cr-12.5Al-0.6Y -0.6Hf	LPCS	17NGBP+HT
e	NiCoCrAlY+Si	Ni-23Co-18Cr-12.5Al-0.6Y -1.5Si	LPCS	17NGBP+HT
f	NiCoCrAlY+Ta	Ni-23Co-18Cr-12.5Al-0.6Y -8.0Ta	LPCS	17NGBP+HT
g	NiCoCrAlY	Ni-23Co-18Cr-12.5Al-0.4Y	APS	17NGBP+HT
h	NiCoCrAlY+Hf	Ni-23Co-18Cr-12.5Al-0.6Y -0.6Hf	APS	17NGBP+HT
i	CoCrAlY	Co-22Cr-12.5Al-0.6Y	LPCS	17NGBP+HT
j	CoCrAlY	Co-22Cr-12.5Al-0.6Y	LPCS	22NGBP+HT
k	CoCrAlY	Co-22Cr-12.5Al-0.6Y	LPCS	HIP+HT
l	CoCrAlY (High Cr Low Al)	Co-29Cr-10Al-0.6Y	LPCS	17NGBP+HT
m	CoCrAlY+Si	Co-22Cr-12.5Al-0.6Y-2.0Si	LPCS	17NGBP+HT
n	CoCrAlY	Co-22Cr-12.5Al-0.6Y	APS	17NGBP+HT
o	CoCrAlY+Si	Co-22Cr-12.5Al-0.6Y-2.0Si	APS	17NGBP+HT

LPCS = Low Pressure Chamber Plasma Spray

APS = One Atmospheric Argon Plasma Spray

HT = Heat Treat at 1352<sup>o</sup>K (1975<sup>o</sup>F) for 4 hours in H<sub>2</sub>

HIP = Hot Isostatic Pressing at 1470<sup>o</sup>K (2185<sup>o</sup>F) for 3 hours at a pressure of 103.4 MPa (15 ksi)

GBP = Glass Bead Peening (at intensity shown e.g. 17N)

these two processes. The process of glass bead peening followed by a heat treatment has been shown to improve coating density and surface finish. Presently, glass bead peening is conducted at a 17N intensity level on vapor deposited MCrAlY coatings. Two glass bead peening intensity levels (17N and 22N) were evaluated for the plasma sprayed coatings.

d) Ni-23Co-18Cr-12.5Al-0.6Y-0.6Hf - low pressure chamber plasma spraying followed by 17N glass bead peening plus 1352<sup>0</sup>K (1975<sup>0</sup>F)/4 hours/H<sub>2</sub> heat treatment.

Hafnium additions to MCrAl alloys (4,5) have been reported to improve the oxidation resistance of these alloys through the mechanism of improved alumina scale adherence. Since plasma sprayed coatings were observed to suffer from poor oxide scale adherence during high temperature oxidation tests conducted in other programs, it was contemplated that a hafnium addition to the basic NiCoCrAlY composition would reduce this deficiency and improve oxidation resistance.

e) Ni-23Co-18Cr-12.5Al-0.6Y-1.5Si - low pressure chamber plasma spraying followed by 17N glass bead peening plus 1352<sup>0</sup>K (1975<sup>0</sup>F)/4 hours/H<sub>2</sub> heat treatment.

f) Ni-23Co-18Cr-12.5Al-0.6Y-8.0Ta - low pressure chamber plasma spraying followed by 17N glass bead peening plus 1352<sup>0</sup>K (1975<sup>0</sup>F)/4 hours/H<sub>2</sub> heat treatment.

Silicon (1,2,3,6,7) and tantalum (8) had also been observed to improve the oxidation resistance of NiCrAl and CoCrAl based alloys. Laboratory investigations conducted at Pratt & Whitney Aircraft had shown that additions of 1 to 2 weight percent silicon and/or 6 to 10 weight percent tantalum to NiCoCrAlY alloys provided significant improvements in coated oxidation lives of D.S. Mar-M200 + Hf alloys. Based on these studies, NiCoCrAlY+Si and NiCoCrAlY+Ta coatings were included for evaluation during this program.



- g) Ni-23Co-18Cr-12.5Al-0.4Y - plasma spraying in one atmospheric argon chamber followed by glass bead peening at 17N plus 1352<sup>0</sup>K (1975<sup>0</sup>F)/4 hours/H<sub>2</sub> heat treatment.
- h) Ni-23Co-18Cr-12.5Al-0.6Y-0.6Hf - plasma spraying in a one atmospheric argon chamber followed by glass bead peening at 17N plus 1352<sup>0</sup>K (1975<sup>0</sup>F)/4hours/H<sub>2</sub> heat treatment.

These two coating candidates, (g) and (h), are similar in composition to candidates (a) and (d) except that plasma spray processing was conducted in a one atmospheric argon environment rather than in a low pressure (about one-tenth of an atmosphere) argon chamber as was the case with latter coating systems. The atmospheric argon sprayed coating systems were included for initial screening to compare quality and performance with similar composition coatings produced by the low pressure process.

- i) Co-22Cr-12.5Al-0.6Y - low pressure chamber plasma spraying followed by glass bead peening at 17N intensity plus 1352<sup>0</sup>K(1975<sup>0</sup>F)/4 hours/H<sub>2</sub> heat treatment.
- j) Co-22Cr-12.5Al-0.6Y - low pressure chamber plasma spraying followed by glass bead peening at 22N intensity plus 1352<sup>0</sup>K (1975<sup>0</sup>F)/4 hours/H<sub>2</sub> heat treatment.

These two post-coating glass bead peening variations on the low pressure chamber spray CoCrAlY coating were included in the initial list of candidates to determine if higher intensity peening (22N vs 17N) improves the microstructural quality of the CoCrAlY coatings.

- k) Co-22Cr-12.5Al-0.6Y - low pressure chamber plasma spraing followed by hot isostatic pressing at 1470<sup>0</sup>K (2185<sup>0</sup>F) for 3 hours at a pressure of 103.4 MPa (15 Ksi) in argon plus 1352<sup>0</sup>K (1975<sup>0</sup>F)/4 hours/H<sub>2</sub> heat treatment.

The process of hot isostatic pressing the plasma sprayed MCrAlY coating has been reported to eliminate structural defects and thereby improve coating performance. Since it had been previously observed that plasma sprayed CoCrAlY coatings normally contained more structural defects (porosity) than plasma sprayed NiCoCrAlY; therefore post-coating hot isostatic pressing was examined for CoCrAlY coated B-1900+Hf samples.

- l) Co-29Cr-10Al-0.6Y - low pressure chamber plasma spraying followed by glass bead peening at 17N intensity plus 1352<sup>0</sup>K (1975<sup>0</sup>F)/4 hours/H<sub>2</sub> heat treatment.
  
- m) Co-23Cr-12.5Al-0.6Y-2.0Si - low pressure chamber plasma spraying followed by glass bead peening at 17N plus 1352<sup>0</sup>K (1975<sup>0</sup>F)/4 hours/H<sub>2</sub> heat treatment.

Increasing the amount of chromium (9) and additions of silicon (10, 11) to an MCrAlY coating had been shown to improve the hot corrosion performance of MCrAlY coatings. In view of this, a high chromium and lowered aluminum modification and a silicon-containing modification of the basic CoCrAlY composition were included in order to improve the hot corrosion behavior of plasma sprayed CoCrAlY coatings.

- n) Co-22Cr-12.5Al-0.6Y - plasma spraying in one atmospheric argon chamber followed by glass bead peening at 17N plus 1352<sup>0</sup>K (1975<sup>0</sup>F)/4 hours/H<sub>2</sub> heat treatment.
  
- o) Co-22Cr-12.5Al-0.6Y-2.0Si - plasma spray in one atmospheric argon chamber followed by glass bead peening at 17N plus 1352<sup>0</sup>K (1975<sup>0</sup>F)/4hours/H<sub>2</sub> heat treatment.

These one-atmospheric argon plasma sprayed candidates were included in the initial screening to compare microstructural quality with that of the similar CoCrAlY-based coatings produced by the low pressure chamber spray process.

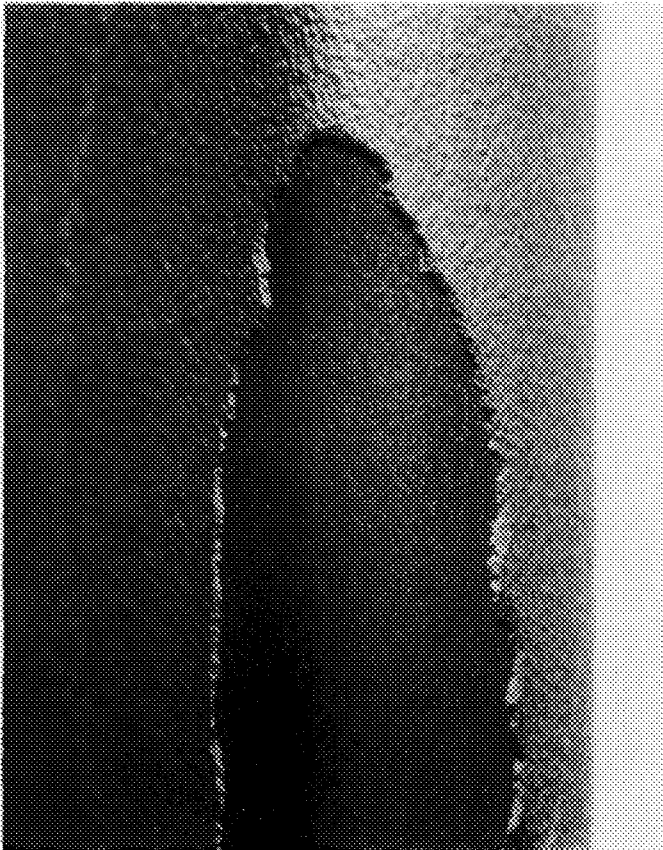
#### 4.1.2 Results of Initial Screening

The selection of the ten best coating systems for subsequent burner rig oxidation and hot corrosion testing was conducted by metallographic evaluation of the fifteen processing/composition variations, described in the previous subsection, for coating quality and thickness uniformity. Coated B-1900+Hf coupons were evaluated for this screening. During initial post-spray glass bead peening (17N intensity level) of the as-sprayed coupons, it was observed that some coatings, especially argon chamber sprayed coatings and the low pressure sprayed NiCoCrAlY + Ta and CoCrAlY + Si coatings, spalled and/or cracked due to either poor interfacial bonding between the coating and the substrate or because of residual stresses present in the as-sprayed coating. An example of this behavior is provided in Figure 13. A heat treatment of one hour at 1352<sup>0</sup>K (1975<sup>0</sup>F) in a hydrogen atmosphere before peening successfully eliminated this problem. Therefore, it was decided that as a precautionary measure all samples representing the various coating variations would be heat treated at 1352<sup>0</sup>K (1975<sup>0</sup>F) for one hour in a hydrogen environment prior to the glass bead peening operation. It should be pointed out that this pre-heat treatment step prior to the glass bead peening may not be necessary for the final coatings optimized in the program and may be eliminated in the future.

The metallographically determined average coating thicknesses and the extent of the thickness variations (standard deviation  $\sigma$ ) observed on the specimens are presented in Table II. The thicknesses of the low pressure chamber sprayed coatings were observed to be more uniform ( $\sigma = 2$  to 8% of mean) compared to those of the one-atmosphere argon chamber sprayed coatings ( $\sigma = 10$  to 17% of mean). However, the thickness control with both processes met the program requirement that the coating thickness on each specimen be within +20% of the 100 to 150 microns (4 to 6 mils) target thickness. In view of this, the selection of ten candidates was primarily based on coating quality.

Representative microstructures of NiCoCrAlY and CoCrAlY coatings processed by the two plasma spray processes are provided in Figure 14. Typically, compared

ORIGINAL PAGE  
BLACK AND WHITE PHOTOGRAPH



7X

Figure 13 Spalling of the Low Pressure Chamber Plasma Sprayed CoCrAlY+Si Coating on the B1900+Hf Substrate During Post-Spray Glass Bead Peening.

ORIGINAL PAGE IS  
OF POOR QUALITY

TABLE II  
THICKNESS OF COATED SPECIMENS  
METALLOGRAPHICALLY EVALUATED IN TASK I

<u>Coating Designation</u>	<u>Coating Type</u>	<u>Plasma Spray Process</u>	<u>Post Coating Processing</u>	<u>Coating Thickness (microns)</u>	
				<u>Mean</u>	<u>Standard Deviation</u>
a	NiCoCrAlY	LPCS	H+17NGBP+HT	148	5
b	NiCoCrAlY	LPCS	HT+17NGBP	140	8
c	NiCoCrAlY	LPCS	H+22NGBP+HT	128	8
d	NiCoCrAlY+Hf	LPCS	H+17NGBP+HT	145	8
e	NiCoCrAlY+Si	LPCS	H+17NGBP+HT	162	8
f	NiCoCrAlY+Ta	LPCS	H+17NGBP+HT	118	8
g	NiCoCrAlY	APS	H+17NGBP+HT	100	10
h	NiCoCrAlY+Hf	APS	H+17NGBP+HT	110	18
i	CoCrAlY	LPCS	H+17NGBP+HT	150	10
j	CoCrAlY	LPCS	H+22NGBP+HT	132	3
k	CoCrAlY	LPCS	H+17NGBP+HIP+HT	142	8
l	CoCrAlY (High Cr Low Al)	LPCS	H+17NGBP+HT	130	10
m	CoCrAlY+Si	LPCS	H+17NGBP+HT	155	10
n	CoCrAlY	APS	H+17NGBP+HT	88	12
o	CoCrAlY+Si	APS	H+17NGBP+HT	92	15

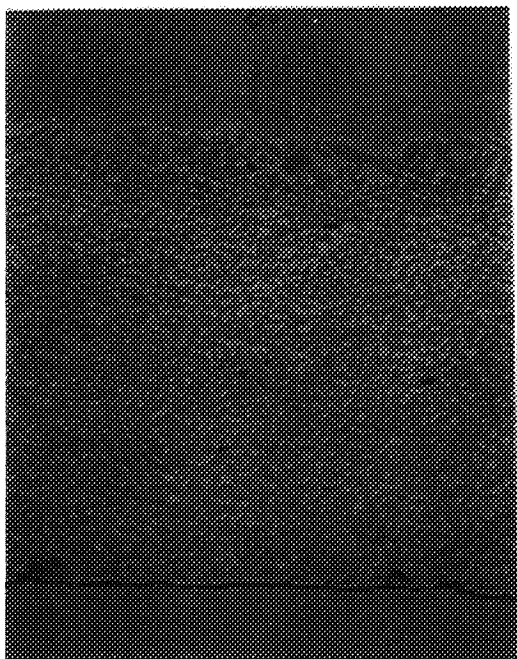
LPCS = Low Pressure Chamber Plasma Spray  
 APS = One Atmospheric Argon Plasma Spray  
 H = Heat Treat at 1325<sup>o</sup>K (1975<sup>o</sup>F) for 1 hour in H<sub>2</sub>  
 HT = Heat Treat at 1352<sup>o</sup>K (1975<sup>o</sup>F) for 4 hours in H<sub>2</sub>  
 HIP = Hot Isostatic Pressing at 1470<sup>o</sup>K (2185<sup>o</sup>F) for 3 hours at a pressure of 103.4 MPa (15 ksi)  
 GBP = Glass Bead Peening (at intensity shown e.g. 17N)

NICOCALY

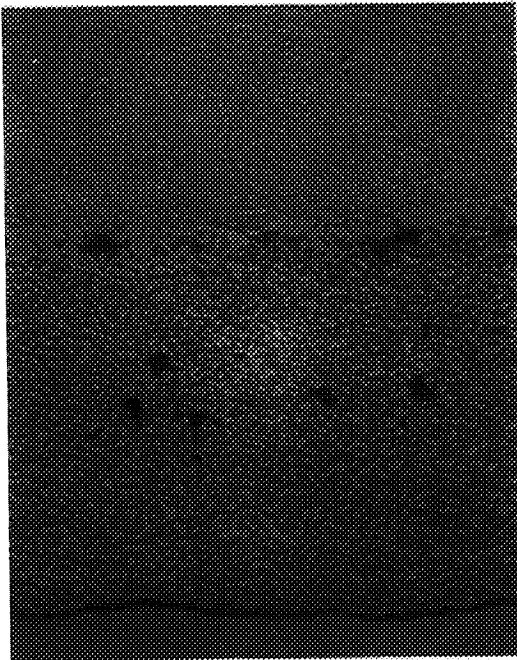
COCALY



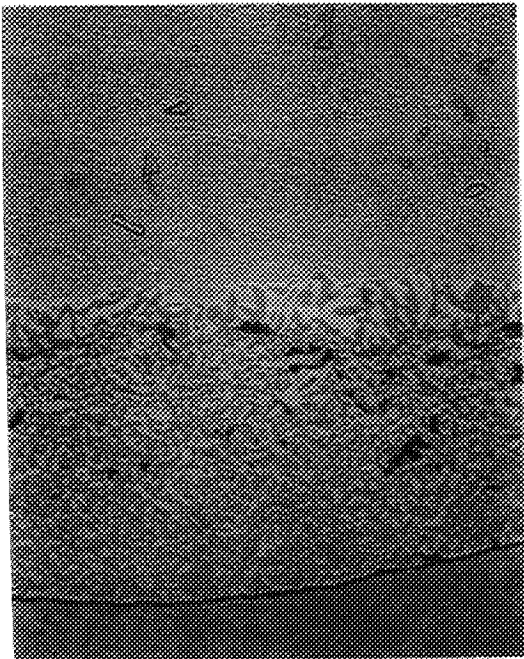
(a) 400 X



(b) 400 X



(c) 400 X



(d) 400 X

Figure 14

Comparison of Microstructures Show Low Pressure Chamber Sprayed Coatings (a and b) are Superior in Quality to One-Atmosphere Argon Chamber Sprayed Coatings (c and d)

to the one-atmosphere argon sprayed coatings, the low pressure chamber sprayed coatings were observed to be more dense (98.5% vs 97%) and displayed lesser amounts of oxide contamination. In view of this, it was decided that all compositional and process modifications to both NiCoCrAlY and CoCrAlY coatings (Hf, Ta, Si additions and post-coating hot isostatic pressed processes) be fabricated by using the low pressure chamber process for subsequent burner rig evaluation. However, argon chamber sprayed NiCoCrAlY and CoCrAlY coatings were considered to be of sufficiently good quality (< 3% porosity) to warrant inclusion in the subsequent burner rig testing. This allowed a comparison to be made with the low pressure chamber sprayed coatings of similar composition.

Microstructures of the low pressure chamber sprayed NiCoCrAlY coatings representing various post-coating process combinations are shown in Figure 15. These coatings were fabricated using the following three post-coating process conditions: (1) 1352<sup>o</sup>K (1975<sup>o</sup>F)/4 hrs + glass bead peening at 17N; (2) 1352<sup>o</sup>K (1975<sup>o</sup>F)/1 hr + glass bead peening (17N) + 1352<sup>o</sup>K (1975<sup>o</sup>F)/4 hrs; and (3) 1352<sup>o</sup>K (1975<sup>o</sup>F)/1 hr + glass bead peening (22N) + 1352<sup>o</sup>K (1975<sup>o</sup>F)/4 hrs. Examination of these specimens indicated that the coating (Figure 15c) given a high intensity glass bead peening (22N) contains the least amount of structural defects. A similar result was found for the CoCrAlY coatings. Therefore, this process and sequence was selected as the post-coating process for all plasma spray MCrAlY coatings to be subsequently evaluated.

Microstructures of the low pressure chamber sprayed NiCoCrAlY + Hf, NiCoCrAlY + Ta, NiCoCrAlY + Si, CoCrAlY + Si and CoCrAlY (high Cr, low Al) coatings were observed to be of good quality (< 2% porosity), and therefore these variations were selected for subsequent burner rig evaluation. The microstructure of the hot isostatically pressed CoCrAlY coating is shown in Figure 16. As expected, this coating was found to contain less porosity compared to CoCrAlY coatings which were not given this process step. However, due to the high temperature exposure for three hours, substantial interdiffusion of various elements between the coating and the alloy took place resulting in a significant loss of aluminum (beta phase depletion) from

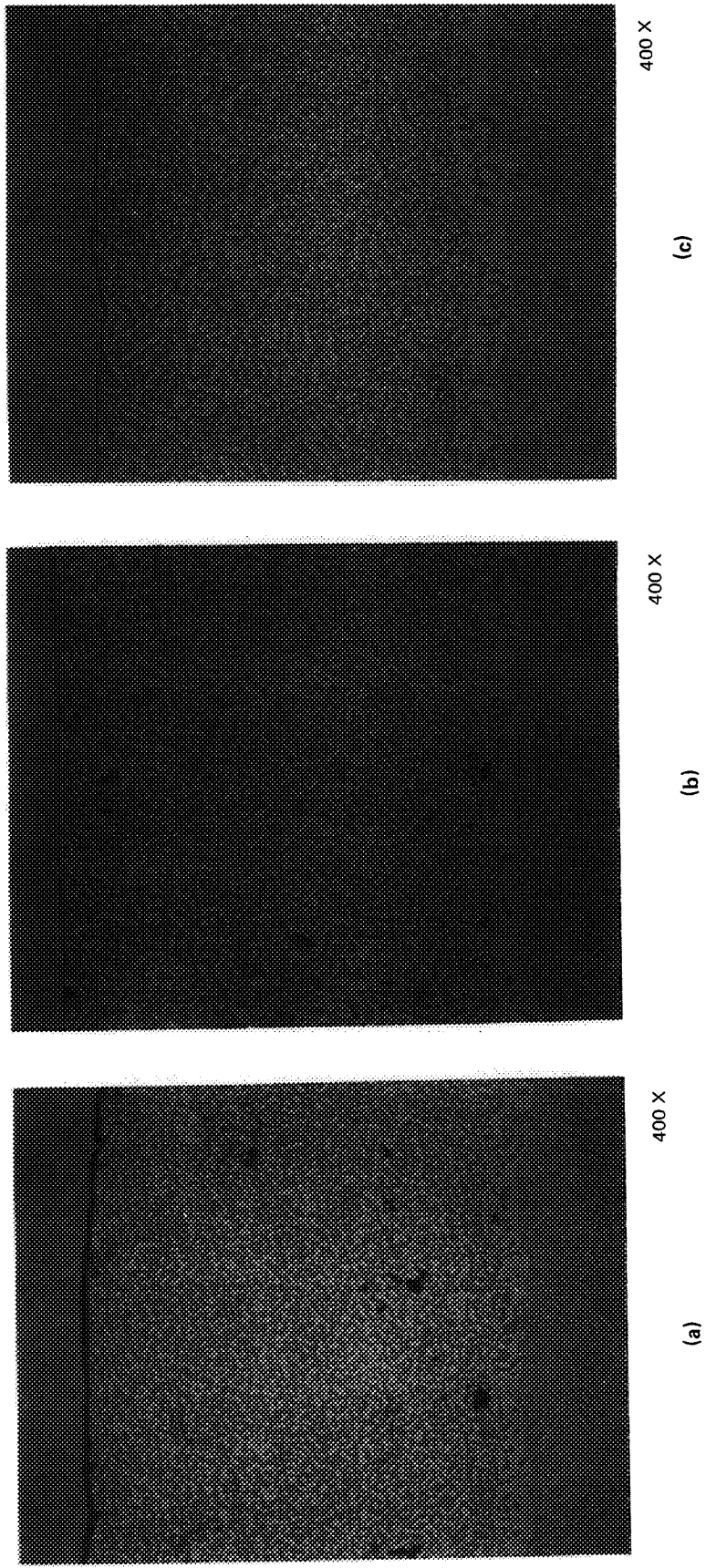


Figure 15 Microstructures of Low Pressure Chamber Sprayed NiCoCrAlY Coatings Fabricated Using (a) 13520K(19750F)/4 hrs + GBP (17N), (b) 13520K (19750F)/1 hr + GBP (17N) + 13520K(19750F)/4 hrs, and (c) 13520K (19750F)/1 hr + GBP (22N) + 13520K (19750F)/4 hrs. GBP = Glass Bead Peening



ORIGINAL PAGE  
BLACK AND WHITE PHOTOGRAPH



500X

ORIGINAL PAGE IS  
OF POOR QUALITY

Figure 16 Microstructure of Low Pressure Chamber Sprayed CoCrAlY+HIP Coating After Post-Coating Processing at 1352°K (1975°F)/1 hr + GBP (17N) + HIP (1470°K (2185°F)/3 hrs/103.4 MPa (15 Ksi)) + 1352°K (1975°F)/4 hrs. HIP = Hot Isostatic Pressing

the coating to the substrate alloy. This coating, however, was selected as one of the ten candidates because this was clearly an easy way to improve coating density at difficult-to-coat locations (e.g. fillets) on actual turbine airfoils.

The selected coating composition/process/alloy combinations which were subsequently burner rig tested in this task are provided in Table III. These coating variations were compared with the baseline vapor deposited NiCoCrAlY and CoCrAlY coatings on the single crystal and B1900 + Hf alloys.

#### 4.1.3 Pre-Test Microstructures of Burner Rig Specimens

Burner rig and ductility test specimens were coated with the ten selected candidate systems using powders procured from Alloy Metals Incorporated. The chemistries and particle size distribution of various powder materials are provided in Tables IV and V. As can be seen from Table IV the actual compositions of the powders were in good agreement to what was ordered. Likewise, the particle size distribution of most received powders fell within the target of 5 to 44 microns (Table V).

Pre-test microstructures of NiCoCrAlY coatings on single crystal alloy burner rig samples produced by vapor deposition and the two plasma spray processes are shown in Figure 17. As expected, these coatings were observed to be two phase alloys consisting of a CsCl type of (Ni,Co)Al intermetallic ( $\beta$ ) phase and a face-centered cubic Ni, Co solid solution ( $\gamma$ ) phase. Further, the vapor deposited NiCoCrAlY coating has a columnar structure in contrast to equiaxed microstructure exhibited by both types of plasma sprayed coatings. The argon plasma sprayed coatings also contained significant amounts of  $Al_2O_3/Y_2O_3$  oxides. Pre-test microstructural quality of the other selected NiCoCrAlY-type coating systems on the single crystal alloy are shown in the fully processed condition in Figure 18. NiCoCrAlY + Si and NiCoCrAlY + Hf microstructures were very similar to the baseline NiCoCrAlY structures except that the silicon addition appeared to have increased the amount of beta phase present in this coating. Electron microprobe x-ray images of these three

TABLE III

SELECTED COATING/PROCESS/ALLOY COMBINATIONS  
WHICH WERE BURNER RIG TESTED IN TASK I

<u>Alloy</u>	<u>Coating</u>	<u>Plasma Spray Process</u>
Single Crystal	Ni-23Co-18Cr-12.5Al-0.4Y	LPCS
Single Crystal	Ni-23Co-18Cr-12.5Al-0.4Y	APS
Single Crystal	Ni-23Co-18Cr-12.5Al-0.6Y-0.6Hf	LPCS
Single Crystal	Ni-23Co-18Cr-12.5Al-0.6Y-1.5Si	LPCS
Single Crystal	Ni-23Co-18Cr-12.5Al-0.6Y-8Ta	LPCS
B1900+Hf	Co-22Cr-12.5Al-0.6Y	LPCS
B1900+Hf	Co-22Cr-12.5Al-0.6Y	APS
B1900+Hf	Co-29Cr-10Al-0.6Y	LPCS
B1900+Hf	Co-22Cr-12.5Al-0.6Y-2.0Si	LPCS
B1900+Hf	Co-22Cr-12.5Al-0.6Y+HIP	LPCS

LPCS = Low Pressure Chamber Plasma Spray

APS = One Atmospheric Argon Plasma Spray

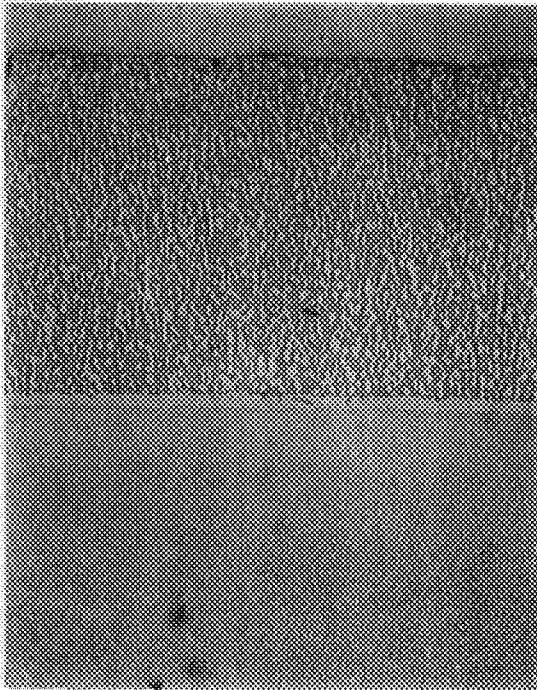
HIP = Hot Isostatic Pressing at 1470<sup>o</sup>K (2185<sup>o</sup>F) for 3 hours at a pressure of 103.4 MPa (15 ksi)

TABLE IV  
CHEMICAL COMPOSITIONS OF COATING VARIATIONS EVALUATED IN TASK I

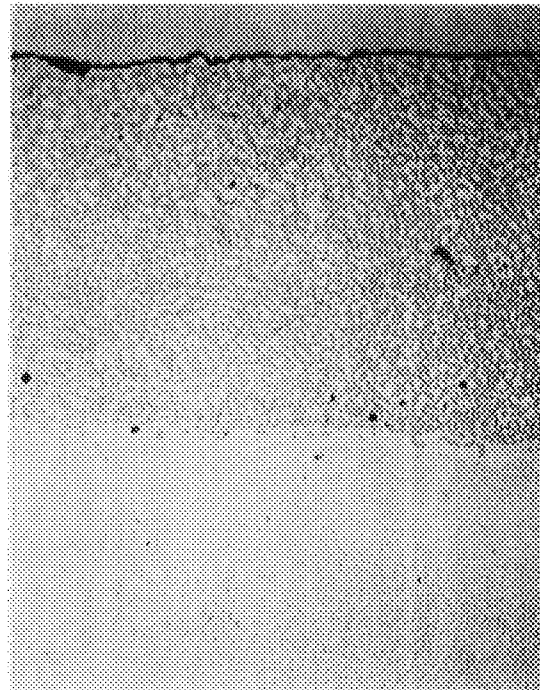
<u>Ordered Alloy</u>	AMI <u>Lot No.</u>	<u>Concentration in Weight Percent</u>							
		<u>Ni</u>	<u>Co</u>	<u>Cr</u>	<u>Al</u>	<u>Y</u>	<u>Hf</u>	<u>Si</u>	<u>Ta</u>
Ni-23Co-18Cr-12Al-0.4Y	10138	Bal.	23.4	17.9	12.6	0.44			
Ni-23Co-18Cr-12Al-0.6Y+0.6Hf	10141	Bal.	20.8	17.8	12.5	0.61	0.7		
Ni-23Co-18Cr-12Al-0.6Y+1.5Si	10265	Bal.	21.1	17.8	12.6	0.72		1.6	
Ni-23Co-18Cr-12Al-0.6Y+8Ta	10267	Bal.	20.9	17.8	12.6	0.56			8.5
Co-22Cr-12Al-0.6Y	10260	-	Bal.	20.1	12.7	0.72			
Co-29Cr-10Al-0.6Y	10258	-	Bal.	29.0	10.8	0.65			
Co-22Cr-12Al-0.6Y+2Si	10262	-	Bal.	21.3	12.6	0.81		2.0	

TABLE V  
PARTICLE SIZE DISTRIBUTION OF VARIOUS POWDER MATERIALS  
EVALUATED IN TASK I

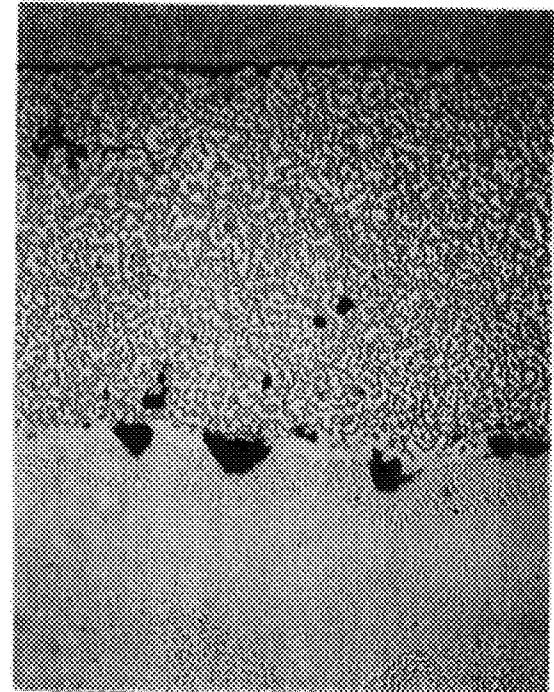
<u>Alloy</u>	<u>Lot No.</u>	<u>Particle Size Weight Percent of Powder in Given Range (Microns )</u>						<u>Mean Particle Size</u>
		<u>0-5</u>	<u>5-10</u>	<u>10-20</u>	<u>20-40</u>	<u>40-44</u>	<u>44-62</u>	
NiCoCrAlY	10138	2.2	7.1	20.7	56.6	5.5	7.9	25.8
NiCoCrAlY+Hf	10141	2.0	7.8	20.7	56.2	6.2	7.0	26.1
NiCoCrAlY+Si	10265	0.2	2.0	11.6	68.7	7.0	10.5	29.6
NiCoCrAlY+Ta	10267	1.0	4.8	14.2	63.0	7.0	10.0	29.4
CoCrAlY	10260	1.0	5.0	18.5	60.0	7.0	7.5	27.7
CoCrAlY	10258	5.5	17.0	38.5	35.4	1.5	2.1	16.5
CoCrAlY+Si	10262	0.5	1.7	15.7	65.0	8.4	8.7	28.3



NiCoCrAlY  
Electron-Beam Physical  
Vapor Deposited  
400X

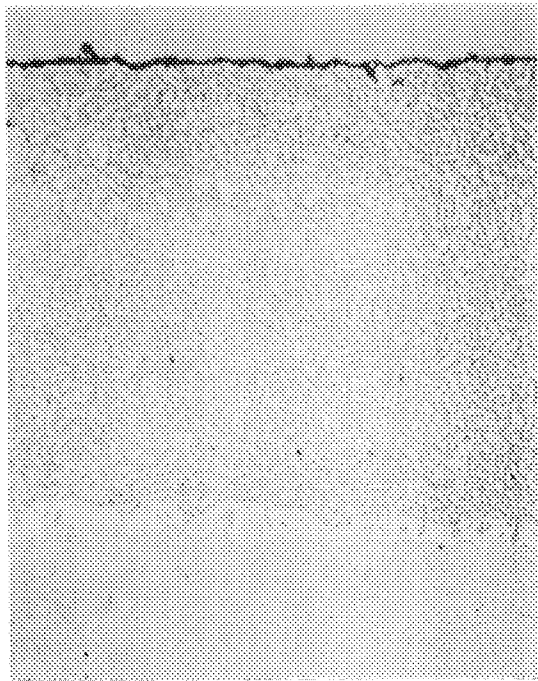


NiCoCrAlY  
Low Pressure Chamber Sprayed  
400X



NiCoCrAlY  
Atmospheric Argon  
Chamber Sprayed  
400X

Figure 17 Pre-Test Microstructures of NiCoCrAlY Coatings Made by  
Electron-Beam Physical Vapor Deposition, Low Pressure Chamber  
Plasma Spraying, and One Atmosphere Argon Chamber Spraying



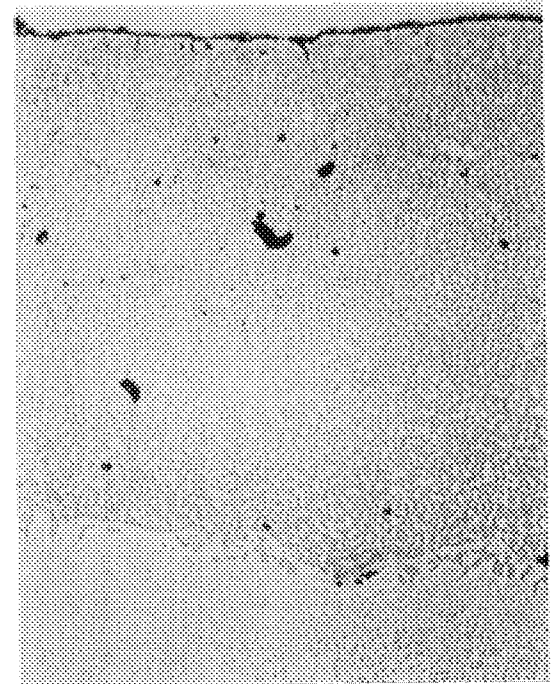
NiCoCrAlY + Hf

400X



NiCoCrAlY + Si

400X



NiCoCrAlY + Ta

400X

Figure 18

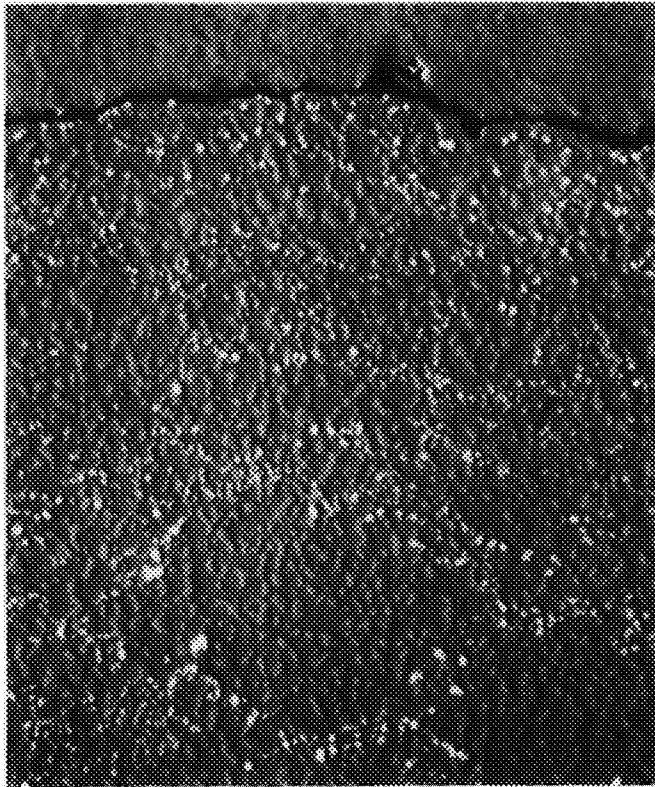
Pre-Test Microstructures of Low Pressure Chamber Sprayed NiCoCrAlY-Type Coatings with Modified Compositions

modified NiCoCrAlY coating systems indicated that only the NiCoCrAlY + Ta system exhibited phases other than gamma and beta (Figure 19). This phase was found to consist mainly of tantalum and nickel. About equal amounts of these elements by weight were present in this phase and, it may therefore be an  $Ni_3Ta$  type  $\gamma'$  phase. Like silicon, the addition of tantalum also increased the amount of beta phase present in the NiCoCrAlY microstructure.

Figures 20 and 21 illustrate the pre-test microstructures of CoCrAlY-type coatings on the B1900 + Hf alloy samples in the fully processed condition. As observed in the case of NiCoCrAlY coatings, the one-atmosphere argon chamber sprayed CoCrAlY coating was slightly less dense compared to the low pressure chamber sprayed CoCrAlY coating (Figure 20). It appeared that the silicon addition to CoCrAlY resulted in slightly increased porosity whereas, as indicated before, post-coating hot isostatic pressing of CoCrAlY coated samples reduced the defects considerably, resulting in almost a totally dense coating. Also observed in the low pressure chamber sprayed CoCrAlY + Si microstructure was an unusually large amount of beta (CoAl) phase in the outer layer of the coating (Figure 21). The CoCrAlY + Si powder which was used to deposit this coating contained a nominal 12.6 weight percent aluminum. Such an aluminum level does not normally result in a continuous beta phase formation in the coating outer layer. Electron microprobe concentration profile traces (Figure 22) for aluminum and silicon indicated the presence of a slight concentration gradient in the beta-rich outer portion of the coating with greater amount of the silicon in the coating being found in this region. Since silicon stabilizes the beta phase, the larger concentration of this element in the outer layer is likely responsible for the observed condition. This structural modification in CoCrAlY + Si system apparently occurs during post coating heat treatment ( $1352^{\circ}K$  ( $1975^{\circ}F$ )/4 hours/ $H_2$ ). It is not clear why silicon segregates in this manner.

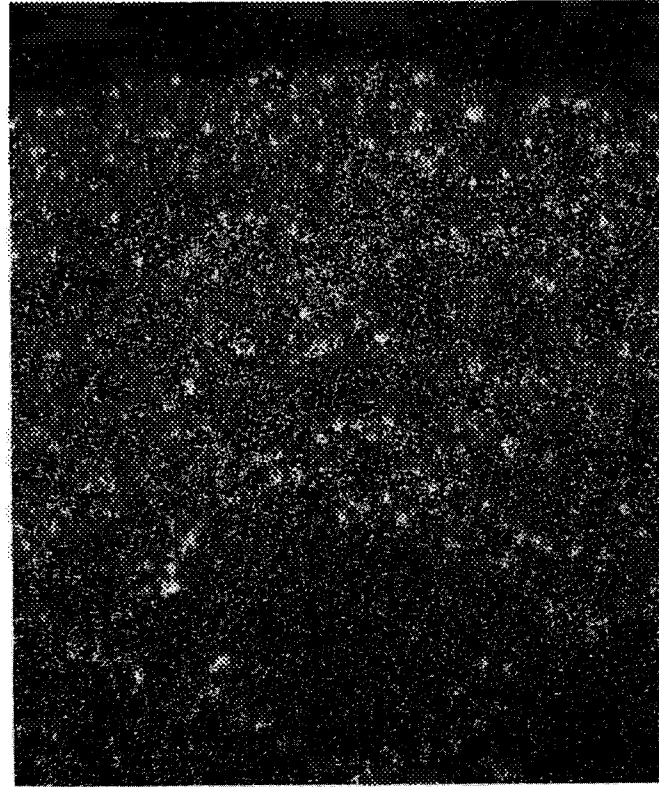
#### 4.1.4 Burner Rig Oxidation Tests

The ten aforementioned plasma sprayed NiCoCrAlY and CoCrAlY based coatings, and the baseline vapor deposited NiCoCrAlY and CoCrAlY systems, were exposed



1000X

BACK SCATTER ELECTRON IMAGE



1000X

Ta X-RAY IMAGE

ORIGINAL PAGE  
BLACK AND WHITE PHOTOGRAPH

Figure 19 Scanning Electron Micrographs of Low Pressure Chamber Sprayed NiCoCrAlY + Ta Coating in the As-Processed Condition Illustrating Presence of a Tantalum Containing Phase in the Coating Microstructure.



ORIGINAL PAGE  
BLACK AND WHITE PHOTOGRAPH

400X  
CoCrAlY  
Atmospheric Argon  
Chamber Sprayed



400X  
CoCrAlY  
Low Pressure Chamber Sprayed



400X  
CoCrAlY  
Electron-Beam Physical  
Vapor Deposited

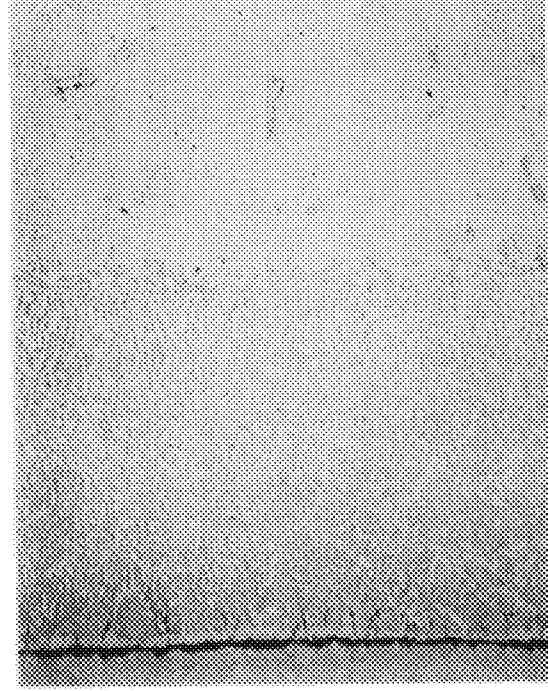
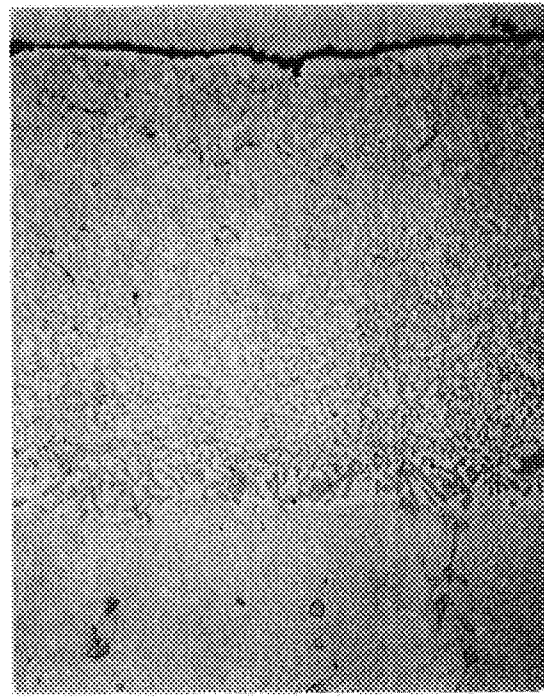


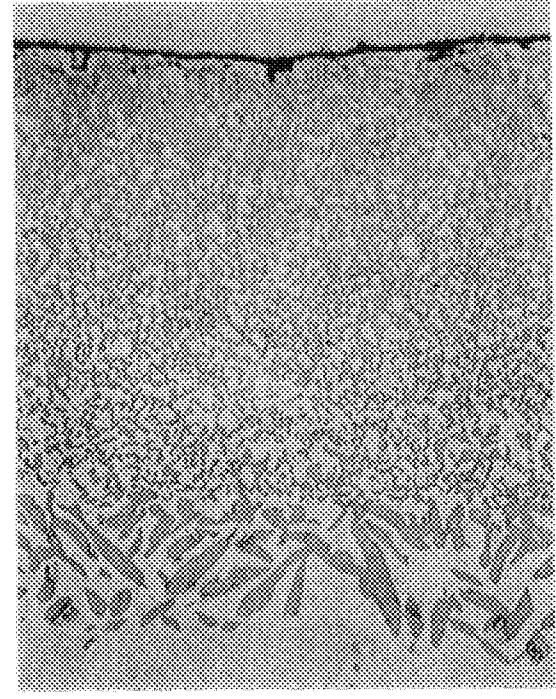
Figure 20  
Pre-Test Microstructures of CoCrAlY Coatings Made by Various  
Processes



CoCrAlY + Si 400X



CoCrAlY (High Cr, Low Al) 400X



CoCrAlY + HIP 400X

Figure 21

Pre-Test Microstructures of Low Pressure Chamber Sprayed  
CoCrAlY-Type Coatings With Modified Composition/Processes.  
HIP = Hot Isostatic Pressing

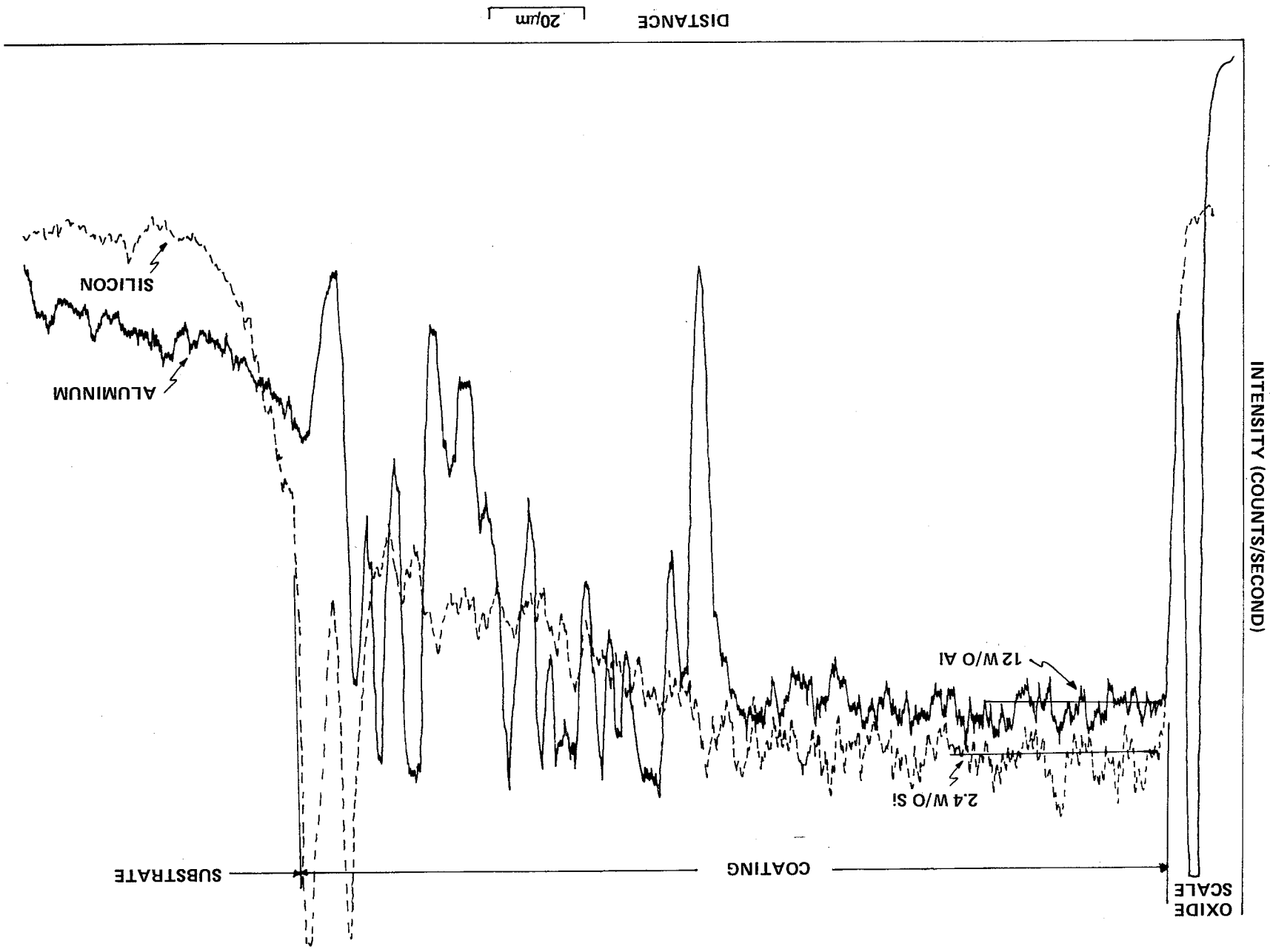


Figure 22 Relative Aluminum and Silicon X-Ray Intensities for Low Pressure Chamber Sprayed CoCrAlY+Si Coating on B1900+Hf Alloy in the Fully Processed Condition.

to a 1394<sup>0</sup>K (2050<sup>0</sup>F) cyclic burner rig test. As described previously, the one hour test cycle was 55 minutes at 1394<sup>0</sup>K (2050<sup>0</sup>F) followed by five minutes of forced air cooling. Visual observations were used to ascertain the degree of coating degradation during testing. The times required for initial localized oxidation to the coating-substrate interface and for failure over 50 percent of the test section were normalized to account for variations in coating thickness from specimen to specimen. The failure time was divided by the coating thickness in microns for the particular specimen (measured metallographically on a section taken from the specimen tip prior to testing) and then multiplied by 127 to give a normalized life for a 127 micron (5 mils) thick coating. This 127 micron value was selected because it represents typical overlay coating thickness on many engine components.

a. NiCoCrAlY-Coated Single Crystal Test Results and Post-Test Microstructural Examination

Tables VI and VII summarize the visual condition of the coated single crystal test samples after 350 and 1000 hours of exposure in the cyclic oxidation test. Throughout the course of this test, the least oxide scale spalling among all of the NiCoCrAlY - type coatings was exhibited by the low pressure chamber sprayed NiCoCrAlY + Si and the NiCoCrAlY + Hf coatings.

Examination of the microstructures of the NiCoCrAlY-type coatings after 350 hours of exposure revealed that low pressure chamber sprayed NiCoCrAlY, NiCoCrAlY + Hf, one atmosphere argon chamber sprayed NiCoCrAlY and the baseline vapor deposited NiCoCrAlY coatings retained only small quantities of the beta phase, whereas the low pressure chamber sprayed NiCoCrAlY + Si and NiCoCrAlY + Ta coatings contained significantly greater amounts of this protective phase (Figures 23 and 24)\* (the increased amount of beta phase remaining in a coating qualitatively indicates a larger remaining reservoir of aluminum, which in turn generally results in superior coating performance).

---

\*The silicon and tantalum additions to NiCoCrAlY increase the amount of beta present in the as processed coating; however, this cannot totally account for the observed behavior.

TABLE VI

VISUAL CONDITIONS OF COATED SINGLE CRYSTAL SAMPLES AFTER 350 HOURS OF EXPOSURE IN THE BURNER RIG OXIDATION TEST AT 1394° (2050°F)

<u>Coating Type</u>	<u>Coating Process*</u>	<u>Coating Thickness (Microns)</u>	<u>Visual Condition</u>
NiCoCrAlY	EB-PVD	100	Moderate Spalling of Oxide Scale
	APS	108	Heavy Spalling of Oxide Scale
	LPCS	125	Light to Moderate Spalling of Oxide Scale
NiCoCrAlY+Hf	LPCS	120	Very Light Spalling of Oxide Scale
NiCoCrAlY+Si	LPCS	142	Light Spalling of Oxide Scale
NiCoCrAlY+Ta	LPCS	152	Light to Moderate Spalling of Oxide Scale

\*EB-PVD - Electron Beam Physical Vapor Deposition

APS - One Atmosphere Argon Plasma Spray

LPCS - Low Pressure Chamber Plasma Spray

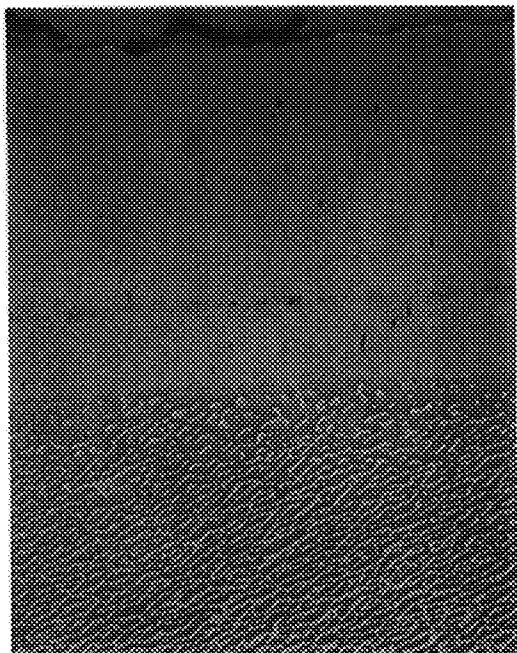
TABLE VII

VISUAL CONDITIONS OF COATED SINGLE CRYSTAL SAMPLES AFTER 1000 HOURS  
TEST TIME IN THE BURNER RIG OXIDATION TEST AT 1394°K (2050°F)

<u>Coating Type</u>	<u>Coating Process*</u>	<u>Coating Thickness (Microns)</u>	<u>Exposure Time (Hours)</u>	<u>Normalized Coating Life (Hours)**</u>	<u>Normalized Time to 1st Coating Penetration</u>	<u>Visual Condition</u>
NiCoCrAlY	EB-PVD	112	655	722	605	Failed
	APS	128	636	635	550	Failed
	LPCS	118	1000	>1064	965	Near Failure
NiCoCrAlY+Hf	LPCS	132	1000	> 943	-	Moderate oxide scale spalling; Light blue spinel at sample edges, no coating penetration.
NiCoCrAlY+Si	LPCS	145	1000	> 876	-	Moderate oxide scale spalling; No blue spinel or coating penetration.
NiCoCrAlY+Ta	LPCS	155	1000	> 820	-	Heavy oxide scale spalling; no blue spinel or coating.

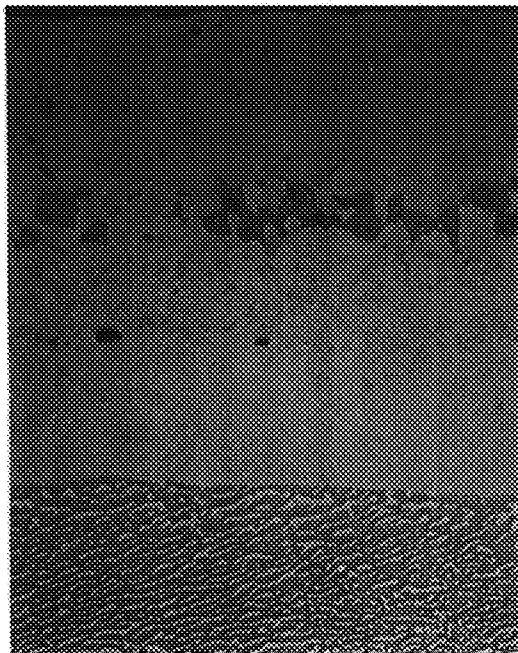
\*EB-PVD - Electron Beam Physical Vapor Deposition; APS - One Atmosphere Argon Plasma Spray; LPCS - Low Pressure Chamber Plasma Spray

\*\*Normalized Coating Life - Coating Life Normalized to "Use" Thickness of 127 Microns



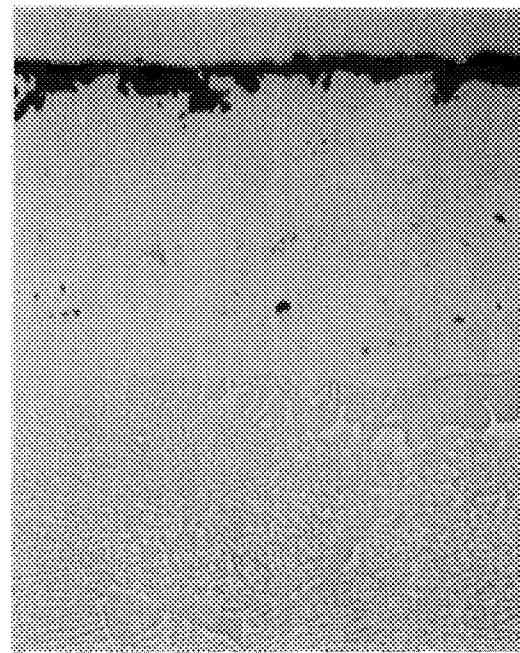
400X

NiCoCrAlY  
Electron-Beam Physical  
Vapor Deposited



400X

NiCoCrAlY  
Low Pressure Chamber Sprayed



400X

NiCoCrAlY  
Atmospheric Argon  
Chamber Sprayed

Figure 23

Post-Test Microstructures of the Test Section of NiCoCrAlY-Type Coatings On the Single Crystal Alloy After 350 hours of Exposure In An Oxidative Environment At 1394<sup>o</sup>K (2050<sup>o</sup>F)

ORIGINAL PAGE  
BLACK AND WHITE PHOTOGRAPH

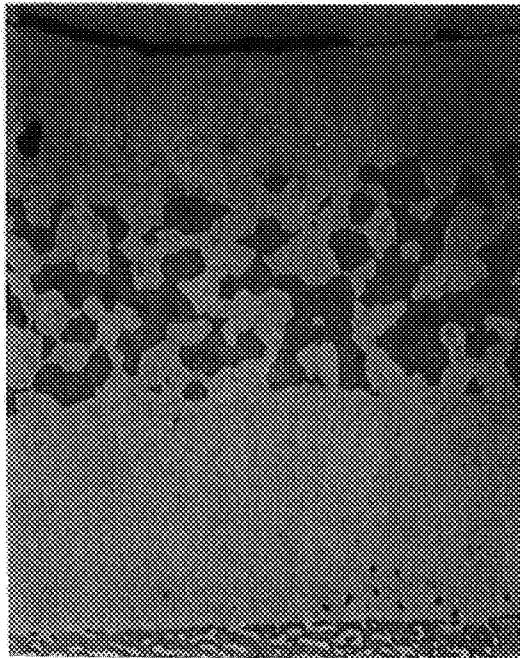
A similar evaluation on samples removed after 650 hours of oxidation testing showed that all coating systems were depleted of the protective beta phase. At about this time, the baseline vapor deposited and the atmospheric argon sprayed NiCoCrAlY coatings exhibited the initial signs of failure with localized oxidation to the coating-substrate interface (Table VII).

The appearance of the low pressure chamber sprayed single crystal samples exposed for 1000 hours of burner rig oxidation testing is presented in Figure 25. This figure also illustrates the surface condition of the baseline vapor deposited NiCoCrAlY coating which failed after 655 hours and the atmospheric argon sprayed NiCoCrAlY which failed after 635 hours. The baseline vapor deposited NiCoCrAlY coating which failed after a total of 655 hours of exposure gave a normalized coating life (performance normalized for 127 microns of typical 'use' thickness) of 722 hours. In comparison the one atmosphere argon plasma sprayed NiCoCrAlY/single crystal sample exhibited a normalized life of 635 hours and the low pressure chamber sprayed NiCoCrAlY sample, although showing considerable degradation (near failure) had endured 1000 hours of exposure in this test. The performance of the atmospheric argon sprayed NiCoCrAlY coating was consistent with previous results observed in other Pratt & Whitney Aircraft programs. It is believed that the lower life of this type of plasma sprayed coating is related to its lower density (less than 97 percent) and higher amount of oxide contamination.

The vapor deposited coating exhibited a normalized life (722 hours) estimated to be at the low end of the scatterband of oxidation data for similarly coated single crystals obtained in other Pratt & Whitney Aircraft programs. The low pressure chamber sprayed NiCoCrAlY coating exhibited durability (more than 1000 hours) slightly greater than the average vapor deposited NiCoCrAlY life on the single crystal alloy.

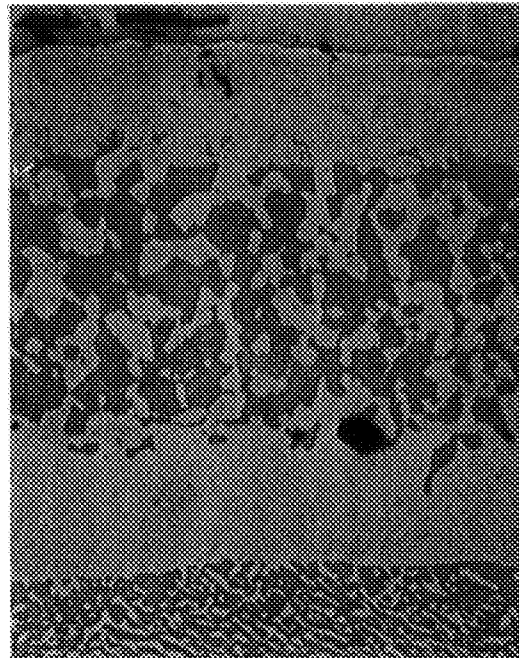
It was consistently observed throughout the 1394<sup>0</sup>K (2050<sup>0</sup>F) cyclic burner rig test that the extent of spalling of the protective aluminum oxide scales on both the vapor deposited and the low pressure chamber sprayed NiCoCrAlY





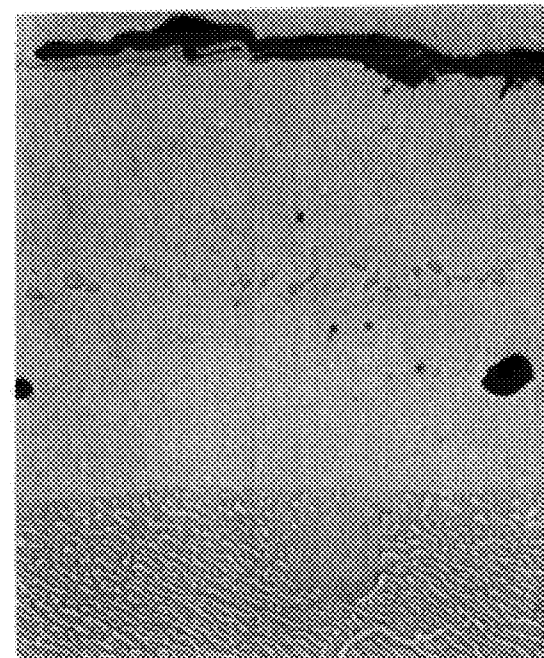
400X

NiCoCrAlY + Si  
Low Pressure Chamber Sprayed



400X

NiCoCrAlY + Ta  
Low Pressure Chamber Sprayed

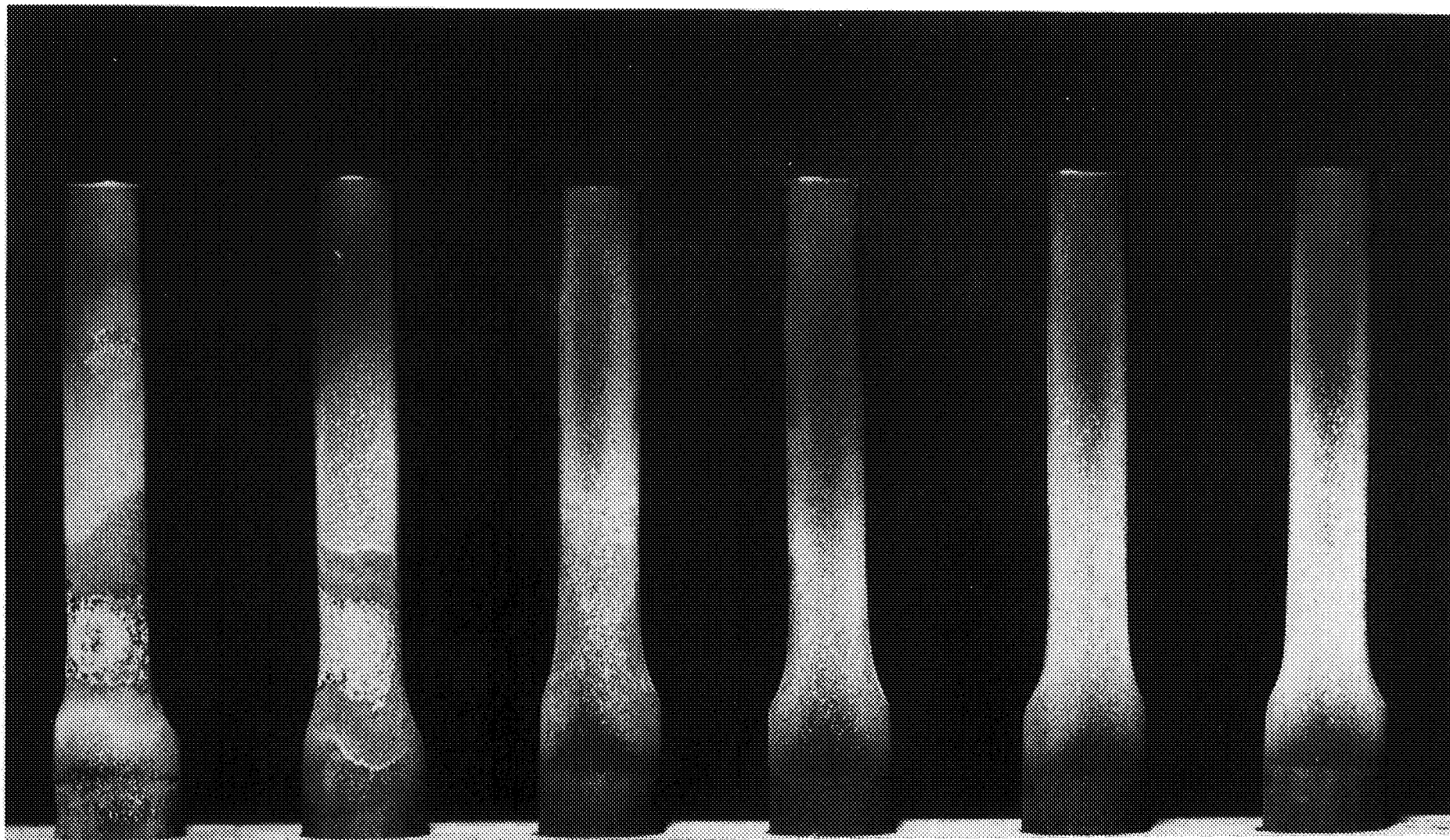


400X

NiCoCrAlY + Hf  
Low Pressure Chamber Sprayed

Figure 24 Post-Test Microstructures of the Test Section of NiCoCrAlY-Type Coatings On the Single Crystal Alloy After 350 hours of Exposure In An Oxidative Environment At 1394°K (2050°F)

ORIGINAL PAGE  
BLACK AND WHITE PHOTOGRAPH



NiCoCrAlY  
(EB-PVD)  
655 hrs  
(Failed)

NiCoCrAlY  
(APS)  
636 hrs  
(Failed)

NiCoCrAlY  
(LPCS)  
1000 hrs

NiCoCrAlY + Hf  
(LPCS)  
1000 hrs

NiCoCrAlY + Si  
(LPCS)  
1000 hrs

NiCoCrAlY + Ta  
(LPCS)  
1000 hrs

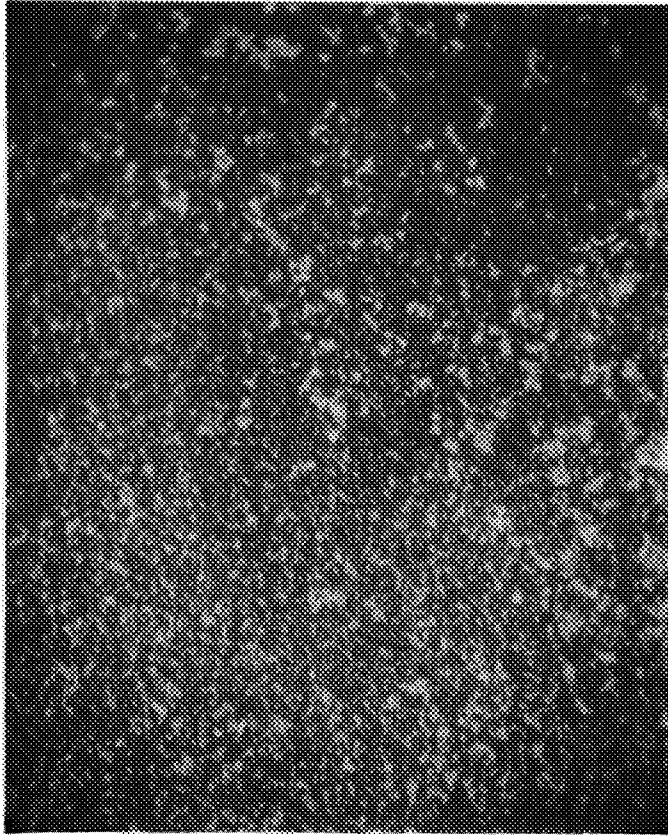
Figure 25

Surface Condition of Test Bars With NiCoCrAlY-Type Coatings on the Single Crystal Alloy, Exposed in Cyclic Burner Rig Oxidation Test at 1394°K (2050°F). EB-PVD = Electron-Beam Physical Vapor Deposited  
APS = Atmospheric Argon Chamber Sprayed; LPCS = Low Pressure Chamber Sprayed

coatings was quite similar. Evidence of this behavior is provided in Figure 26. During the early stages of testing (20 to 80 hours of exposure), oxide scale spalling was slightly more evident on the vapor deposited coating. This, however, is believed to be due to the lesser amount of yttrium (0.21 vs 0.44 weight percent) possessed by the vapor deposited material. A furnace annealing study was also performed on the NiCoCrAlY coated single crystal coupons. It was found that tantalum from the base alloy diffused at a slightly faster rate in the low pressure chamber sprayed coating compared to its mobility in the vapor deposited coating (Figure 27). The increased amount of available tantalum in the low pressure chamber sprayed coating is believed to provide beneficial effects in oxidation resistance to this coating.

In summary, it appears that in this cyclic 1394<sup>0</sup>K (2050<sup>0</sup>F) burner rig oxidation test, the durability of the low pressure chamber sprayed NiCoCrAlY coating on the single crystal sample was slightly superior to that of the vapor deposited NiCoCrAlY coating because of: 1) the presence of a slightly higher amount of yttrium, and 2) a beneficial effect of tantalum, derived from the single crystal alloy, and that present to a slightly larger extent in the plasma sprayed coating. Regardless, it appears that the low pressure chamber sprayed process can produce coatings which are at least equivalent in oxidation resistance to those produced by the state-of-the-art method -- electron beam physical vapor deposition.

As indicated in Table VII, the three low pressure chamber sprayed NiCoCrAlY + X (where X stands for Si, Ta or Hf additions) coating modifications on the single crystal alloy successfully lasted for 1000 hours of exposure in the 1394<sup>0</sup>K (2050<sup>0</sup>F) burner rig oxidation test. During visual inspection of these coated specimens, the least amount of oxide scale spalling was exhibited by the NiCoCrAlY + Hf coated sample, followed by the NiCoCrAlY + Si sample. The most amount of spalling of the alumina scale was shown by the NiCoCrAlY + Ta coating system. This behavior is illustrated in Figure 28 where surface photographs of the NiCoCrAlY + Ta, NiCoCrAlY + Si and NiCoCrAlY + Hf coatings are compared after 198 hours of exposure.



(a)

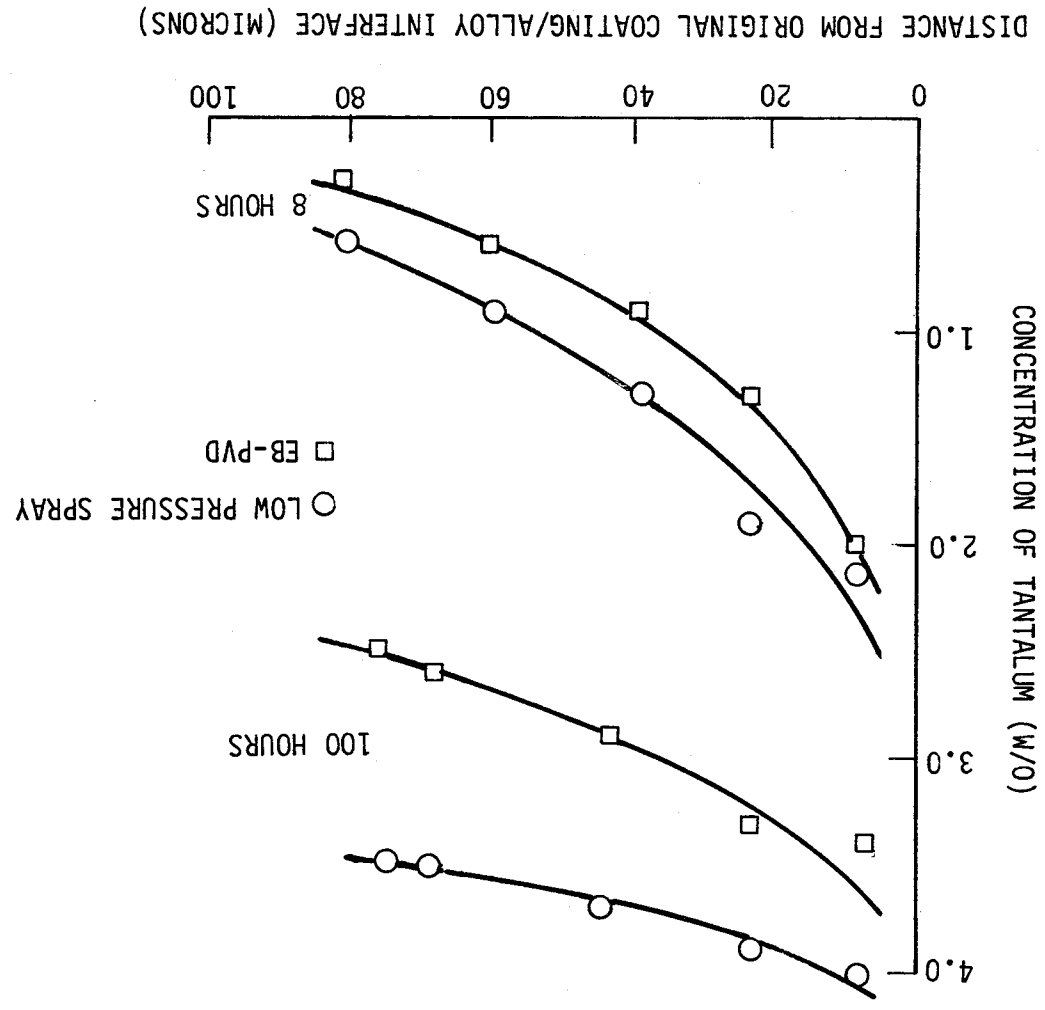


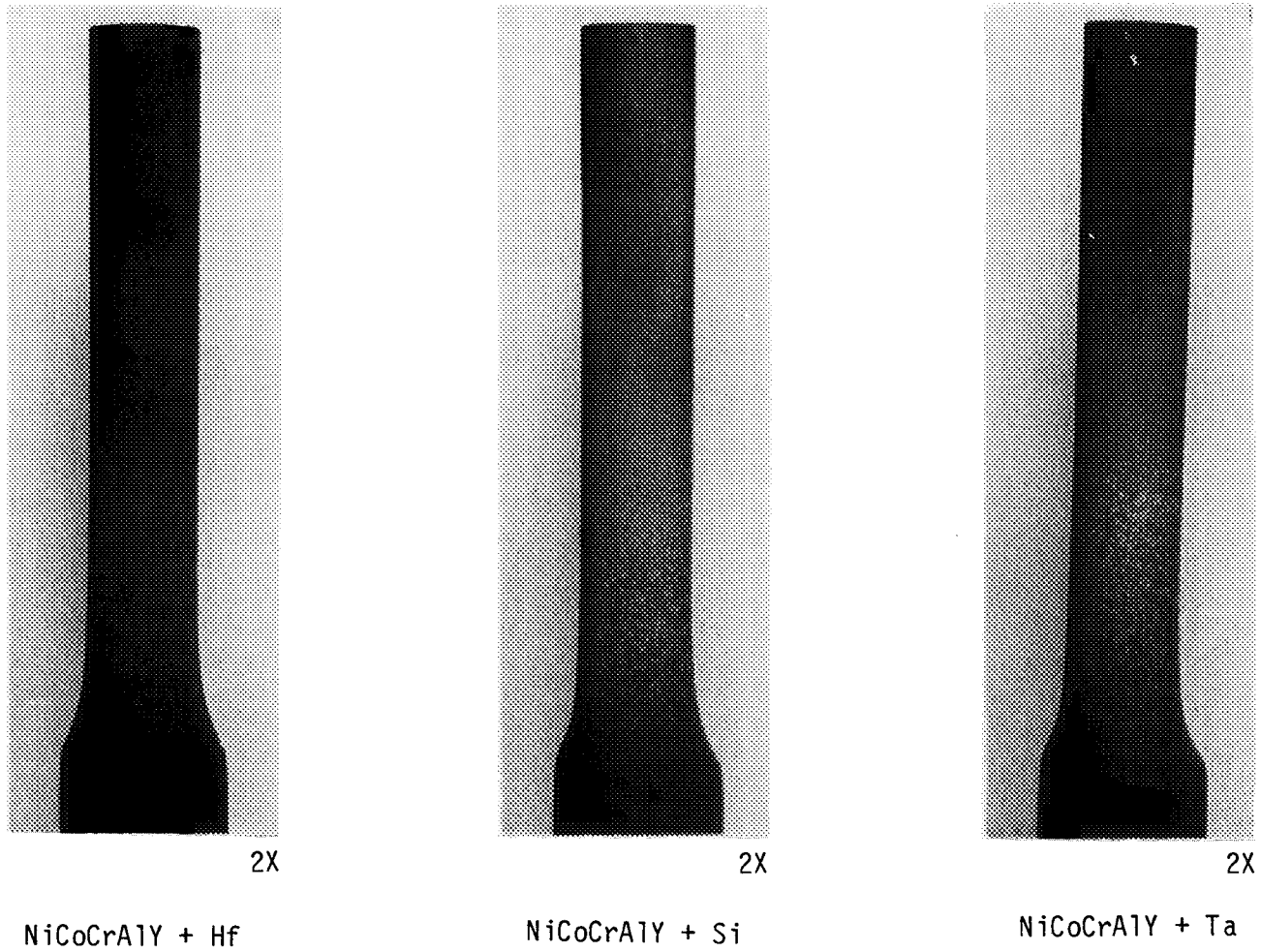
(b)

Figure 26 Surface Photographs (10X) of Burner Rig Test Samples After 100 Hours of Oxidation Testing at 1394°K (2050°F). (a) Vapor Deposited NiCoCrAlY on the Single Crystal Alloy; (b) Low Pressure Chamber Sprayed NiCoCrAlY on the Same Alloy. Note Essentially Similar Spalling of Al<sub>2</sub>O<sub>3</sub> on Both Systems.

ORIGINAL PAGE  
BLACK AND WHITE PHOTOGRAPH

Figure 27 Tantalum Diffusion from Single Crystal Alloy into NiCoCrAlY Coatings at 1422oK (2100oF)





ORIGINAL PAGE  
BLACK AND WHITE PHOTOGRAPH

Figure 28 Surface Photographs of Low Pressure Chamber Sprayed Single Crystals Exposed for 198 Hours In a Oxidative Environment at 1394<sup>o</sup>K (2050<sup>o</sup>F) In a Cyclic Burner Rig. Note the Least Oxide Scale Spalling Exhibited by Hafnium Modified NiCoCrAlY Coating Followed by Si and Ta Modified Coatings Respectively.

Hafnium is an active element and therefore it improves the oxide scale adherence capability of a coating through  $\text{HfO}_2$  "peg" formation underneath the alumina scale. In view of this the improved oxide scale adherence of the NiCoCrAlY + Hf coated system was not unexpected. However, this coating also showed an increased beta phase consumption rate compared to that exhibited by other plasma sprayed NiCoCrAlY-type systems (Figure 24; 350 hours post-test microstructures). This behavior has been previously observed in other programs. In these efforts (12), it was shown that during the oxidation process these  $\text{HfO}_2$  stringers ("pegs") underneath the alumina scale are partially incorporated into the  $\text{Al}_2\text{O}_3$  scale since the growth of the alumina takes place by inward diffusion of oxygen. The local regions of alumina scales modified in this manner allow increased transport of oxygen. This in turn results in increased formation of alumina around and underneath the partially consumed  $\text{HfO}_2$  stringers. Thus more aluminum is consumed in this process which translates into an increased rate of beta depletion. In view of this evidence, it was concluded that although hafnium additions to the NiCoCrAlY system considerably improved oxide scale adhesion capability, it failed to increase the oxidation resistance of the coating and, therefore, was not a candidate system for further optimization in Task II.

The exact mechanisms of how the additions of silicon or tantalum to NiCoCrAlY result in large increases in coating life over the basic NiCoCrAlY chemistry are not fully understood. However, it appears that silicon improves the NiCoCrAlY durability by improving oxide scale adhesion without increasing beta consumption rate as is the case with hafnium modified NiCoCrAlY. In fact, as can be seen in Figures 23 and 24, more beta is present in the NiCoCrAlY + Si coating compared to that present in both plasma sprayed and vapor deposited NiCoCrAlY materials. It is also believed that silicon may modify the outer oxide scale resulting in a reduced oxide growth rate (which in turn translates into lessened spalling and improved oxidation resistance). This behavior was qualitatively observed by examining furnace tested NiCoCrAlY and NiCoCrAlY + 1% Si alloys isothermally oxidized at  $1422^{\circ}\text{K}$  ( $2100^{\circ}\text{F}$ ). Figure 29 compares the microstructure of these two alloys after exposure for the indicated time intervals; the silicon modified alloy exhibited a thinner and more adherent oxide scale compared to unmodified NiCoCrAlY material.



ORIGINAL PAGE  
BLACK AND WHITE PHOTOGRAPH

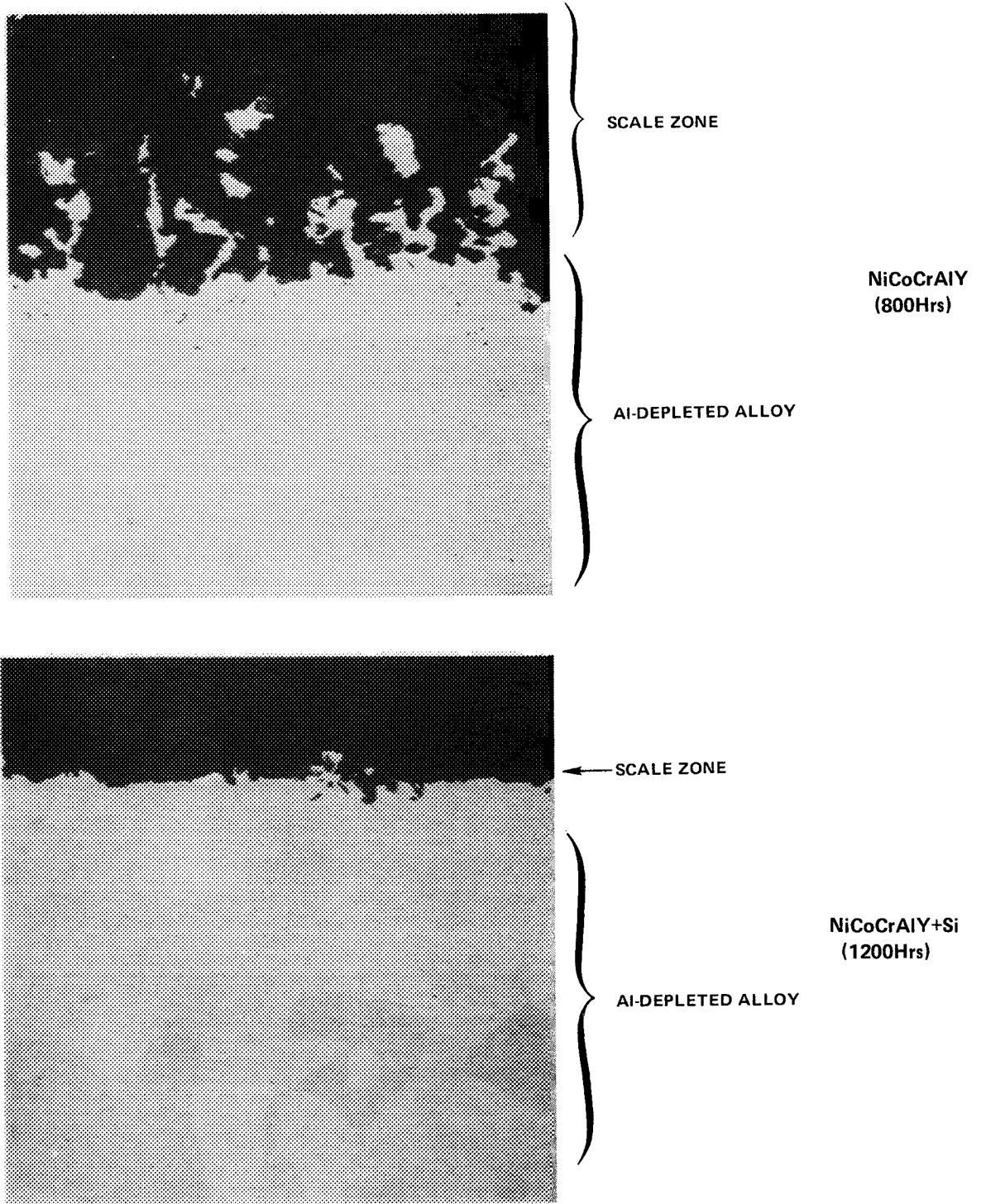


Figure 29 Photomicrographs (200X) of NiCoCrAlY and NiCoCrAlY + 1% Si After Oxidation at 1422<sup>o</sup>K (2100<sup>o</sup>F). Much more severe Degradation of the non-silicon alloy has occurred (note shorter time)

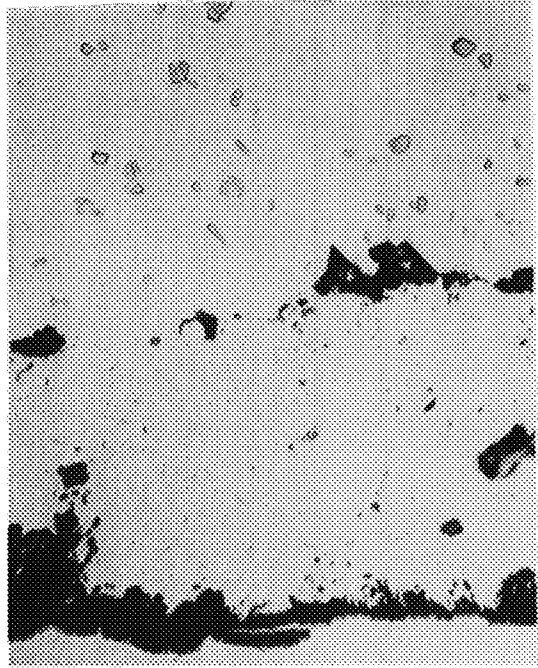


The reason for the beneficial effects of tantalum on NiCoCrAlY oxidation life, as illustrated in Figure 24 where this coating contains the most amount of beta phase, may be related to the reformation of relatively thin but protective alumina scales during thermal cycling. This behavior which is expected to reduce aluminum consumption was observed during early stages of testing of NiCoCrAlY + Ta coating on the single crystal alloy samples. Tantalum most probably causes this effect by reducing the transient oxidation time thereby accelerating the process of alumina formation.

b. CoCrAlY Coated B1900 + Hf Test Results and Post-Test Microstructural Examination.

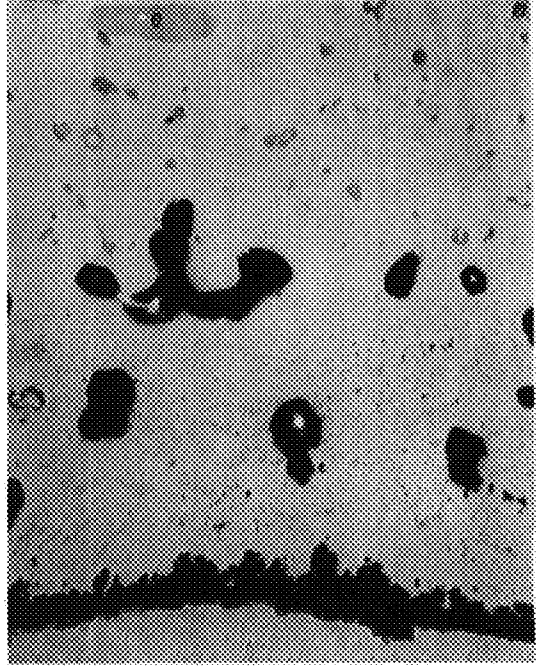
Throughout the cyclic oxidation testing all of the CoCrAlY based coatings on the B1900 + Hf alloy samples appeared less durable than the NiCoCrAlY type-coatings evaluated on the single crystal alloy specimens. The primary reason for these results was that the CoCrAlY-type coatings on the B1900 + Hf alloy exhibited small "pits" (localized coating distress) on their test surfaces (highest temperature zone of the sample) within 50 to 200 hours of exposure whereas, no such local degradation was observed on the NiCoCrAlY coated single crystal bars. It is presently believed that selective diffusion of some substrate element(s) is the primary cause of pit formation and therefore, this phenomenon is more dependent on the base alloy composition than on the coating characteristics. Further, it is also known that due to greater compositional difference cobalt-based coatings on nickel-base alloys exhibit accelerated coating-substrate interdiffusion compared to that shown by nickel-based coatings. Therefore coating degradation is expected to be faster with the former type of coatings.

Microstructural evaluation of the samples removed after 350 hours of burner rig oxidation testing revealed complete depletion of the beta phase in all CoCrAlY-type coatings (Figures 30 and 31) on the B1900 + Hf alloy, although the CoCrAlY+Si coating system exhibited significantly less surface degradation when visually examined during testing. Further, all CoCrAlY systems exhibited a varied degree of voids in the coating and/or at the coating-substrate



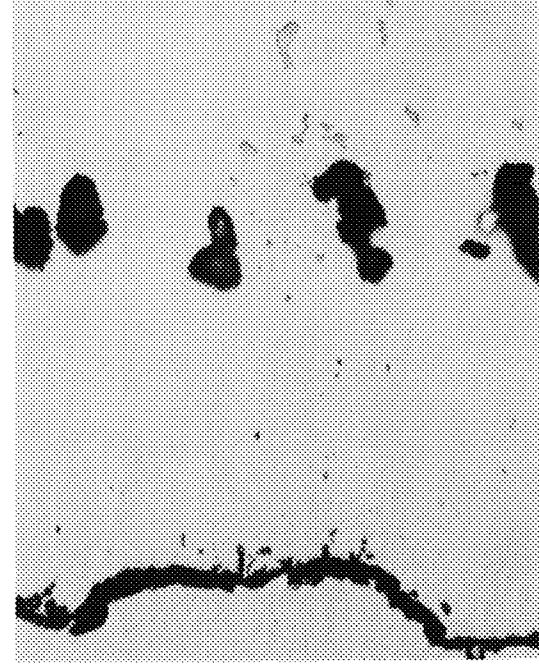
CoCrAlY  
Atmospheric Argon

400X



CoCrAlY  
Low Pressure Chamber Sprayed

400X



CoCrAlY  
Electron-Beam Physical  
Vapor Deposited

400X

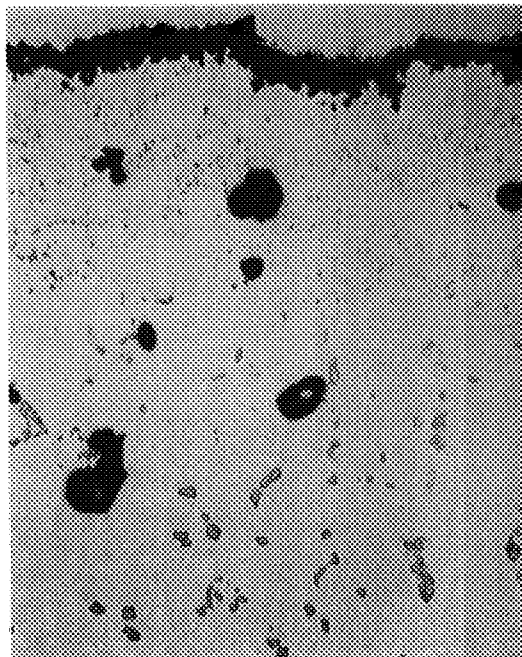
Post-Test Microstructures of the Test Section of CoCrAlY  
Coatings on B-1900+Hf Alloy After 350 hours of Exposure In An  
Oxidative Environment At 1394°K (2050°F)

Figure 30



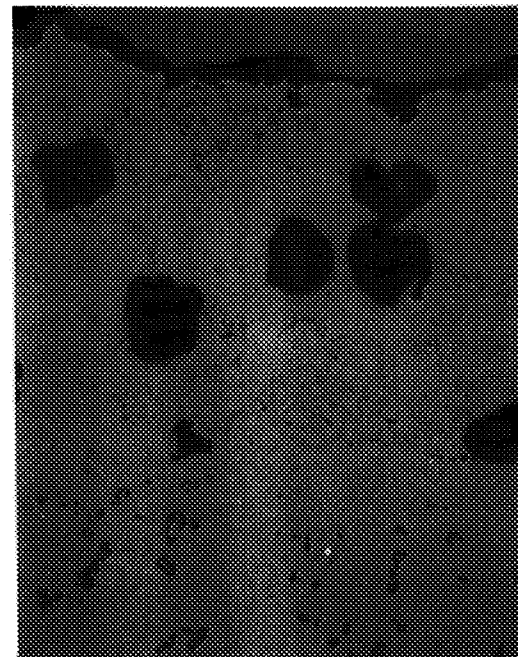
400X

CoCrAlY + Si



400X

CoCrAlY (High Cr, Low Al)



400X

CoCrAlY + HIP

ORIGINAL PAGE  
BLACK AND WHITE PHOTOGRAPH

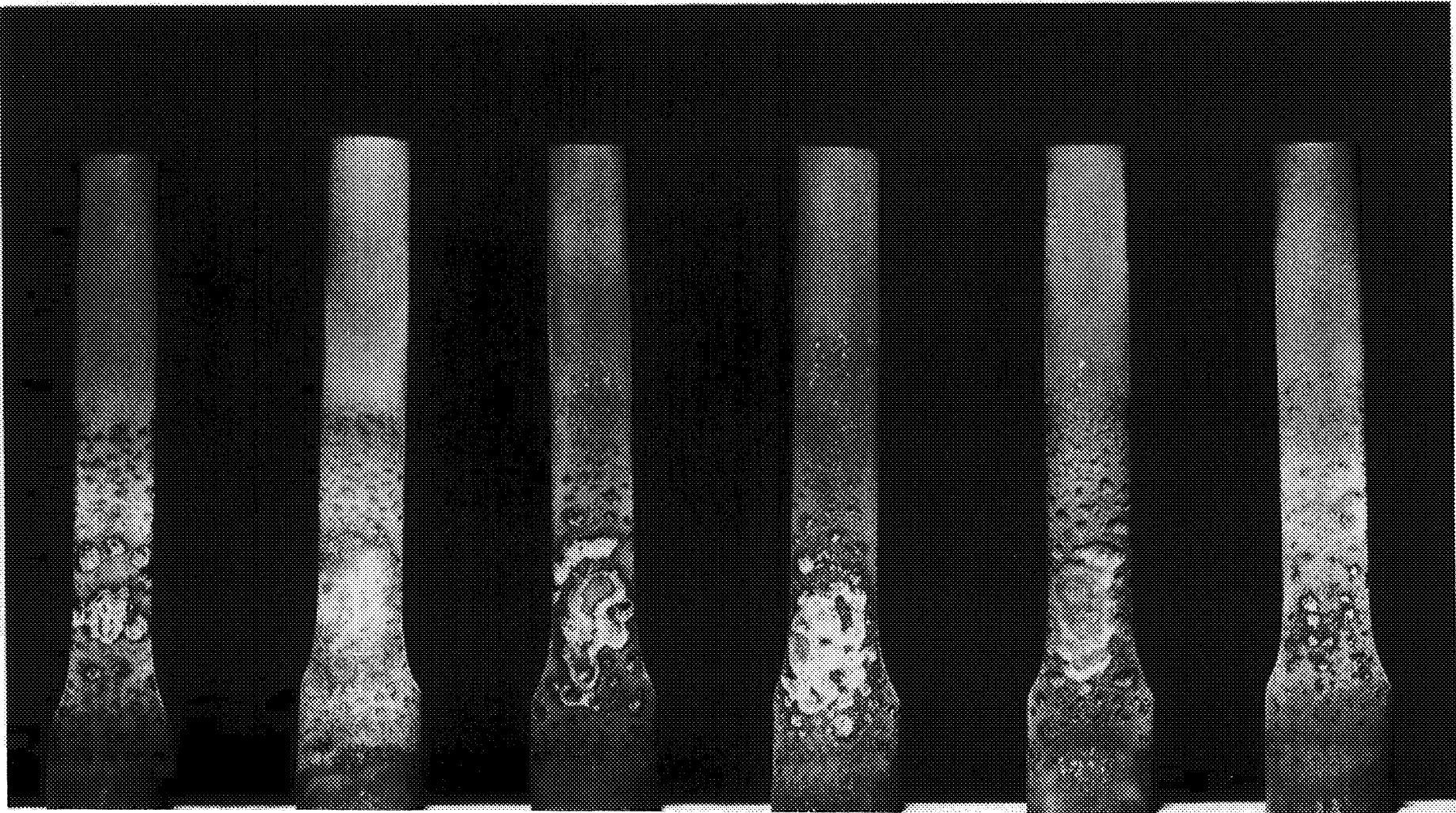
Figure 31 Post-Test Microstructures of the Test Section of Low Pressure Chamber Sprayed CoCrAlY-Type Coatings On B-1900+Hf Alloy After 350 hours of Exposure In An Oxidative Environment At 1394°K (2050°F)  
HIP = Hot Isostatic Pressing

ORIGINAL PAGE  
OF POCG 6041

interface. These voids are believed to be diffusion-induced porosity and have been previously observed in CoCrAlY-coated nickel base alloys. This behavior is not surprising because, as previously mentioned, a large amount of interdiffusion is expected between a cobalt based coating and a nickel base substrate.

The appearance of the CoCrAlY-based coatings after 1000 hours of testing is shown in Figure 32. Among the unmodified CoCrAlY coatings produced by the three processes, the baseline vapor deposited CoCrAlY coating exhibited the best performance. The one atmosphere argon sprayed material performed the poorest (Table IX). These were expected results in view of the observation that the vapor deposited system consistently showed greater oxide scale adherence compared to the two plasma spray CoCrAlY systems.

Among the modified CoCrAlY coatings produced by the low pressure chamber plasma spray process, the CoCrAlY + Si exhibited the least surface degradation (Figure 32) and its performance was superior to what was shown by the baseline vapor deposited CoCrAlY coating. This observation was based primarily on visual examination where the CoCrAlY + Si coating exhibited the least amount of pitting (Figure 32 and Tables VIII and IX). Further, the silicon-containing CoCrAlY showed oxide scale adherence capability similar to that of the vapor deposited CoCrAlY suggesting that the silicon addition in the plasma sprayed coating increased oxide scale adherence to the same degree possessed by the vapor deposited coating. The relatively lower rate of formation and growth of pits in the low pressure chamber sprayed CoCrAlY + Si coating may be due to the longer retention of the beta phase present in this coating compared to that in the baseline vapor deposited CoCrAlY (compare Figures 21(a) and 20(a)). Qualitatively, it is expected that a coating containing a larger amount of beta phase will experience less diffusion from the substrate (diffusion of substrate elements into a MCrAlY coating predominantly occurs through the gamma phase; beta being an intermetallic phase normally allows a very limited diffusion of elements other than nickel and aluminum through its structure) compared to the coating having a lesser quantity of this phase. Since pit formation and growth is a coating-substrate interdiffusion related



CoCrAlY  
(EB-PVD)  
1000 hrs

CoCrAlY  
(APS)  
391 hrs  
(Failed)

CoCrAlY  
(LPCS)  
991 hr  
(Failed)

CoCrAlY + HIP  
(LPCS)  
892 hrs  
(Failed)

CoCrAlY (High Cr)  
(LPCS)  
909 hrs  
(Failed)

CoCrAlY + Si  
(LPCS)  
1000 hrs

Figure 32

Surface Condition of Test Bars With CoCrAlY-Type Coatings on B1900+Hf Alloy, Exposed in Cyclic Burner Rig Oxidation Test at 1394<sup>o</sup>K (2050<sup>o</sup>F). EB-PVD = Electron-Beam Physical Vapor Deposited APS = Atmospheric Argon Chamber Sprayed; LPCS = Low Pressure Chamber Sprayed

TABLE VIII

VISUAL CONDITIONS OF COATED B1900+Hf SAMPLES AFTER 350 HOURS OF EXPOSURE IN THE BURNER RIG OXIDATION TEST AT 1394°K (2050°F)

<u>Coating Type</u>	<u>Coating Process*</u>	<u>Coating Thickness (Microns)</u>	<u>Visual Condition</u>
CoCrAlY	EB-PVD	118	Light to Moderate Pitting
	APS	112	Very Heavy Pitting
	LPCS	138	Moderate Pitting
CoCrAlY + HIP	LPCS	135	Heavy Pitting
CoCrAlY (High Cr, Low Al)	LPCS	128	Heavy Pitting
CoCrAlY+Si	LPCS	112	Very Light Pitting

TABLE IX

VISUAL CONDITIONS OF COATED B1900+Hf SAMPLES AFTER 1000 HOURS TEST TIME IN THE BURNER RIG OXIDATION TEST AT 1394°K (2050°F)

<u>Coating Type</u>	<u>Coating Process*</u>	<u>Coating Thickness (Microns)</u>	<u>Exposure Time (Hours)</u>	<u>Normalized Coating Life (Hours)**</u>	<u>Normalized Time to 1st Coating Penetration</u>	<u>Visual Condition</u>
CoCrAlY	EB-PVD	118	1000	>1064	113	Near Failure
	APS	102	391	477	56	Failed
	LPCS	138	991	901	78	Failed
CoCrAlY+HIP	LPCS	152	892	731	16	Failed
CoCrAlY (High Cr, Low Al)	LPCS	132	909	858	81	Failed
CoCrAlY+Si	LPCS	162	1000	> 769	186	No coating penetration. Very light pitting.

\*EB-PVD - Electron Beam Physical Vapor Deposition; APS - One Atmosphere Argon Plasma Spray; LPCS - Low Pressure Chamber Plasma Spray; HIP = Hot Isostatic Pressing

\*\*Normalized Coating Life - Coating Life Normalized to "Use" Thickness of 127 Microns

phenomenon, the coating with slower interdiffusion should exhibit a reduced "pitting" rate.

As indicated in Table IX, the hot isostatically pressed CoCrAlY and the higher chromium (29 vs 22 w/o) plus lower aluminum (10.5 vs 13 w/o) containing CoCrAlY systems exhibited slightly lower durability (normalized coating life) compared to that shown by the baseline vapor deposited and low pressure chamber sprayed CoCrAlY coatings. The inferior performance of these two coating systems in this 1394<sup>0</sup>K (2050<sup>0</sup>F) cyclic burner rig oxidation test is thought to have been due to the lower amount of aluminum present in the as-processed condition of these systems. Although the hot isostatically pressed CoCrAlY system was analysed to contain 12.6 w/o aluminum after low pressure chamber plasma spraying, this concentration was reduced significantly (to an estimate of about 11.0 weight percent based on beta phase fraction) after high temperature hot isostatic pressing at 1470<sup>0</sup>K (2185<sup>0</sup>F)/3 hours/103.4 MPa (15 Ksi). Apparently, interdiffusion of various elements (primarily outward diffusion of nickel and inward diffusion of aluminum between the coating and the substrate during the high temperature post-coating processing) was the cause of this beta phase reduction (compare Figures 21(c) and 20(b)). The lower aluminum concentration in the high chromium containing CoCrAlY system was intentional and is explained previously. This candidate was included in Task I screening specifically for improving hot corrosion performance.

#### 4.1.5 Burner Rig Hot Corrosion Test Results

Burner rig cyclic hot corrosion testing at 1172<sup>0</sup>K (1650<sup>0</sup>F) was conducted on the ten experimental plasma spray coating systems and two vapor deposited MCrAlY baselines, in the test cycle described previously. After 500 hours of exposure, most of the coating systems showed slight to moderate surface degradation. Only one sample (the one atmosphere argon plasma sprayed CoCrAlY coating on B1900 + Hf) failed in this test. The surface conditions of various coatings after 500 hours are illustrated in Figures 33 and 34 and the visual observations associated with these test samples are summarized in Table X.

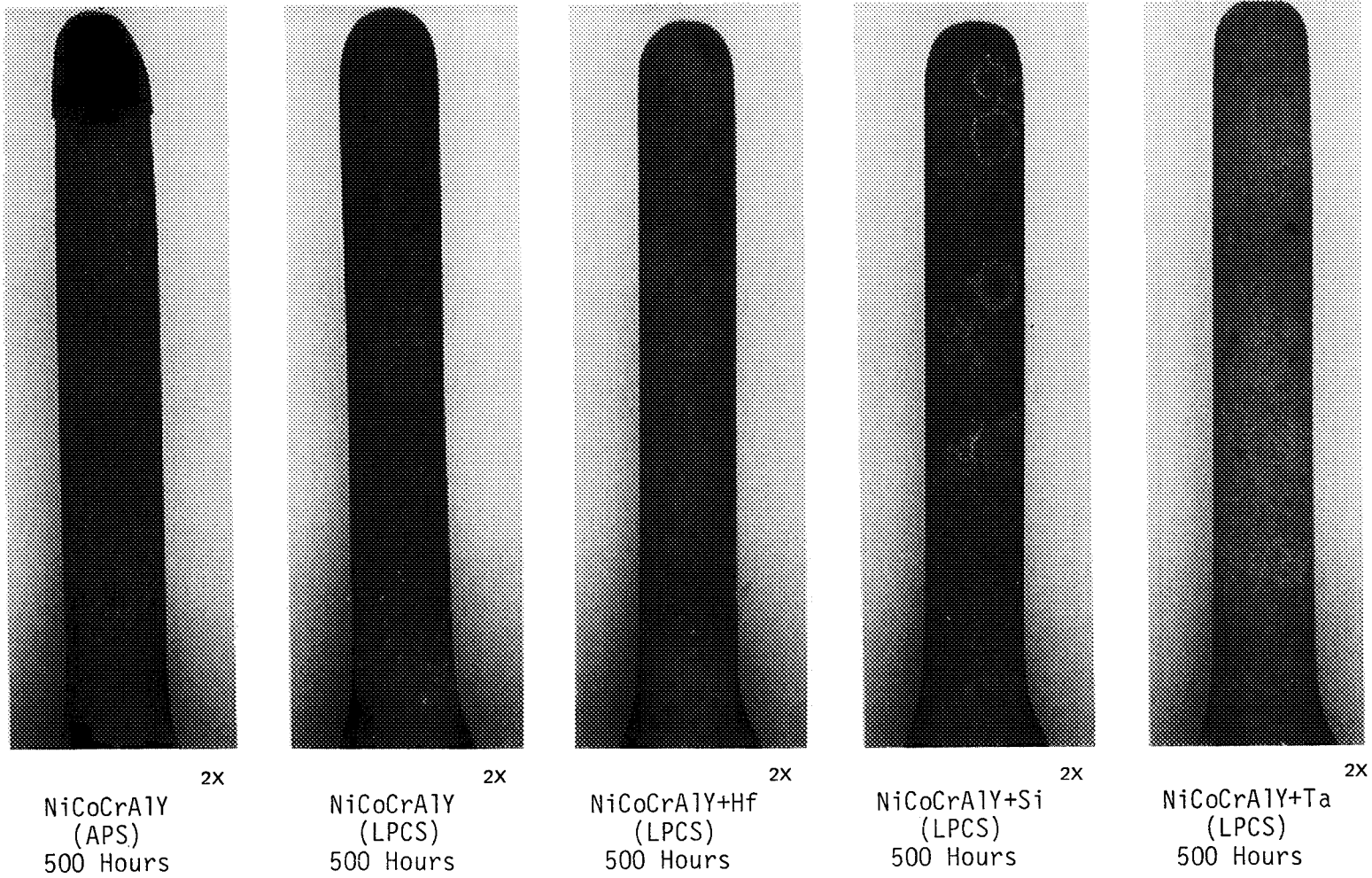
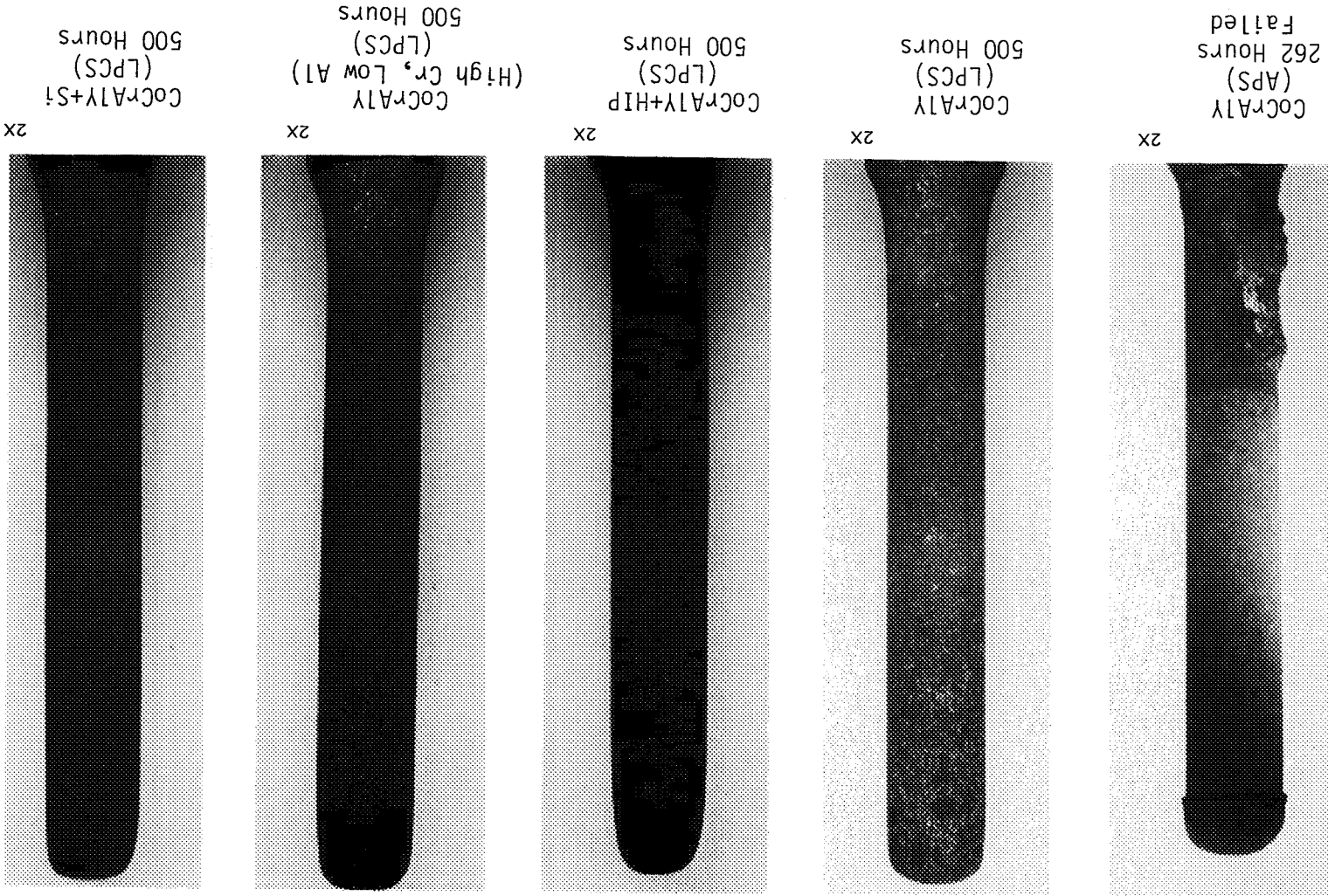


Figure 33

Surface Photographs of Test Samples with NiCoCrAlY-Type Plasma Sprayed Coatings on the Single Crystal Alloy Exposed to a Hot Corrosive Environment at 1172<sup>o</sup>K (1650<sup>o</sup>F), APS = Atmospheric Argon Chamber Sprayed; LPCS = Low Pressure Chamber Sprayed



ORIGINAL PAGE  
BLACK AND WHITE PHOTOGRAPH



Surface Photographs of Test Samples with CoCrAlY-Type Plasma Sprayed Coatings on B-1900+HF Alloy Exposed to a Hot Corrosive Environment at 1172°K (1650°F). APS = Atmospheric Argon Chamber Sprayed; LPCS = Low Pressure Chamber Sprayed

Figure 34

TABLE X

VISUAL CONDITIONS OF SAMPLES EVALUATED IN BURNER RIG HOT  
CORROSION TESTING AT 1172°K (1650°F)

Test Time: 500 hours

<u>Alloy</u>	<u>Coating Composition</u>	<u>Coating Process</u>	<u>Exposure Time (Hours)</u>	<u>Visual Observations on Test Section*</u>
B1900+Hf	CoCrAlY	EB-PVD	500	Moderate surface degradation
B1900+Hf	CoCrAlY	APS	262	Failed
B1900+Hf	CoCrAlY	LPCS	500	Moderate surface degradation
B1900+Hf	CoCrAlY+HIP	LPCS	500	Slight surface degradation
B1900+Hf	CoCrAlY (High Cr, Low Al)	LPCS	500	Slight surface degradation
B1900+Hf	CoCrAlY+Si	LPCS	500	Slight surface degradation
Single Crystal	NiCoCrAlY	EB-PVD	500	Slight surface degradation
Single Crystal	NiCoCrAlY	APS	500	Moderate surface degradation
Single Crystal	NiCoCrAlY	LPCS	500	Moderate surface degradation
Single Crystal	NiCoCrAlY+Hf	LPCS	500	Slight surface degradation
Single Crystal	NiCoCrAlY+Si	LPCS	500	Slight to moderate surface degradation
Single Crystal	NiCoCrAlY+Ta	LPCS	500	Slight surface degradation

\*Pre-Test coating thicknesses were not obtained on these samples since sectioning of the sample tips for thickness measurement would have resulted in premature hot corrosive attack on the bare tip and the nearby coating.

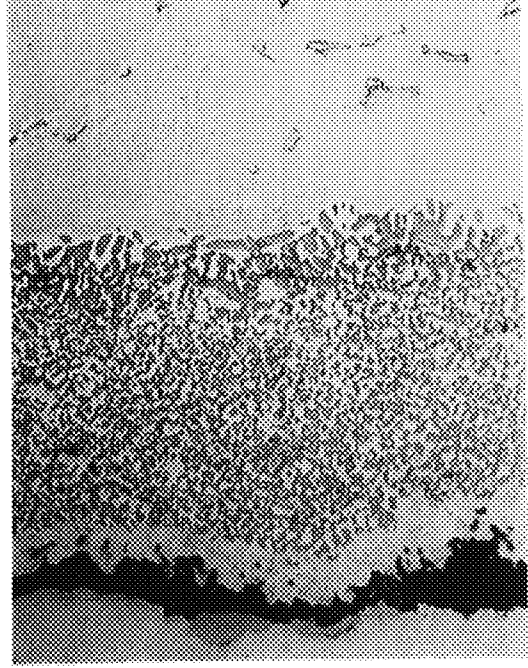
EB-PVD = Electron Beam Physical Vapor Deposition  
 LPCS = Low Pressure Chamber Plasma Spray  
 APS = One Atmosphere Argon Plasma Spray  
 HIP = Hot Isostatic Pressing

Coating microstructures of the samples removed after 350 hours of burner rig testing are provided in Figures 35 through 38. As these photomicrographs indicate, all coatings were reasonably resistant to degradation for 350 hours of exposure to the hot corrosion test conditions. All coatings had more than eighty percent of their beta plus gamma structure intact with no selective hot corrosion penetration. With respect to surface depletion of beta phase, the low pressure chamber sprayed CoCrAlY + Si coating on the B1900 + Hf alloy and the low pressure chamber sprayed NiCoCrAlY + Ta coating on the single crystal alloy exhibited the least amount of aluminum consumption. Microstructural examination of samples exposed to a total of 500 hours of the hot corrosive environment showed the same trends; however degradation to coatings at this time interval had not progressed significantly to what was microstructurally observed after 350 hours.

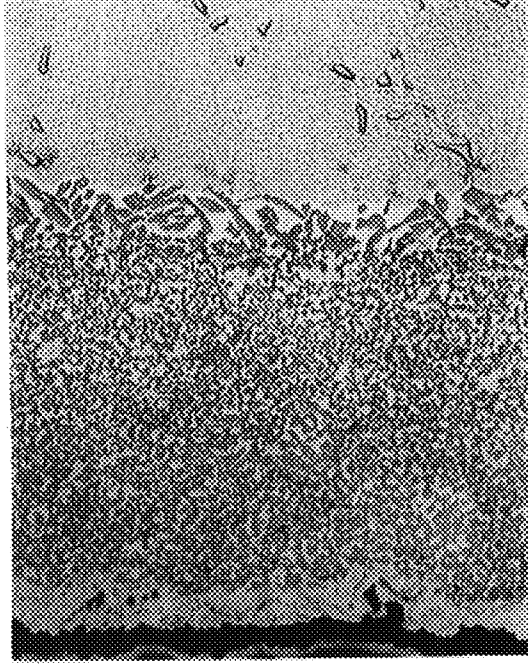
All of the low pressure chamber sprayed overlay coatings provided satisfactory protection to the single crystal and the B1900 + Hf alloys in cyclic hot corrosion testing. These coatings along with the baseline vapor deposited MCrAlY coatings were still highly protective after 500 hours of exposure. Only one sample (the one atmosphere argon plasma sprayed CoCrAlY coated B1900 + Hf system) failed in this test and it is believed that this failure was more related to poor coating quality than to any inferior characteristics typical of the process or of the coating composition. The second sample of this coating/alloy system which was metallographically examined after 350 hours of exposure exhibited no sign of imminent failure (see Figure 35).

With respect to the relative performance, of the different coatings (as is evident from Figures 33 through 38), it was difficult to differentiate between the CoCrAlY-based and the NiCoCrAlY-based coatings. Further, because of the limited degradation, ranking of hot corrosion resistance among the coatings belonging to the same MCrAlY group was not possible. However, based on beta phase retention, it is expected that the CoCrAlY + Si coating in the CoCrAlY group and the silicon and tantalum-modified NiCoCrAlY systems belonging to the NiCoCrAlY group will exhibit the most durability.

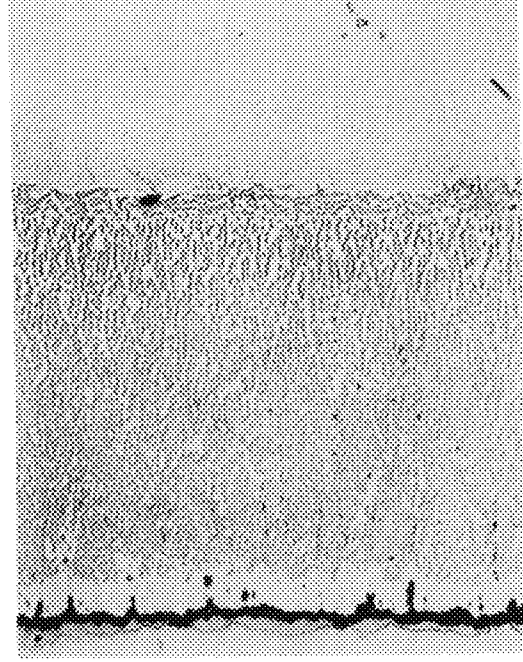
ORIGINAL PAGE  
BLACK AND WHITE PHOTOGRAPH



400x  
CoCrAlY  
Atmospheric Argon Chamber Sprayed  
Unfilled Sample



400x  
CoCrAlY  
Low Pressure Chamber Sprayed



400x  
CoCrAlY  
Electron-Beam Physical  
Vapor Deposited

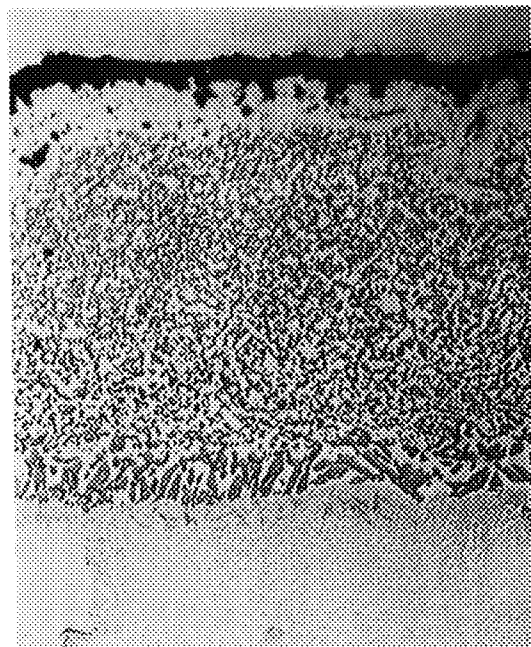
Post-Test Microstructures of the Test Section of CoCrAlY  
Coatings on B-1900+Hf Alloy After 350 Hours of Exposure in a Hot  
Corrosive Environment at 1172oK (1650oF)

Figure 35

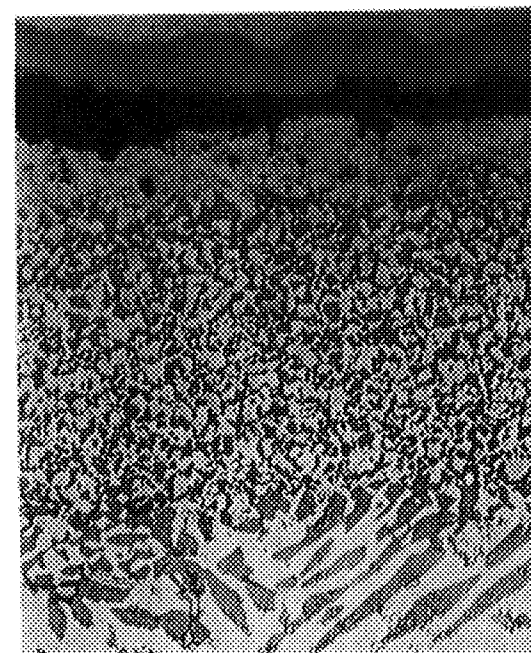
ORIGINAL PAGE IS  
OF POOR QUALITY



CoCrAlY+Si 400x



CoCrAlY (High Cr, Low Al) 400x



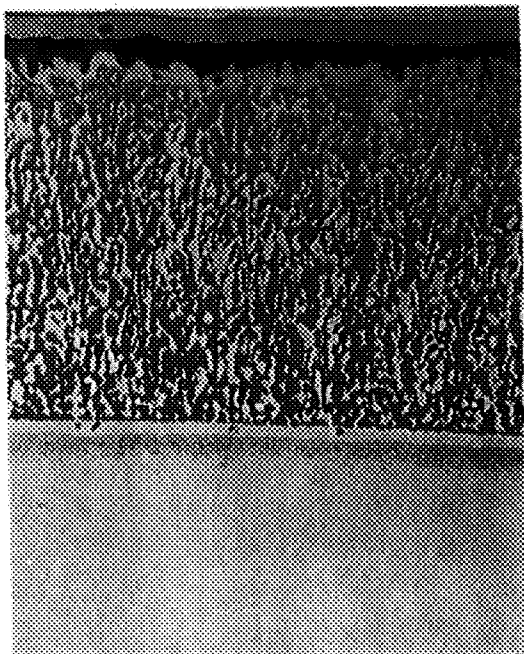
CoCrAlY+HIP 400x

BLACK AND WHITE PHOTOGRAPH

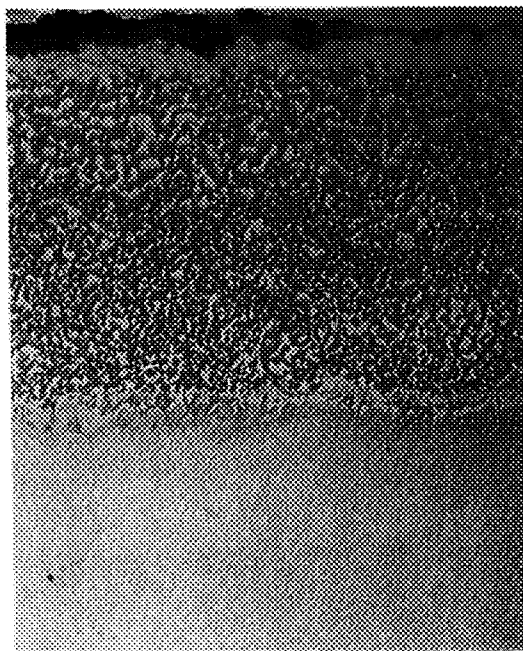
Figure 36

Post-Test Microstructures of the Test Section of Low Pressure Chamber Sprayed CoCrAlY-Type Coatings on B-1900+Hf Alloy After 350 Hours of Exposure in a Hot Corrosive Environment at 1172°K (1650°F), HIP = Hot Isostatic Pressing

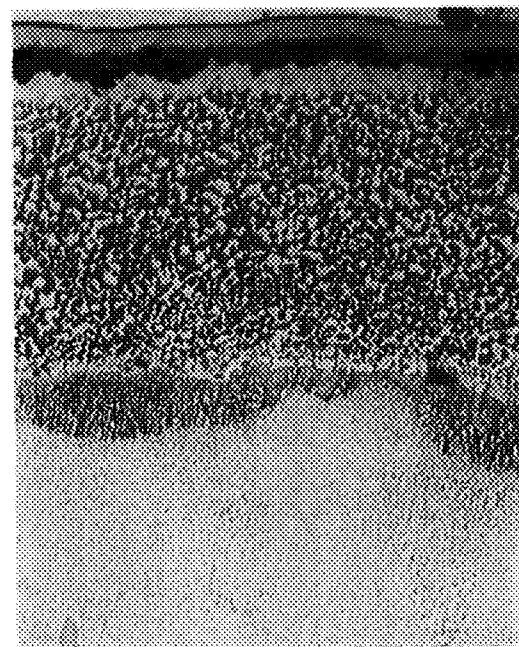
ORIGINAL PAGE IS  
OF POOR QUALITY  
73



NiCoCrAlY  
Electron-Beam Physical  
Vapor Deposited 400x



NiCoCrAlY  
Low Pressure Chamber Sprayed 400x



NiCoCrAlY  
Atmospheric Argon  
Chamber Sprayed 400x

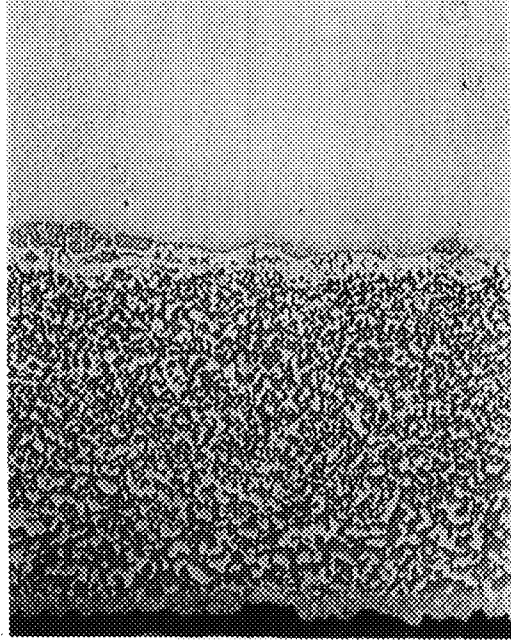
Figure 37 Post-Test Microstructure of the Test Section of NiCoCrAlY Coatings on the Single Crystal Alloy After 350 Hours of Exposure in a Hot Corrosive Environment at 1172°K (1650°F)

ORIGINAL PAGE  
BLACK AND WHITE PHOTOGRAPH



ORIGINAL PAGE IS  
BLACK AND WHITE PHOTOGRAPH

400x



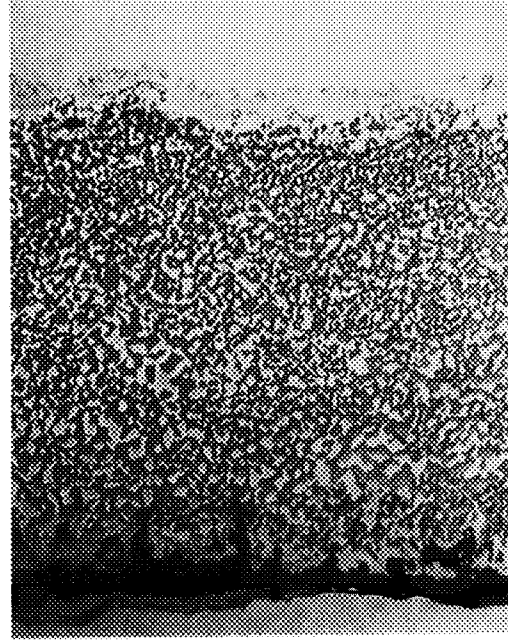
NiCoCrAlY+Hf

400x



NiCoCrAlY+Ta

400x



NiCoCrAlY+Si

Post-Test Microstructure of the Test Section of Low Pressure  
Chamber Sprayed NiCoCrAlY-Type Coatings on the Single Crystal  
Alloy After 350 Hours of Exposure in a Hot Corrosive Environment  
at 1172°K (1650°F)

Figure 38

ORIGINAL PAGE IS  
OF POOR QUALITY

#### 4.1.6 Coating Ductility Test Results

Results of the tensile ductility (strain to first coating crack) tests at 588<sup>0</sup>K (600<sup>0</sup>F) of all low pressure chamber plasma sprayed coatings are provided in Table XI, along with the ductility data of the baseline vapor deposited NiCoCrAlY and CoCrAlY coatings. These data are illustrated in Figure 39. Based on the results of two test samples for each coating system, it appears that the low pressure chamber sprayed MCrAlY coatings exhibited superior ductility (strain to cracking) compared to that shown by the vapor deposited MCrAlY coatings. Further, within the NiCoCrAlY group, the additions of tantalum or silicon to the basic NiCoCrAlY chemistry resulted in a decrease in coating ductility with tantalum exhibiting a substantial effect. The effect of hafnium is believed to be negligible with data falling within experimental error. However, the low pressure chamber sprayed NiCoCrAlY + Si coating exhibited cracking strains (ductility) approximately in the same range as that shown by the baseline vapor deposited NiCoCrAlY coating.

In the CoCrAlY group of coatings produced by the low pressure chamber plasma spray process, it was again observed that the silicon addition reduced ductility. The high chromium-low aluminum variation of the CoCrAlY system also exhibited slightly lower ductility compared to the unmodified plasma sprayed CoCrAlY indicating that a 2 weight percent decrease in aluminum concentration was not sufficient to alleviate the effect caused by the 7 weight percent increase in chromium content of the CoCrAlY coating. The hot isostatic pressed CoCrAlY system exhibited a substantial increase in the resistance of the coating to crack initiation. This increase was due to the reduced aluminum content of the coating brought about by the high temperature post-coating processing (as was discussed previously).

Post-test microstructural examination of cracked MCrAlY coatings from both groups (NiCoCrAlY and CoCrAlY based systems) revealed that most cracks were associated with micro defects rather than large irregularities (Figure 40). Examination of the vapor deposited coatings verified that they did not contain any pit or flake defects. In the case of plasma sprayed coatings, cracks did



TABLE XI

## TENSILE DUCTILITY OF VARIOUS COATINGS AT 588°K (600°F)

<u>Coating Composition</u>	<u>Substrate Alloy</u>	<u>Coating Process*</u>	<u>Strain to First Observed Crack (Percent)</u>
Co-22Cr-12.6Al-0.4Y	B1900+Hf	EB-PVD	0.3; 0.5
Co-22Cr-12.5Al-0.6Y	B1900+Hf	LPCS	0.5; 0.7
Co-29Cr-10.8Al-0.6Y	B1900+Hf	LPCS	0.4; 0.5
Co-22Cr-12.5Al-0.6Y-2.0Si	B1900+Hf	LPCS	0.3; 0.3
Co-22Cr-12.5Al-0.6Y+HIP	B1900+Hf	LPCS	1.4; 1.7
Ni-21Co-19Cr-12.3Al-0.2Y	B1900+Hf	EB-PVD	0.9; 1.1
Ni-23Co-18Cr-12.5Al-0.4Y	B1900+Hf	LPCS	1.4; 1.7
Ni-21Co-18Cr-12.5Al-0.6Y-0.7Hf	B1900+Hf	LPCS	1.1; 1.4
Ni-21Co-18Cr-12.6Al-0.6Y-1.6Si	B1900+Hf	LPCS	0.9; 0.9
Ni-21Co-18Cr-12.6Al-0.6Y-8.5Ta	B1900+Hf	LPCS	0.4; 0.6

\*EB-PVD = Electron Beam Physical Vapor Deposition  
 LPCS = Low Pressure Chamber Plasma Spray  
 HIP = Hot Isostatic Pressing

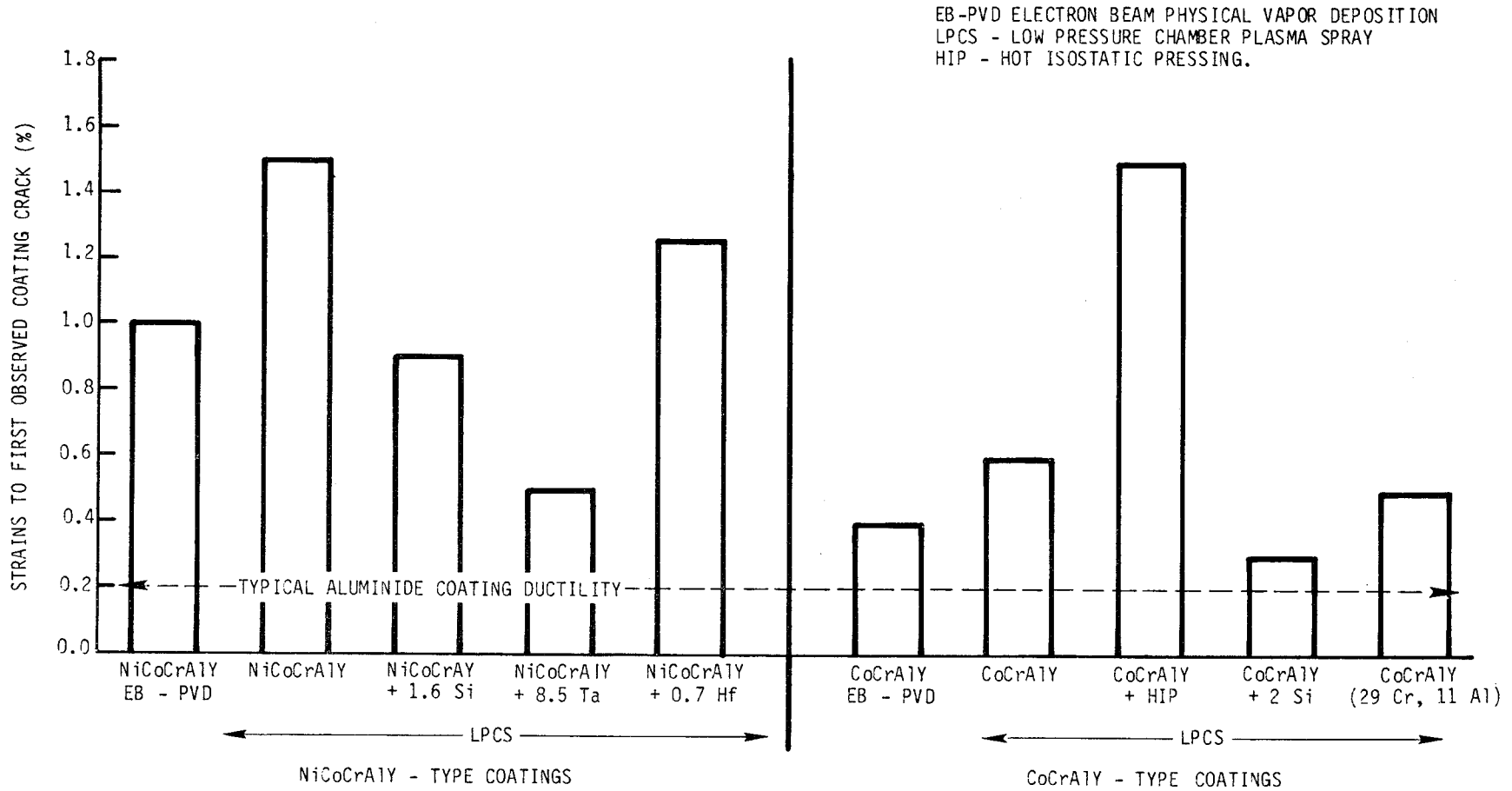
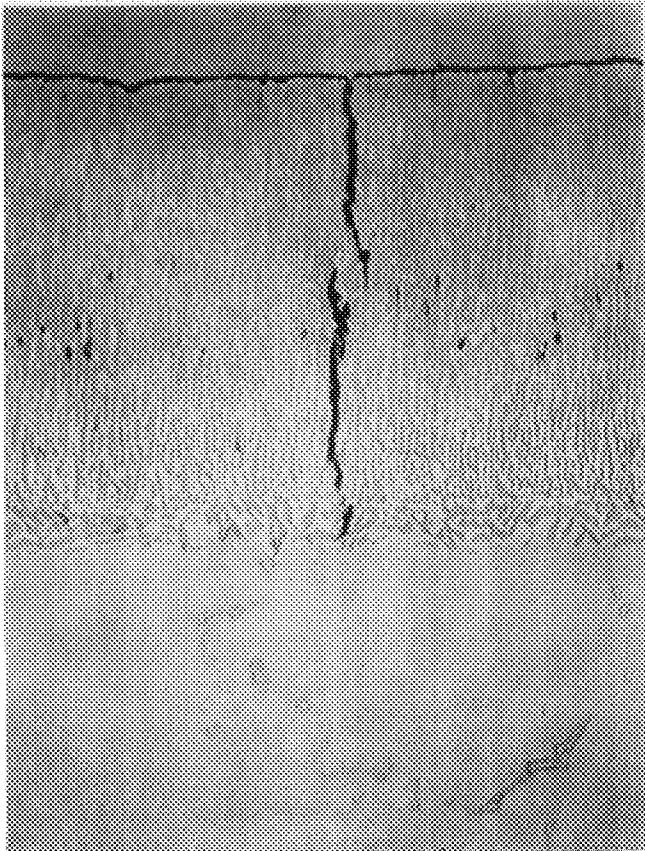


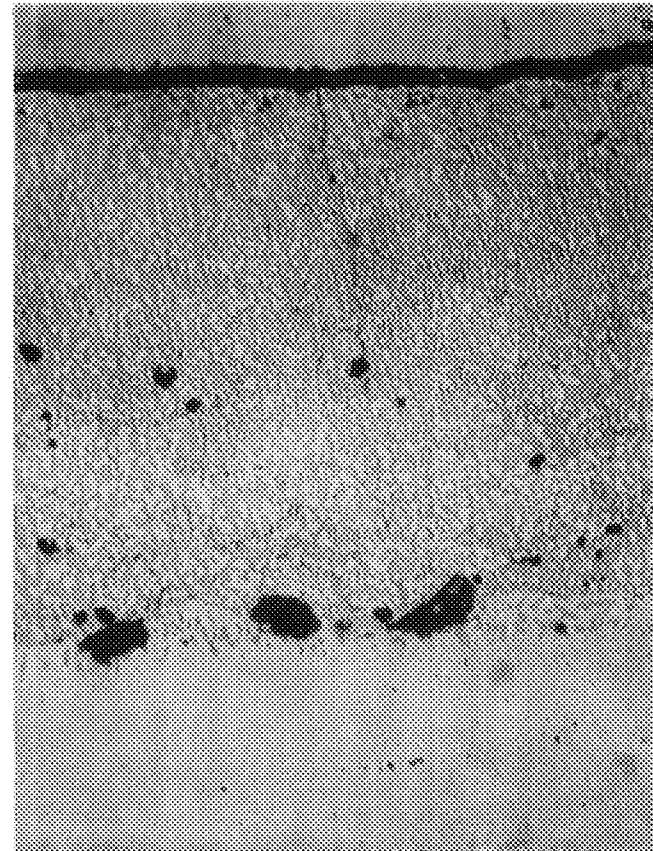
Figure 39 Average Cracking Strains of Coated B1900 + Hf Alloy at 588°K (600°F)



500X

ELECTRON BEAM PHYSICAL VAPOR DEPOSITION

NiCoCrAlY



500X

LOW PRESSURE CHAMBER SPRAY

NiCoCrAlY

Figure 40 Post-Test Microstructural Condition of NiCoCrAlY Coated B1900 + Hf Ductility Specimens.

ORIGINAL PAGE  
BLACK AND WHITE PHOTOGRAPH

not initiate at any large oxide inclusions. Instead, it appears that crack initiation was either at the sample surfaces or at micro defects (voids) present in the coating.

The aforementioned results indicate that for both NiCoCrAlY and CoCrAlY overlay coatings, microstructure-related characteristics exert influence upon the coating strain to first cracking. The vapor deposited MCrAlY coatings exhibited lower ductility compared to that shown by the plasma sprayed MCrAlY coatings of similar compositions because of microstructural differences. Another significant factor affecting coating ductility is the amount of beta (a relatively hard and brittle phase) present in the coating. Qualitatively, the higher the amount of beta phase, the lower is the ductility; with a 100% beta containing overlay coating, or a pack cementation diffusion aluminide coating, exhibiting the lowest fracture strain (typically 0.2% at 588<sup>0</sup>K (600<sup>0</sup>F)). As can be seen in Table XII, both silicon and tantalum additions to NiCoCrAlY and the silicon addition to CoCrAlY increase the beta concentration; therefore it is not surprising that these modifications exhibited lower ductility compared to their respective unmodified compositions.

Finally, in order to put these results into perspective, it should be recalled that the purpose of the tensile ductility testing was to verify that the fracture strains of the experimental coatings would exceed values in the order of 0.2 percent in case of CoCrAlY coatings and 0.4 percent strain in case of NiCoCrAlY based coatings which are currently used successfully on gas turbine airfoils. The ductility results of this investigation indicate that the fracture strains of all the coating systems evaluated exceed the magnitude of anticipated thermomechanical strains in commercial engine operation. Further the ductility (strain to first observed crack) of all low pressure chamber sprayed coating systems exceeded the typical ductility of aluminide coatings (0.2%) at 588<sup>0</sup>K (600<sup>0</sup>F).

TABLE XII

BETA PHASE CONCENTRATIONS OF VARIOUS COATINGS  
IN THE AS-PROCESSED CONDITION

<u>Coating Composition</u>	<u>Average* Beta Concentration of the Coating (%)</u>	<u>Average Coating Cracking Strain (Percent)</u>
Ni-23Co-18Cr-12.5Al-0.4Y	54	1.55
Ni-21Co-18Cr-12.5Al-0.6Y-0.7Hf	53	1.25
Ni-21Co-18Cr-12.6Al-0.6Y-1.6Si	58	0.90
Ni-21Co-18Cr-12.6Al-0.6Y-8.5Ta	66	0.50
Co-22Cr-12.5Al-0.6Y	63	0.60
Co-22Cr-12.5Al-0.6Y-2.0Si	74	0.30
Co-22Cr-12.5Al-0.6Y+HIP	55	1.55

\*Average of Four Evaluated Areas in the Coating. Data obtained by Qualitative Metallographic Analysis.

#### 4.2 Summary of Task I Results and Selection of Coatings for Task II

Based on the results of the cyclic burner rig oxidation and hot corrosion evaluations plus the tensile ductility testing of ten experimental plasma sprayed overlay coating systems the following conclusions were made.

- In all tests in which they were compared, the low pressure chamber plasma sprayed MCrAlY coatings were superior to the one atmosphere argon plasma sprayed MCrAlY coatings.
- The low pressure chamber sprayed NiCoCrAlY coating on the single crystal alloy provided equivalent or slightly greater protection compared to that of the baseline vapor deposited NiCoCrAlY coating of similar composition. However, the oxidation behavior of the low pressure chamber sprayed CoCrAlY coating was inferior to that of the vapor deposited CoCrAlY on the B1900 + Hf alloy.
- The silicon, hafnium and tantalum additions to NiCoCrAlY and the silicon addition to CoCrAlY exhibited improved oxidation resistance at 1394<sup>o</sup>K (2050<sup>o</sup>F) compared to the unmodified vapor deposited and low pressure chamber sprayed NiCoCrAlY and CoCrAlY coatings respectively. All these modified coating systems successfully provided protection to the single crystal and B1900 + Hf alloys for 1000 hours at 1394<sup>o</sup>K (2050<sup>o</sup>F) in a cyclic rig test.
- Hot isostatic pressing at 1470<sup>o</sup>K (2185<sup>o</sup>F) for three hours of the CoCrAlY coating resulted in improved coating density. However, due to increased coating-substrate interdiffusion during the high temperature (1470<sup>o</sup>K (2185<sup>o</sup>F)) operation, the aluminum concentration of the coating was substantially reduced. This resulted in inferior oxidation resistance but improved ductility for this coating system compared to the baseline CoCrAlY material.

- In cyclic hot corrosion burner rig testing at 1172<sup>0</sup>K (1650<sup>0</sup>F), all experimental plasma sprayed candidates as well as the baseline vapor deposited MCrAlY coatings successfully protected the base alloys for 500 hours (the program goal), under severe corrosive conditions (35 ppm salt plus 1.3% sulfur).
- Low pressure chamber sprayed MCrAlY coatings exhibited greater ductility than similar compositions fabricated by electron-beam physical vapor deposition. Additions of 8 w/o tantalum or 1.5 w/o silicon to the basic NiCoCrAlY chemistry and the 2.0 w/o silicon addition to the CoCrAlY composition resulted in decreases in coating ductility. However, the low pressure chamber sprayed NiCoCrAlY + 1.5 Si and CoCrAlY + 2.0 Si coatings exhibited cracking strains (ductility) in the same range as that shown by the vapor deposited NiCoCrAlY and CoCrAlY baseline coatings respectively.

#### Selection of Coatings for Task II Evaluation

Based on the aforementioned results, four coating systems for the single crystal alloy and four coating systems for the B1900 + Hf alloy were selected for further optimization in Task II.

Since the NiCoCrAlY + 1.5Si and NiCoCrAlY + 8Ta coatings on the single crystal alloy were superior to all other coating systems on this alloy, a total of four modifications of these two basic systems were selected for this alloy in Task II.

- NiCoCrAlY + Si (1.0 w/o)
- NiCoCrAlY + Si (2.0 w/o)
- NiCoCrAlY + Si (1.6 w/o) + Ta (8.0 w/o)
- NiCoCrAlY + Si (1.6 w/o) + Ta (4.0 w/o)

The CoCrAlY + 2Si coating on B1900 + Hf performed superior to all other coatings evaluated on this substrate. Further, the CoCrAlY coating containing

a higher amount of chromium and lower amount of aluminum had visually appeared to show some potential for improved performance under the hot corrosive test conditions. The hot isostatically pressed CoCrAlY (1470<sup>0</sup>K (2185<sup>0</sup>F)/3 hours/103.4 MPa (15 Ksi)) coating exhibited a greatly improved coating density, but substantial interdiffusion between the coating and the substrate occurred during hot isostatic pressing which is believed to have adversely affected its performance. Therefore, a reduced hot isostatic pressing temperature (1352<sup>0</sup>K (1975<sup>0</sup>F)) was selected to be used in Task II to decrease the extent of interdiffusion but still achieve substantially the same improvement in coating density. In view of above observations, three compositional modifications of the CoCrAlY + Si coating system, and a post-coating hot isostatic pressing modification of the CoCrAlY system were selected for further optimization in Task II:

- CoCrAlY + Si (1.5 w/o)
- CoCrAlY + Si (2.5 w/o)
- CoCrAlY (high Cr, low Al) + Si (2.0 w/o)
- CoCrAlY + HIP (1352<sup>0</sup>K (1975<sup>0</sup>F)/4 hrs/103.4 MPa (15 Ksi))

#### 4.3 Task II Evaluations

In Task II, the eight selected low pressure chamber plasma sprayed coating systems, described in the previous section, were evaluated by oxidation and hot corrosion burner rig tests as in Task I. Vapor deposited NiCoCrAlY and CoCrAlY coatings were tested concurrently in these evaluations as baselines. Metallographic analyses were carried out on the eight systems prior to and after burner rig testing to assist in the evaluation of coating performance. Based on the testing and analyses the best plasma sprayed coating system for each of the B1900 + Hf and single crystal alloys were selected for engine testing in Task III.



#### 4.3.1 Pre-Test Microstructures

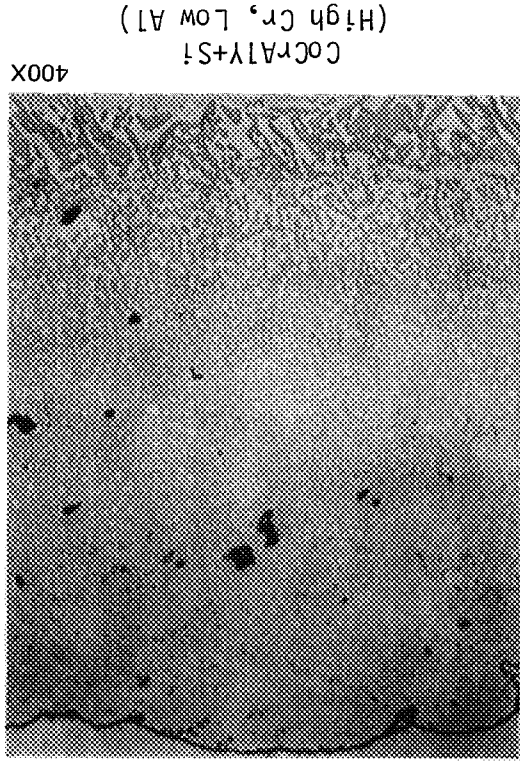
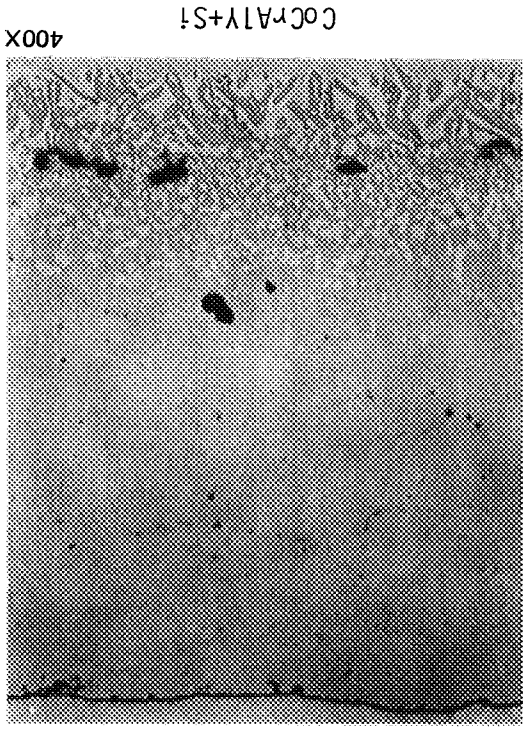
A metallographic section was obtained from the tip end of each test bar of the eight coating systems to document and analyze the initial microstructural characteristics and coating thickness prior to oxidative and corrosive exposure in the burner rigs. Figures 41 through 43 show the typical representative initial microstructural characteristics of the CoCrAlY-type and NiCoCrAlY-type coatings on the B1900 + Hf and the single crystal alloy, respectively. Both variations in the NiCoCrAlY + Si system (1.2Si and 2.2Si additions) were observed to have similar microstructures; therefore the microstructure of only one variation (NiCoCrAlY + 1.2Si) is presented in Figure 43. Similar behavior was observed for the two variations in the NiCoCrAlY + Si + Ta and the CoCrAlY + Si systems and therefore the microstructure of only one variation in each of these two systems is provided in Figure 43 and 41 respectively.

The aluminum content of all the coating systems shown in these figures was measured to be 12.7  $\pm$ 0.1 weight percent except for the high Cr, low Al CoCrAlY + Si system which contains 10.8 weight percent aluminum. As was observed in Task I specimens the CoCrAlY coating systems containing silicon and the NiCoCrAlY coating systems containing silicon and/or tantalum had a higher than normal (for the aluminum content present) volume percent of beta phase present in the coating. For comparison, low pressure chamber sprayed CoCrAlY and NiCoCrAlY coatings are also provided in Figures 41 and 43 respectively.

Examination of the microstructure of the hot isostatically pressed CoCrAlY coating system revealed that hot isostatically pressing at 1352<sup>0</sup>K (1975<sup>0</sup>F) for four hours at 103.4 MPa (15 Ksi), instead of 1470<sup>0</sup>K (2185<sup>0</sup>F)/3 hrs/103.4 MPa (15 Ksi) as previously done in Task I, substantially reduced the coating/substrate interdiffusion and apparently almost total coating densification was achieved on these test bar samples (Figure 42).

The thickness of various coating systems on test bars were measured to be within  $\pm$ 20 percent of the 100 to 150 microns (4-6 mils) range requested. This satisfactorily met the program requirements.

ORIGINAL PAGE  
BLACK AND WHITE PHOTOGRAPH



Pre-Test Microstructures of Low Pressure Chamber Sprayed  
CoCrAlY-Type Coatings on B-1900+Hf Alloy After Post-Coating  
Processing

Figure 41

ORIGINAL PAGE IS  
OF POOR QUALITY

C-2

ORIGINAL PAGE  
BLACK AND WHITE PHOTOGRAPH



CoCrAlY+HIP  
(1470K (2185°F)/3hrs/103.4 MPa (15 Ksi))

400X



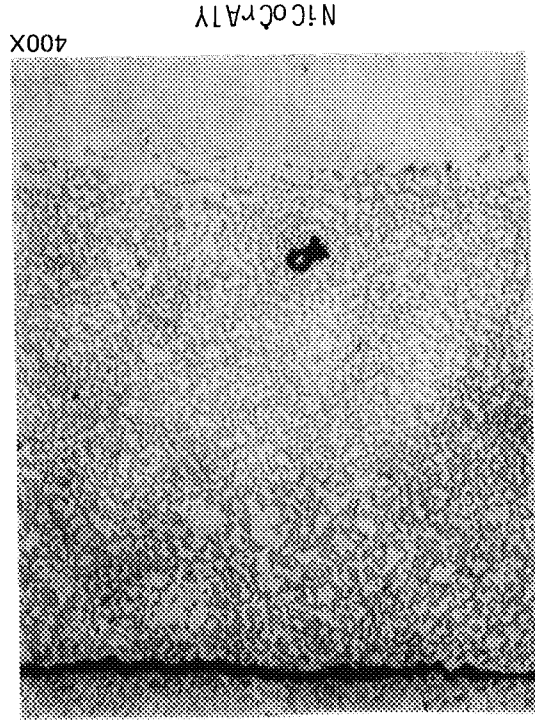
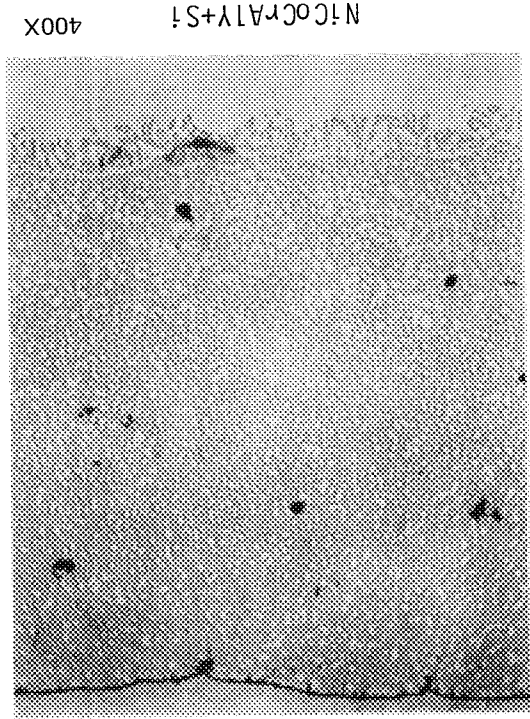
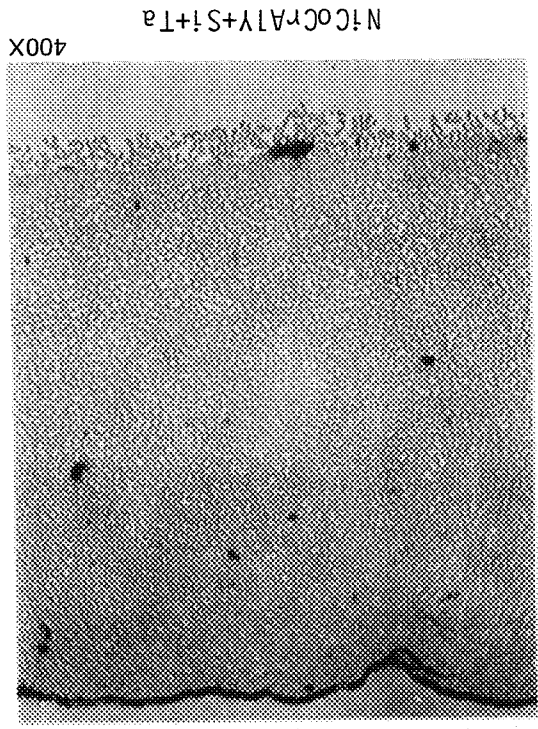
CoCrAlY+HIP  
(1352K (1975°F)/4hrs/103.4 MPa (15 Ksi))

400X

Pre-Test Microstructures of Low Pressure Chamber Sprayed  
CoCrAlY+HIP Coatings on B-1900+Hf Alloy After Post-Coating  
Processing. Note Reduced Coating-Substrate Interdiffusion and  
Lower Aluminum Loss in Case of Lower Temperature HIP'ed CoCrAlY  
Coating. HIP = Hot Isostatic Pressing

Figure 42

ORIGINAL FACE  
BLACK AND WHITE PHOTOGRAPH



Pre-Test Microstructures of Low Pressure Chamber Sprayed  
NiCoCrAlY-Type Coatings on the Single Crystal Alloy After  
Post-Coating Processing

Figure 43

#### 4.3.2 Burner Rig Oxidation Testing

##### a. NiCoCrAlY-Type Coatings on the Single Crystal Alloy

The visual appearance of the four NiCoCrAlY-type low pressure chamber sprayed coating systems on the single crystal after exposure for 350 hours and 1000 hours in the 1394<sup>o</sup>K (2050<sup>o</sup>F) cyclic burner rig test are summarized in Tables XIII and XIV. Figure 44 shows the surface conditions of these specimens after 1000 hours of exposure. Also included in this figure is the vapor deposited NiCoCrAlY coated single crystal which failed after 730 hours of exposure (811 hours of normalized life). Throughout the course of the Task II burner rig oxidation testing, less spalling of coating oxide scales was exhibited by all of the modified NiCoCrAlY low pressure chamber sprayed coating systems compared to that exhibited by the baseline vapor deposited NiCoCrAlY coating samples. A similar improvement was shown by these coating systems in comparison to the low pressure chamber sprayed NiCoCrAlY coating tested in Task I. This improved oxide scale adherence shown by the plasma sprayed modified NiCoCrAlY coatings is believed to be due to the presence of silicon in these coatings.

In addition to the evaluation of these Task II coating systems, the low pressure chamber sprayed NiCoCrAlY + Si and NiCoCrAlY + Ta coated single crystal specimens tested for 1000 hours in Task I were further exposed to the oxidative environment in Task II for a total of 1905 hours before failure. The surface conditions of these two samples after 1785 hours of testing are documented in Figure 45. This illustration indicates that the low pressure chamber sprayed NiCoCrAlY + Si and NiCoCrAlY + Ta coatings, even after 1785 hours of exposure, appear in better surface condition than does the baseline vapor deposited NiCoCrAlY coating shown in Figure 44 after 730 hours of exposure. When the two Task I specimens failed at 1905 hours, their normalized coating life was calculated to be 1642 hours for the NiCoCrAlY + Si system and 1536 hours for the NiCoCrAlY + Ta system. Thus, the plasma sprayed, compositionally modified coatings exhibited about twice the coating life of the baseline vapor deposited system.

TABLE XIII

VISUAL CONDITIONS OF TASK II SINGLE CRYSTAL SPECIMENS AFTER 350 HOURS  
OF EXPOSURE IN THE BURNER RIG OXIDATION TEST AT 1394°K (2050°F)

<u>Coating Composition</u>	<u>Coating Process*</u>	<u>Coating Thickness (Microns)</u>	<u>Visual Condition</u>
NiCoCrAlY	EB-PVD	112	Moderate spalling of oxide scale
NiCoCrAlY+1.2Si	LPCS	145	Moderate spalling of oxide scale
NiCoCrAlY+2.2Si	LPCS	153	Moderate spalling of oxide scale
NiCoCrAlY+1.6Si+4.5Ta	LPCS	138	Heavy spalling of oxide scale
NiCoCrAlY+1.6Si+8.5Ta	LPCS	150	Moderate spalling of oxide scale

\*EB-PVD = Electron Beam Physical Vapor Deposition  
LPCS = Low Pressure Chamber Plasma Spray

TABLE XIV

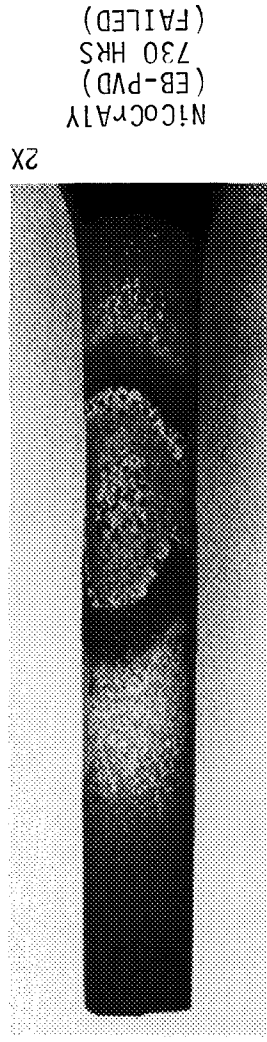
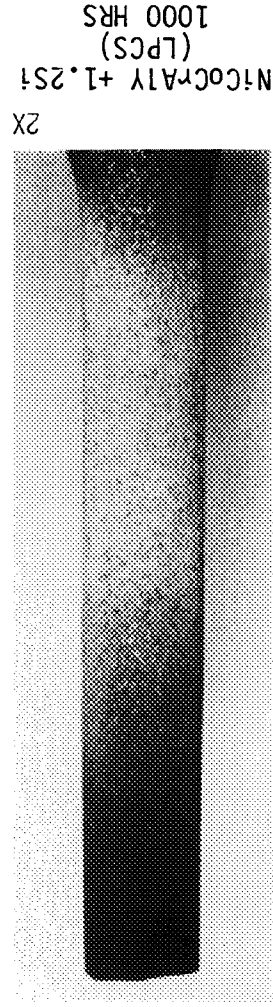
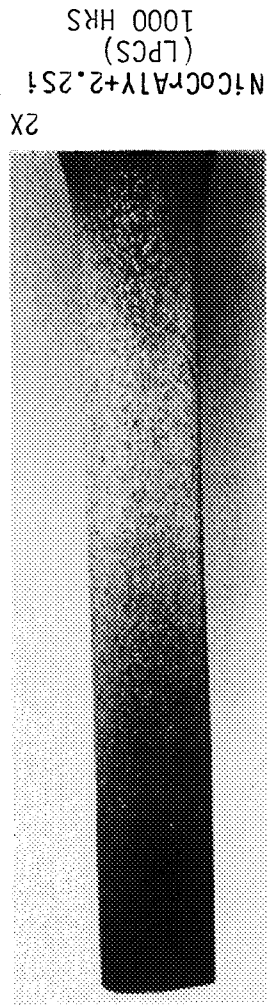
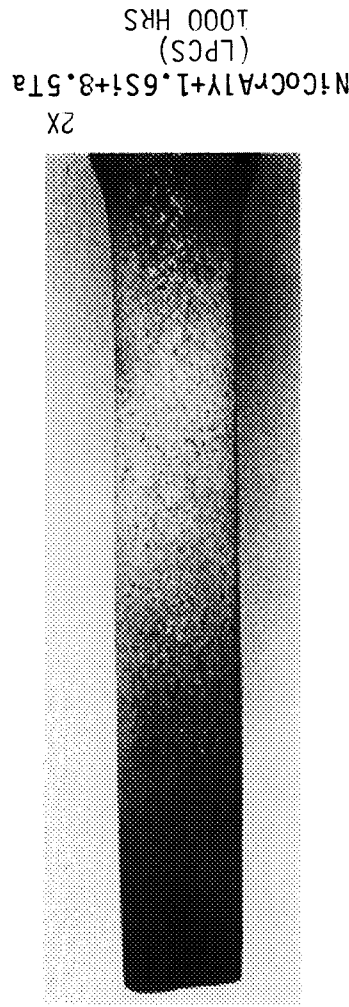
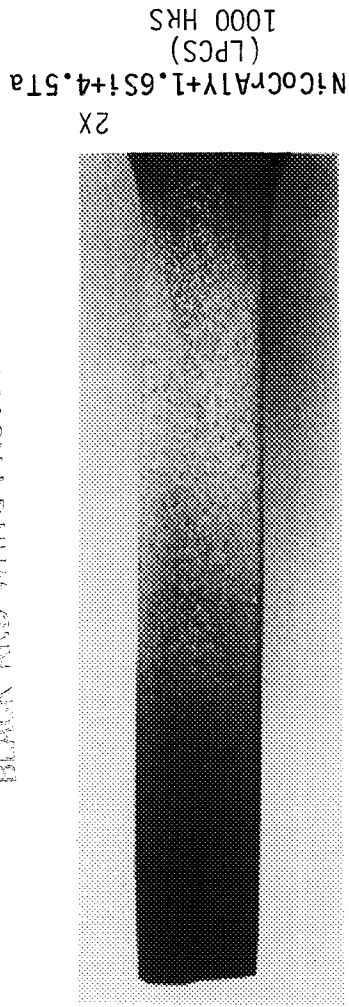
VISUAL CONDITIONS OF TASK II SINGLE CRYSTAL SPECIMENS EVALUATED IN  
BURNER RIG OXIDATION TESTING AT 1394°K (2050°F)

<u>Coating Composition</u>	<u>Coating Process*</u>	<u>Exposure Time (Hours)</u>	<u>Normalized Coating Life** (Hours)</u>	<u>Normalized Time to 1st Coating Penetration</u>	<u>Visual Observation on Test Section</u>
NiCoCrAlY	EB-PVD	730	811	633	Failed
NiCoCrAlY+1.2Si	LPCS	1000	-	-	Moderate spal- ling of oxide scale
NiCoCrAlY+2.2Si	LPCS	1000	-	-	Moderate spal- ling of oxide scale
NiCoCrAlY+1.6Si+8.5Ta	LPCS	1000	-	-	Moderate spal- ling of oxide scale
NiCoCrAlY+1.6Si+4.5Ta	LPCS	1000	-	-	Moderate spal- ling of oxide scale
NiCoCrAlY+1.6Si (Task I System)	LPCS	1905	1642	1424	Failed
NiCoCrAlY+8.5Ta (Task I System)	LPCS	1905	1536	1341	Failed

\*EB-PVD = Electron Beam Physical Vapor Deposition  
LPCS = Low Pressure Chamber Plasma Spray

\*\*Normalized Coating Life: Coating's Life Normalized to Typical 'Use' Thick-  
ness of 127 microns (5.0 mils).

BLACK AND WHITE PHOTOGRAPH

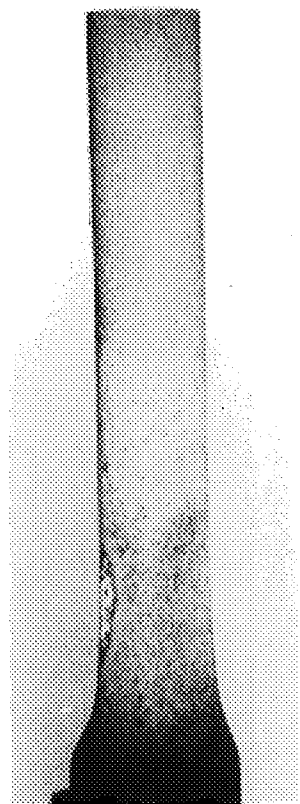


Surface Photographs of Test Samples with NiCoCrAlY-Type Coatings on the Single Crystal Alloy Exposed to an Oxidative Environment at 13940K (20500F). EB-PVD = Electron-Beam Physical Vapor Deposited LPCS = Low Pressure Chamber Sprayed

Figure 44

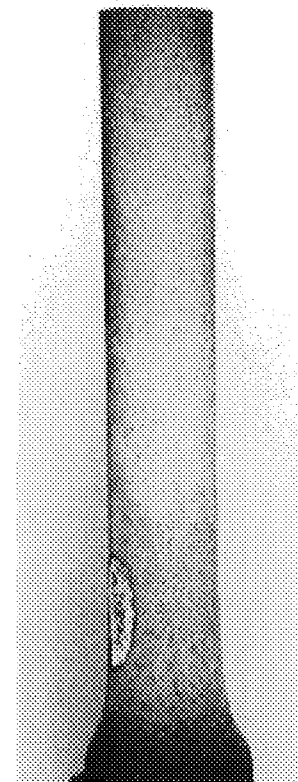


ORIGINAL PAGE IS  
OF POOR QUALITY



NiCoCrAlY+1.6Si  
(LPCS)

2X



NiCoCrAlY+8.5Ta  
(LPCS)

2X

ORIGINAL PAGE IS  
BLACK AND WHITE PHOTOGRAPH

Figure 45 Surface Photographs of Task I Test Samples with NiCoCrAlY-Type Coatings on the Single Crystal Alloy Exposed for 1785 Hours to an Oxidative Environment at 1394°K (2050°F). LPCS = Low Pressure Chamber Sprayed

A metallographic section was obtained from the test section (hot zone) of each test bar exposed for 350 hours and 650 hours to the oxidative environment. Shown in Figure 46 are the representative post-test microstructures of the NiCoCrAlY-type coating systems after 350 hours of exposure. After this test interval, the two NiCoCrAlY + Si (1.2 and 2.2 w/o silicon) and the two NiCoCrAlY + 1.6Si + Ta (8.5 and 4.5 w/o tantalum) coatings exhibited similar post-test microstructures. The quantity of beta phase remaining in the low pressure chamber sprayed NiCoCrAlY + 1.2Si and NiCoCrAlY + 1.6Si + 8.5Ta coatings is greater than the quantity of beta phase remaining in the vapor deposited NiCoCrAlY coating.

Examination of the microstructures of the coated test bars after 650 hours of exposure revealed that the vapor deposited NiCoCrAlY coating system was near failure, while the low pressure chamber sprayed NiCoCrAlY + Si and NiCoCrAlY + Si + Ta coating systems still had some beta phase remaining. This is shown in Figure 47, where the post-test (650 hours) microstructures of these coatings revealed that the quantity of beta phase (and therefore life remaining) in the NiCoCrAlY + Si + Ta coatings increased with the concentration of tantalum. For both the NiCoCrAlY + Si coating systems (1.2 and 2.2 silicon addition), the quantity of beta phase remaining in the coating was approximately similar and was in between the quantity remaining in the two NiCoCrAlY + Si + Ta coating systems. In view of these observations, it is expected that the high tantalum containing NiCoCrAlY + Si + Ta will exhibit the best oxidation resistance followed by the two NiCoCrAlY + Si systems. However, as observed in the Task I testing, the addition of 8.5 weight percent tantalum to NiCoCrAlY resulted in a significant debit in coating ductility. Because the NiCoCrAlY + Si (1 to 2 w/o silicon) coating has a better overall balance of properties, it is the preferred system.

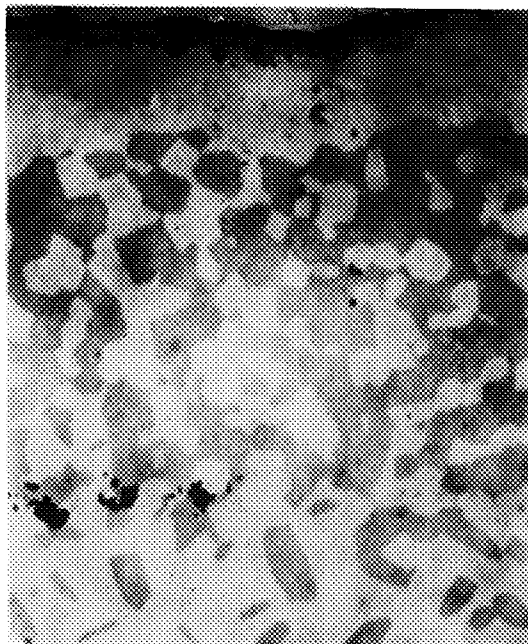
#### b. CoCrAlY-Type Coatings on the B1900 + Hf Alloy

The surface conditions of the modified CoCrAlY plasma sprayed coatings burner rig tested in Task II are summarized in Tables XV and XVI. Table XV presents the observations after 350 hours of oxidation exposure at 1394<sup>0</sup>K (2050<sup>0</sup>F),



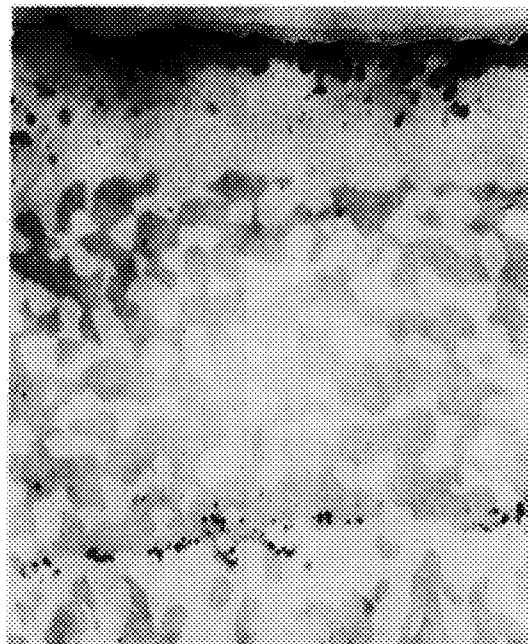
400X

NiCoCrAlY  
Electron-Beam Physical  
Vapor Deposited



400X

NiCoCrAlY+1.2Si  
Low Pressure Chamber Sprayed



400X

NiCoCrAlY+1.6Si+8.5Ta  
Low Pressure Chamber Sprayed

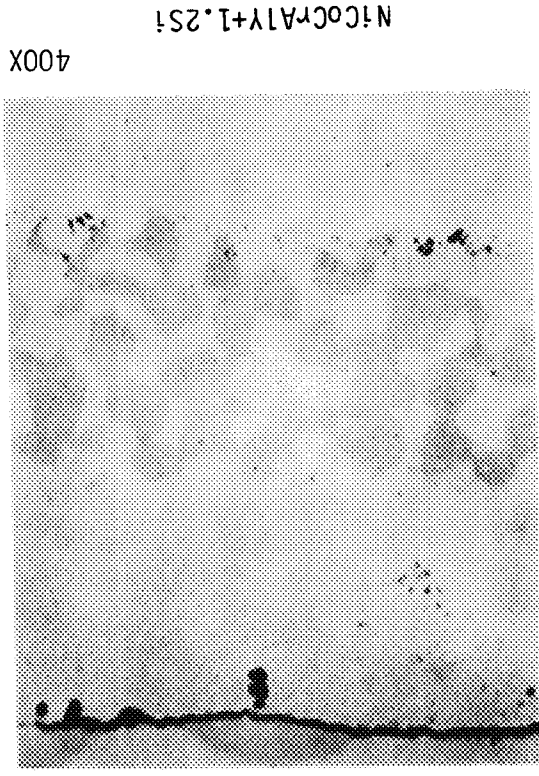
Figure 46

Post-Test Microstructures of the Test Section of NiCoCrAlY-Type Coatings on the Single Crystal Alloy After 350 Hours of Exposure in an Oxidative Environment at 1394<sup>o</sup>K (2050<sup>o</sup>F) during Task II Testing

ORIGINAL PAGE  
BLACK AND WHITE PHOTOGRAPH

ORIGINAL PAGE IS  
OF POOR QUALITY

ORIGINAL PAGE  
BLACK AND WHITE PHOTOGRAPH



Post-Test Microstructures of the Test Section of Low Pressure Chamber Sprayed NiCoCrAlY-Type Coatings on the Single Crystal Alloy After 650 Hours of Exposure in an Oxidative environment at 13940K (2050°F). EB-PVD NiCoCrAlY coating was Near Failure at this Interval

Figure 47

TABLE XV

VISUAL CONDITIONS OF TASK II B1900+Hf SPECIMENS AFTER 350 HOURS OF EXPOSURE IN THE BURNER RIG OXIDATION TEST AT 1394°K (2050°F)

<u>Coating Composition</u>	<u>Coating Process*</u>	<u>Coating Thickness (Microns)</u>	<u>Visual Condition</u>
CoCrAlY	EB-PVD	118	Very light pitting
CoCrAlY+1.6Si	LPCS	170	Light pitting
CoCrAlY+2.7Si	LPCS	162	Very light pitting
CoCrAlY+2.1Si (High Cr, Low Al)	LPCS	165	Moderate pitting
CoCrAlY+HIP (1352°K (1975°F))	LPCS	142	Moderate pitting and blue spinel formed

TABLE XVI

VISUAL CONDITIONS OF COATED B1900+Hf SAMPLES EVALUATED IN BURNER RIG OXIDATION TESTING AT 1394°K (2050°F)

<u>Coating Composition</u>	<u>Coating Process*</u>	<u>Exposure Time (Hours)</u>	<u>Normalized Coating Life** (Hours)</u>	<u>Normalized Time to 1st Coating Penetration</u>	<u>Visual Observation on Test Section</u>
CoCrAlY	EB-PVD	990	1031	147	Failed
CoCrAlY+1.6Si	LPCS	1000	-	149	Light pitting
CoCrAlY+2.7Si	LPCS	1000	-	184	Very light pitting
CoCrAlY+2.1Si (High Cr, Low Al)	LPCS	1000	-	56	Near failure
CoCrAlY+HIP (1352°K (1975°F))	LPCS	838	838	99	Failed
CoCrAlY+HIP (1470°K (2185°F)) (Task I System)	LPCS	892	731	16	Failed

\*EB-PVD = Electron Beam Physical Vapor Deposition  
 LPCS = Low Pressure Chamber Plasma Spray  
 HIP = Hot Isostatic Pressing

\*\*Normalized Coating Life: Coating's Life Normalized to Typical 'Use' Thickness of 127 microns (5.0 mils).

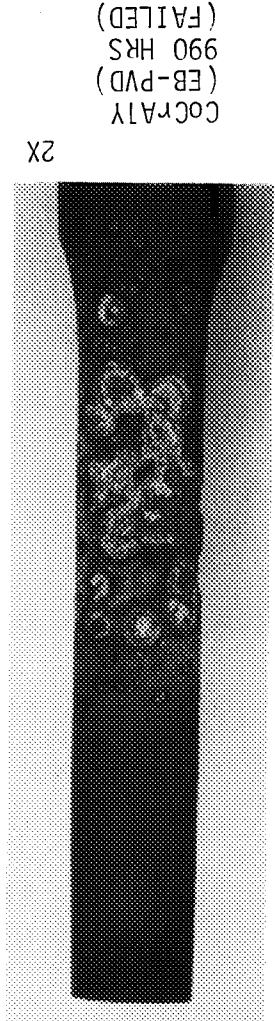
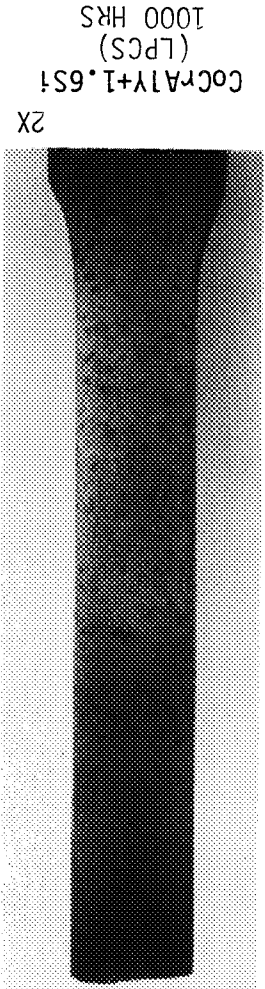
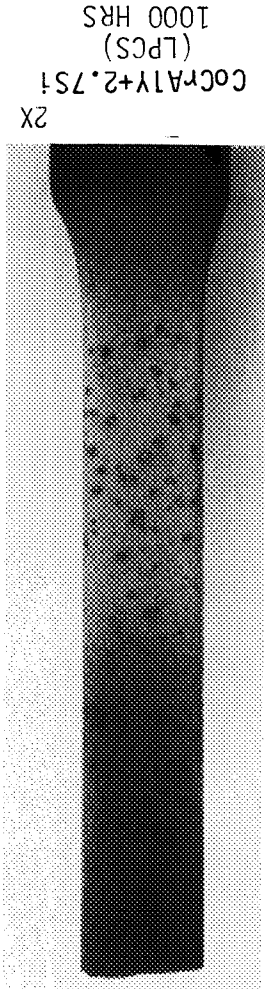
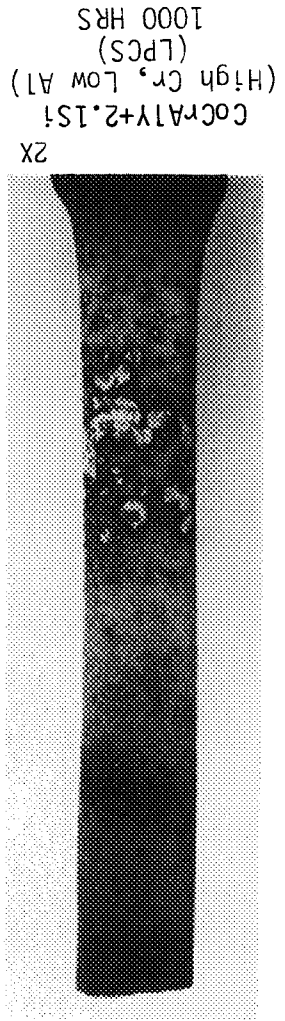
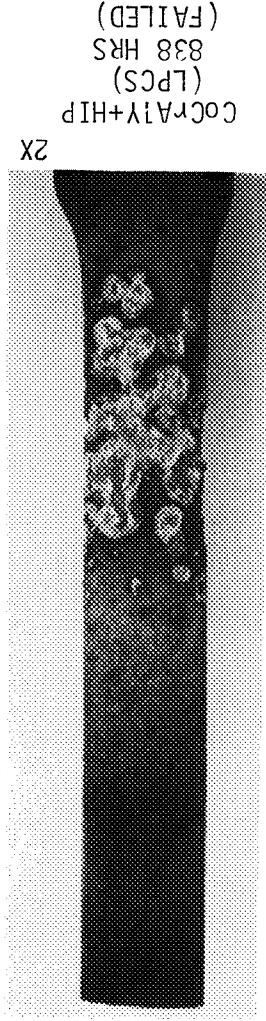
while the surface conditions after 1000 hours are listed in Table XVI. Shown in Figure 48 are the oxidation tested Task II CoCrAlY-base coatings on B1900 + Hf alloy samples after 1000 hours of exposure. As seen in this figure, the two low pressure chamber sprayed CoCrAlY + Si coating systems exhibited the least amount of pitting compared to all other CoCrAlY-type coating systems tested in Task II. In addition, in this test, the hot isostatically pressed CoCrAlY coating system (lower process temperature of 1352<sup>0</sup>K (1975<sup>0</sup>F) appears to have performed slightly better than the Task I hot isostatically pressed CoCrAlY coating system (1470<sup>0</sup>K (2185<sup>0</sup>F) process temperature) examined in Task I. This performance improvement, as noted in Table XVI, is believed to be attributable to lower temperature hot isostatic pressing which resulted in significantly less interdiffusion related aluminum loss to the base alloy during processing (see Figure 42). However, while hot isostatic pressing improved coating density, the process did not provide any improvement in coating durability compared to normally processed low pressure chamber sprayed CoCrAlY.

Shown in Figure 49 are the representative post-test microstructures of the test section of the CoCrAlY-type coated B1900 + Hf alloy samples exposed for 350 hours to the 1394<sup>0</sup>K (2050<sup>0</sup>F) cyclic oxidative environment. All the coating systems except for the low pressure chamber sprayed CoCrAlY + 1.2Si coating system were depleted of beta phase. This microstructural condition is in agreement with the observed surface condition of this coating system (Table XV) which indicated its superior oxidation resistance (less pitting). Silicon modification of the high chromium plus lower aluminum containing CoCrAlY coating did not result in any significant improvement in performance indicating that the effects of aluminum on oxidative resistance are more potent than that of silicon.

#### 4.3.3 Burner Rig Hot Corrosion Testing

The surface conditions of the Task II NiCoCrAlY and CoCrAlY-type coatings after 500 hours of exposure to the 1172<sup>0</sup>K (1650<sup>0</sup>F) burner rig cyclic hot corrosion test are shown in Figures 50 and 51. Only slight to moderate surface

ORIGINAL PAGE  
BLACK AND WHITE PHOTOGRAPH



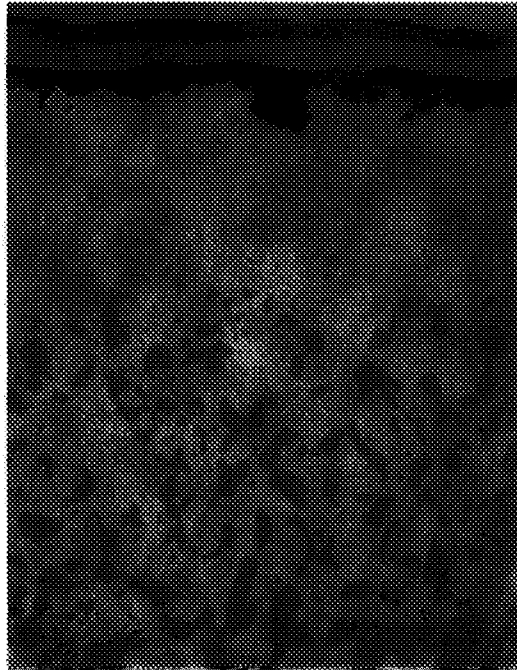
Surface Photographs of Test Samples With CoCrAlY-Type coatings on B-1900+Hf Alloy Exposed to an Oxidative Environment at 13940K (2050°F). EB-PVD = Electron-Beam Physical Vapor Deposited LPCS = Low Pressure Chamber Sprayed

Figure 48



400X

CoCrAlY  
Electron-Beam Physical  
Vapor Deposited



400X

CoCrAlY+1.6Si  
Low Pressure Chamber Sprayed



400X

CoCrAlY+HIP  
Low Pressure Chamber Sprayed

Figure 49

Post-Test Microstructures of the Test Section of CoCrAlY-Type Coatings on B-1900+Hf Alloy After 350 Hours of Exposure in an Oxidative environment at 1394°K (2050°F)

ORIGINAL PAGE  
BLACK AND WHITE PHOTOGRAPH

ORIGINAL PAGE IS  
OF POOR QUALITY



ORIGINAL PAGE  
BLACK AND WHITE PHOTOGRAPH



Figure 50 Surface Photographs of Test Samples With CoCrAlY-Type Coatings on B-1900+Hf Alloy Exposed 500 Hours to a Hot Corrosive Environment at 11720K (1650°F). EB-PVD = Electron-Beam Physical Vapor Deposited; LPCS = Low Pressure Chamber Sprayed

ORIGINAL PAGE IS  
OF POOR QUALITY

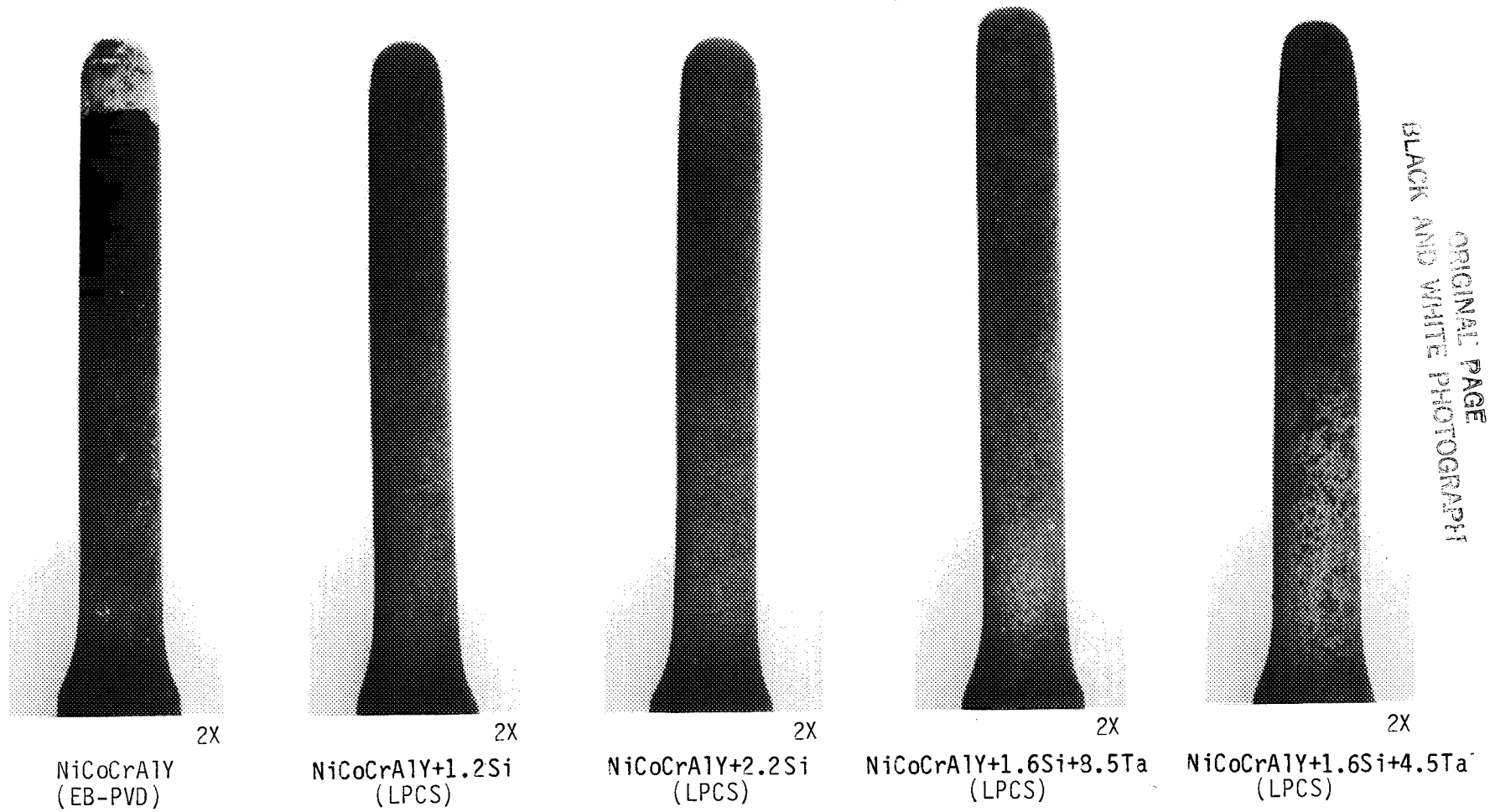


Figure 51 Surface Photographs of Test Samples With NiCoCrAlY-Type Coatings on the Single Crystal Alloy Exposed 500 Hours to a Hot Corrosive Environment at 1172°K (1650°F). EB-PVD = Electron-Beam Physical Vapor Deposited; LPCS = Low Pressure Chamber Sprayed

degradation was experienced by all the coating systems and those visual observations are summarized in Table XVII. Based on visual appearance, the best hot corrosion resistant low pressure chamber sprayed coatings were observed to be CoCrAlY + 1.6Si for the B1900 + Hf alloy, and the NiCoCrAlY + Si and both NiCoCrAlY + Si + Ta systems for the single crystal alloy\*.

As in the Task II oxidation test, some of the Task I tested coating systems were further exposed in the Task II hot corrosion test. The low pressure chamber sprayed CoCrAlY + 2.0Si and vapor deposited CoCrAlY coated B1900 + Hf alloy samples were additionally exposed for 500 more hours in Task II. After a total of 1000 hours of exposure to this hot corrosive environment, the surface conditions of these two coatings were as shown in Figure 52. As can be seen, even after 1000 hours of testing these coatings only show moderate surface degradation. This behavior supports the previously made statements that most coatings evaluated during this program on both the single crystal and the B1900 + Hf alloy samples exhibited good hot corrosion resistance with no evidence of coating failure.

---

\*The surface photographs in Figures 50 and 51 show test samples with rounded tips which are unlike the test samples in Figures 44, 45 and 49. This is because when testing in hot corrosive environment the base metal is usually subjected to severe hot corrosive attack. To eliminate this base metal attack and the resultant undercutting which may lead to premature failure of the coating through internal base metal hot corrosion, the tip areas of the test samples were not cut off for pre-test metallographic examination and therefore appear rounded. In some cases the coating was thin near the tip resulting in premature coating failure in this area. When this occurred, the area was repaired and this resulted in a distorted tip area as can be seen in these figures. The failure of the coating in the tip area of some samples is not indicative of the hot corrosion resistance of the coating on that particular alloy.

TABLE XVII

VISUAL CONDITIONS OF SAMPLES EVALUATED IN THE TASK II  
BURNER RIG HOT CORROSION TEST AT 1172°K (1650°F)

Test Time: 500 Hours

<u>Substrate Alloy</u>	<u>Coating Composition</u>	<u>Coating Process*</u>	<u>Visual Observation on Test Section</u>
B1900+Hf	CoCrAlY	EB-PVD	Slight surface degradation
	CoCrAlY+1.6Si	LPCS	Slight surface degradation
	CoCrAlY+2.7Si	LPCS	Slight surface degradation
	CoCrAlY+2.1Si (High Cr, Low Al)	LPCS	Moderate surface degradation
	CoCrAlY+HIP	LPCS	Moderate surface degradation
Single Crystal	NiCoCrAlY	EB-PVD	Slight surface degradation
	NiCoCrAlY+1.2Si	LPCS	Slight surface degradation
	NiCoCrAlY+2.2Si	LPCS	Slight surface degradation
	NiCoCrAlY+1.6Si+8.5Ta	LPCS	Slight surface degradation
	NiCoCrAlY+1.6Si+4.5Ta	LPCS	Slight surface degradation

\*EB-PVD = Electron Beam Physical Vapor Deposition  
LPCS = Low Pressure Chamber Plasma Spray  
HIP = Hot Isostatic Pressing

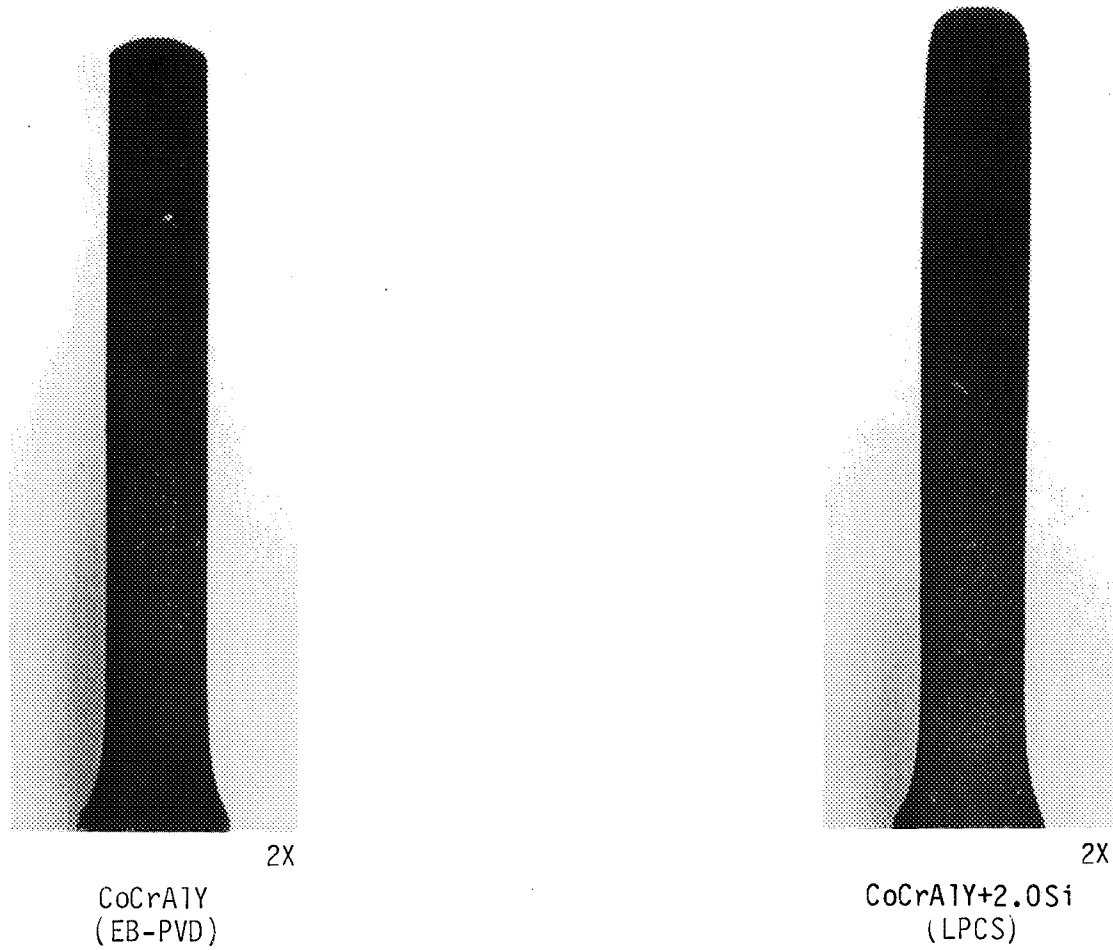


Figure 52

Surface Photographs of Test Samples With CoCrAlY-Type Coatings on the Single Crystal Alloy Exposed 1000 Hours to a Hot Corrosive Environment at 1172°K (1650°F), EB-PVD = Electron-Beam Physical Vapor Deposited; LPCS = Low Pressure Chamber Sprayed

A metallographic section was obtained from the test section (hot zone area) of each test bar exposed for 350 hours and 500 hours to the hot corrosive environment. As stated previously, all coating/alloy systems showed slight or moderate surface degradation. The post-test microstructural conditions confirmed this observation, i.e., only minimal amounts of beta phase depletion was observed under the oxide scale of all coating systems. Shown in Figures 53 and 54 are the post-test microstructures of the test sections of the CoCrAlY-type coatings after 500 hours of exposure to the hot corrosive environment. The least amount of beta phase depletion was observed in both of the CoCrAlY + Si coating variations (1.6 and 2.7 w/o silicon additions). Based on this result and the results of the CoCrAlY-type coatings in the oxidation test, the CoCrAlY + Si coating with silicon additions of 1.5 to 2.5 weight percent was considered to be the best system for the B1900 + Hf alloy.

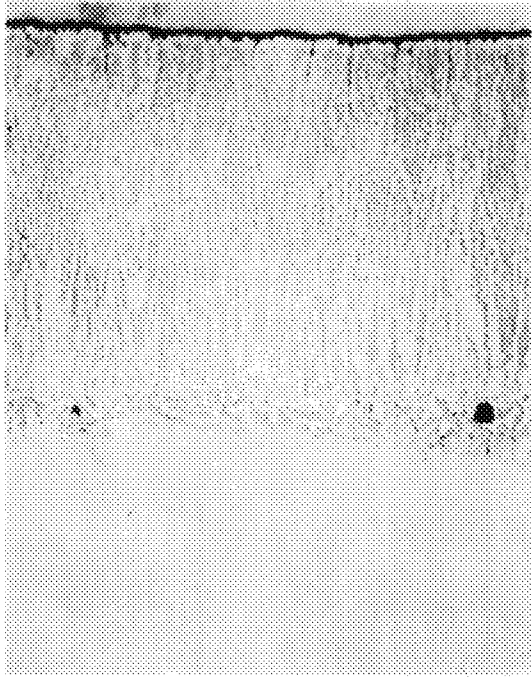
Hot corrosion degradation was observed to be minimal in the case of every coating system of the various NiCoCrAlY based coatings on the single crystal alloy. This is illustrated in Figure 55 and 56 where post-test microstructures of the coated single crystal alloy samples are shown after 500 hours of exposure to the hot corrosive environment (35 ppm salt plus 1.3 w/o sulfur added in the form of  $\text{SO}_2$ ).

#### 4.4 Summary of Task II Results and Selection of Coatings for Task III Engine Testing

From the results of the cyclic burner rig oxidation and hot corrosion evaluations of eight modified low pressure chamber plasma sprayed overlay coatings, the following conclusions were derived.

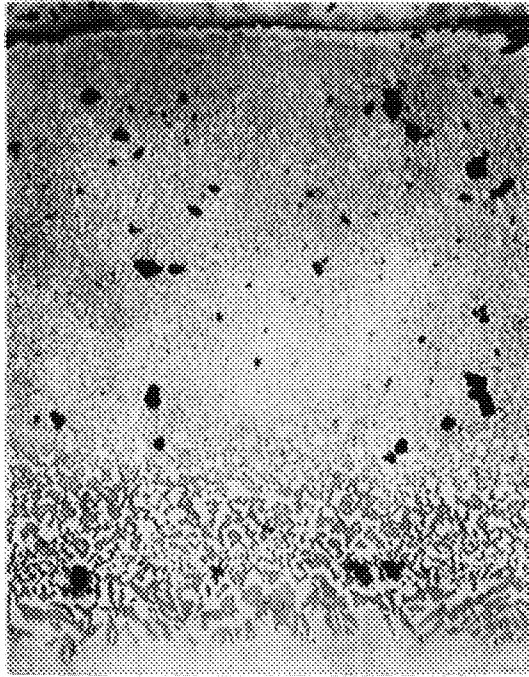
- The low pressure chamber sprayed NiCoCrAlY + 1.6Si coating system had the best balance of properties for protecting the single crystal alloy. This system provided a life improvement of about twice that of the baseline vapor deposited NiCoCrAlY coating.

ORIGINAL PAGE IS  
OF POOR QUALITY



CoCrAlY  
Electron-Beam Physical  
Vapor Deposited

400X



CoCrAlY+1.6Si  
Low Pressure Chamber Sprayed

400X

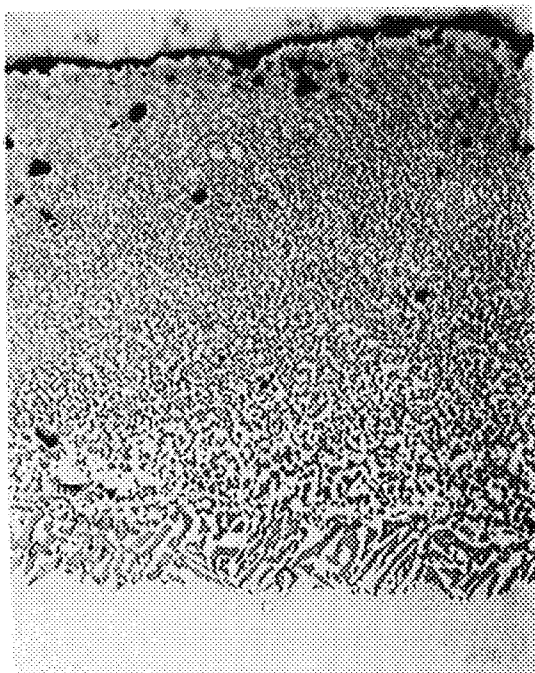


CoCrAlY+2.7Si  
Low Pressure Chamber Sprayed

400X

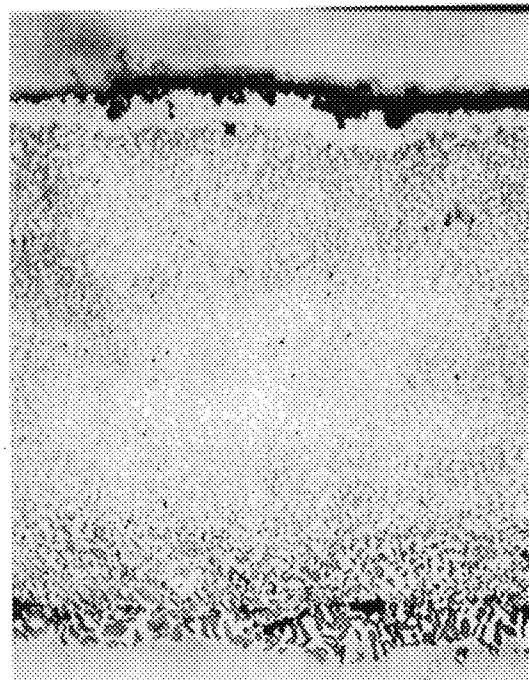
Figure 53 Post-Test Microstructures of the Test Section of CoCrAlY-Type Coatings on B-1900+Hf Alloy After 500 Hours of Exposure in a Hot Corrosive Environment at 1172°K (1650°F)

ORIGINAL PAGE  
BLACK AND WHITE PHOTOGRAPH



400X

CoCrAlY+2.1Si  
(High Cr, Low Al)  
Low Pressure Chamber Sprayed



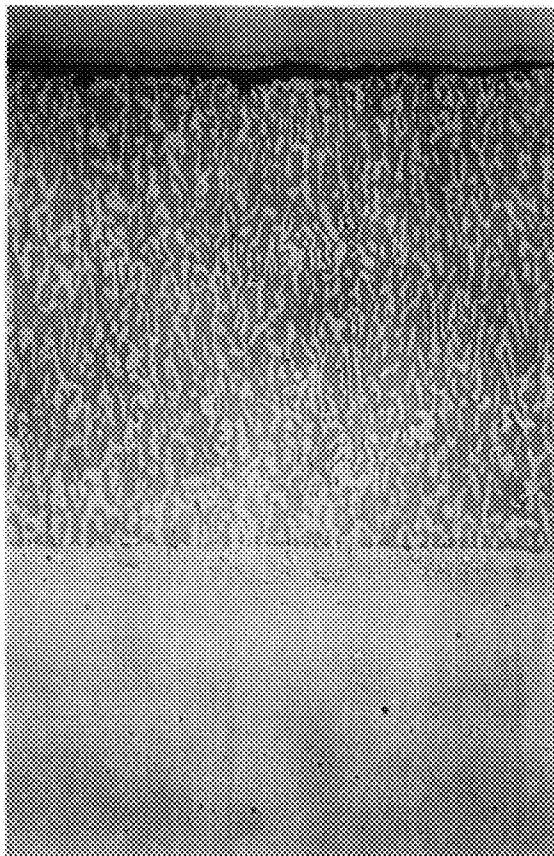
400X

CoCrAlY+HIP (1975°F)  
Low Pressure Chamber Sprayed

Figure 54 Post-Test Microstructures of the Test Section of CoCrAlY-Type Coatings on B-1900+Hf Alloy After 500 hours of Exposure in a Hot Corrosive Environment at 1172°K (1650°F)

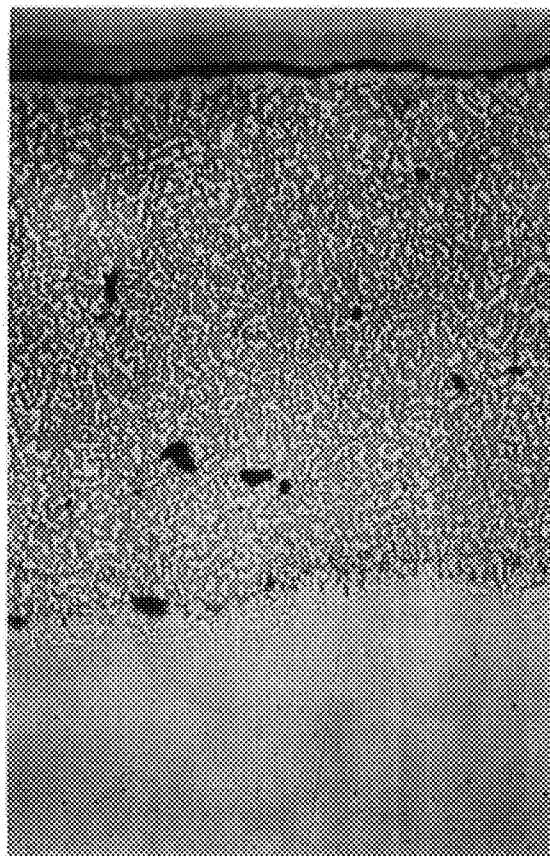
ORIGINAL PAGE  
BLACK AND WHITE PHOTOGRAPH





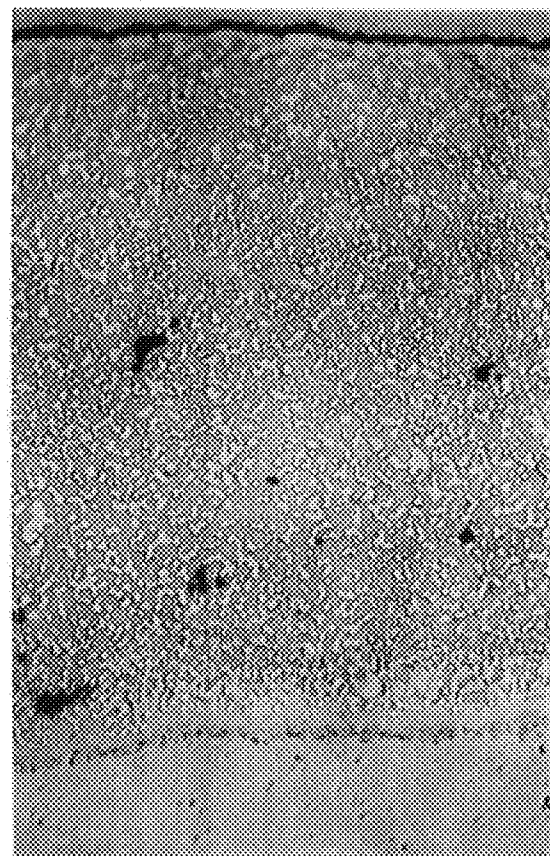
NiCoCrAlY  
Electron-Beam Physical  
Vapor Deposited

500X



NiCoCrAlY + 1.2Si  
Low Pressure Chamber Sprayed

500X

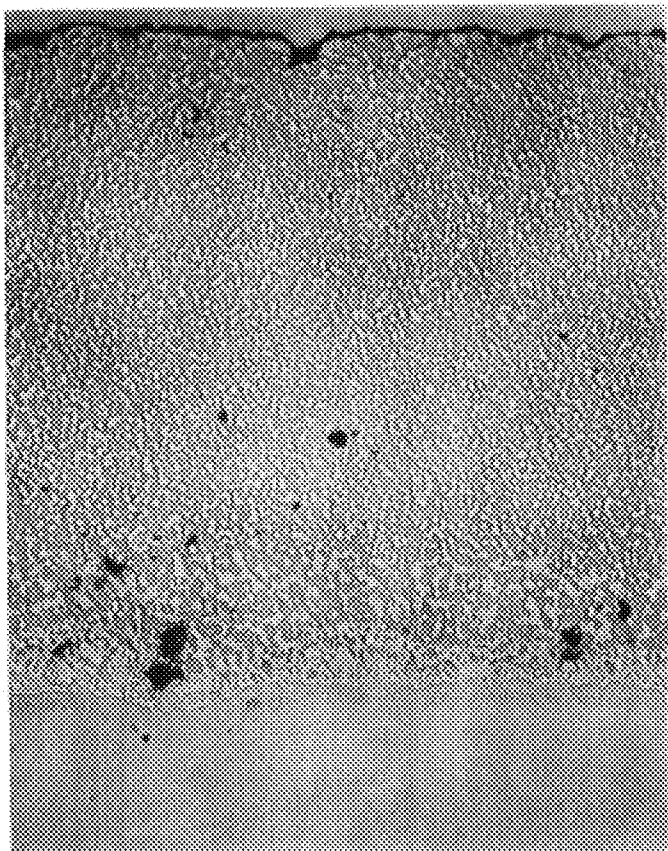


NiCoCrAlY + 2.2Si  
Low Pressure Chamber Sprayed

500X

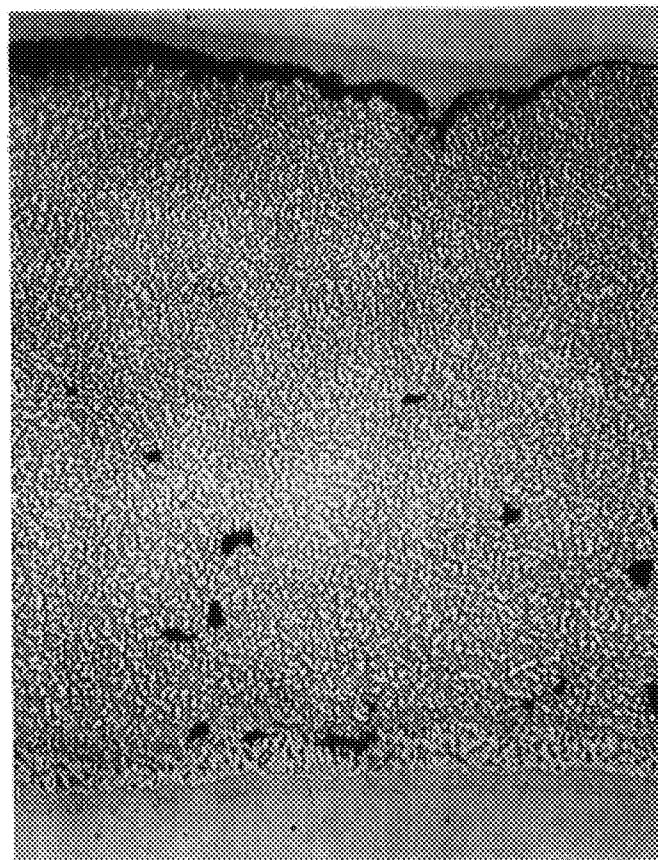
Figure 55 Post-Test Microstructures of the Test Sections of NiCoCrAlY Based Coatings on the Single Crystal Alloy After 500 Hours of Exposure in a Hot Corrosive Environment at 1172<sup>o</sup>K (1650<sup>o</sup>F). Note No Measureable Degradation on Any Coating.

ORIGINAL PAGE  
BLACK AND WHITE PHOTOGRAPH



500X

NiCoCrAlY + 1.6Si + 4.5Ta  
Low Pressure Chamber Sprayed



500X

NiCoCrAlY + 1.6Si + 8.5Ta  
Low Pressure Chamber Sprayed

ORIGINAL PAGE  
BLACK AND WHITE PHOTOGRAPH

Figure 56 Post-Test Microstructures of the Test Sections of Both NiCoCrAlY + Si + Ta Modifications on the Single Crystal Alloy After 500 Hours of Exposure in a Hot Corrosive Environment at 1172°K (1650°F). Note No Measureable Degradation on Any of the Two Modifications.

- Both variations of the NiCoCrAlY + Si system (1.2 and 2.2 w/o silicon additions) oxidation tested in this task exhibited almost the same but considerably superior durability to that shown by the baseline vapor deposited NiCoCrAlY. This result indicates that a silicon addition between 1 and 2 percent will be acceptable and provides a broad enough composition range to be controllable in large scale coating operations.
- In the cyclic oxidative environment at 1394<sup>0</sup>K (2050<sup>0</sup>F), the best performing low pressure chamber plasma sprayed coating for the single crystal alloy was judged to be NiCoCrAlY + 1.6Si + 8.5Ta. However, coating ductility results obtained in Task I, demonstrated that the addition of 8.5 weight percent tantalum to NiCoCrAlY reduced its resistance to cracking significantly thereby making the tantalum addition less attractive.
- The hot corrosion resistance of all of the NiCoCrAlY based coatings on the single crystal alloy was observed to be excellent. None of the evaluated coating systems exhibited observable degradation after 500 hours of exposure in the Task II ducted burner rig test at 1172<sup>0</sup>K (1650<sup>0</sup>F).
- In the cyclic oxidation test, the best system in the CoCrAlY group of coatings for the B1900 + Hf alloy was judged to be the low pressure chamber sprayed CoCrAlY + Si system. Both variations of this coating (1.6 and 2.7 w/o silicon additions) were the only plasma sprayed systems which outperformed the baseline vapor deposited CoCrAlY coating.
- All CoCrAlY based candidates on the B1900 + Hf alloy exhibited excellent hot corrosion resistance. Task II specimens were exposed for 500 hours in the test without any visual degradation.

Based on above results and various property data obtained in Task I the following two coating systems have been selected for engine testing during Task III.

- Ni-22Co-18Cr-12Al-0.5Y-1.5Si for protection of the single crystal JT9D-7R4 first stage turbine blade.
- Co-22Cr-12Al-0.5Y-2.0Si for protection of the B1900 + Hf JT8D-17 first stage turbine blade.

#### 4.5 Task III Engine Test Evaluations

In Task III, the durability of the optimized low pressure chamber plasma sprayed NiCoCrAlY + Si and CoCrAlY + Si coatings will be evaluated in experimental engines to verify the results obtained in Tasks I and II. The former coating will be compared with the baseline vapor deposited NiCoCrAlY system on the single crystal alloy first stage turbine blades of an operating JT9D-7R4 engine. Similarly, the CoCrAlY + Si coating will be compared with the baseline vapor deposited CoCrAlY system on the B1900 + Hf first stage turbine blades of an operating JT8D-17 engine.

Five single crystal and five B1900 + Hf first stage turbine blades are currently being low pressure chamber plasma sprayed by Howmet Corporation using the same process parameters utilized to coat samples during Tasks I and II. Coating thickness and quality control will be maintained according to typical Pratt & Whitney Aircraft standards and specifications for blade alloy coatings. Conformity of coating structure and thickness will be determined by destructive analysis of one blade representing each alloy/coating system. All pre- and post-coating processing used for blade components will be identical to those used for Task I and II samples to ensure exact correspondence of burner rig and engine test coatings regarding coating structure and composition.

The performance of the plasma sprayed coatings in both engines will be assessed and compared with the corresponding vapor deposited coatings on the basis of visual appearance and post-test microstructural examination.

#### 4.6 Discussion

Plasma sprayed MCrAlY coatings, prior to this investigation, failed to perform as well in laboratory and engine tests as similar coatings produced by the electron beam physical vapor deposition process. This program has identified a plasma spray process and coating compositions which exhibit considerable improvement over the performance of baseline vapor deposited NiCoCrAlY and CoCrAlY coatings, thus exceeding the program objectives. As indicated in previous sections the low pressure chamber plasma sprayed NiCoCrAlY + Si and CoCrAlY + Si coatings provided the best high temperature oxidation and corrosion resistance for the single crystal and B1900 + Hf alloy respectively. With the successful completion of this program, for the first time, it is possible to exploit the potential economic and technical benefits of plasma spraying for gas turbine airfoil coatings. The next logical step is to establish the manufacturing technology needed to translate the process into production and overhaul usage.

Several process procedures must be put in place or optimized in order to scale-up the low pressure chamber plasma spray coating process. Methods for controlling process parameters during the coating operation must be established so that reproducible coating quality and thickness will be obtained on a high parts volume basis. To economically achieve this, automated processing and part manipulation will be required. Acceptable tolerances for the improved pre- and post-coating procedures must be identified along with production-oriented methods for carrying out these operations. Realistic quality standards must be determined for the starting powder feedstock and the resultant coatings along with the required postcoating quality assurance procedures. Throughout all of this work, care must be exercised not to impose overly complicated methods or excessively stringent requirements leading to cost burdens which will defeat a major potential advantage of the plasma spray

process. More extensive laboratory and engine testing will also be mandatory to validate the durability of plasma sprayed coatings compared to state-of-the-art electron beam physical vapor deposited MCrAlY coatings. These tasks are similar to those required for any new coating system/process.

The plasma spray coatings optimized in this program can potentially be used in two ways. First, they can be implemented as replacements of electron beam physical vapor deposited MCrAlY coatings to reduce coating costs and/or improve durability of gas turbine airfoils. A second important use is to provide a more durable metallic sublayer for ceramic thermal barrier coatings. The use of these insulative ceramic coatings on airfoils and platforms will increase component durability and/or improve engine performance.

Until now, the weak link of thermal barrier coatings has been thermal stress-induced spalling of the ceramic. The recent significant progress achieved in spall resistance, however, has led to oxidation of the underlying metallic coating causing the ceramic to buckle and rupture from the eruption of voluminous oxidation products. The problem is caused by the pervious nature of ceramics such as zirconia to oxygen transport at elevated temperature and poor oxidation resistance of air plasma sprayed MCrAlY coatings. Use of the low pressure chamber plasma spray process would increase the oxidation resistance of the underlying MCrAlY coating. The plasma sprayed NiCoCrAlY + Si coating optimized in this program is believed to be the best candidate for such a metallic sublayer.

## 5.0 CONCLUSIONS

Burner rig cyclic oxidation and hot corrosion, and tensile ductility tests indicated that low pressure chamber plasma sprayed NiCoCrAlY + Si (Ni-22Co-18Cr-12Al-0.5Y-1.5Si) and CoCrAlY + Si (Co-22Cr-12Al-0.5Y-2.0Si) coatings are capable of protecting the high temperature-high pressure gas path surfaces of single crystal and B1900 + Hf turbine airfoils respectively. These coatings outperformed the baseline electron beam physical vapor deposited NiCoCrAlY and CoCrAlY coatings on the aforementioned alloys, thus exceeding the program goals.

A brief summary of the principal findings resulting from this program is presented below.

- Plasma sprayed NiCoCrAlY and CoCrAlY coatings produced in an atmospheric argon chamber exhibited lives inferior to those shown by coatings of similar composition but plasma sprayed in a low pressure argon environment. The one-atmosphere argon sprayed coatings did not provide adequate protection to either the single crystal or the B1900 + Hf alloy in cyclic oxidation testing at 1394<sup>0</sup>K (2050<sup>0</sup>F). However, these coatings lasted satisfactorily for 500 hours in a cyclic hot corrosive environment at 1172<sup>0</sup>K (1650<sup>0</sup>F).
- The low pressure chamber plasma sprayed NiCoCrAlY coating on the single crystal alloy endured 1000 hours of cyclic exposure at 1394<sup>0</sup>K (2050<sup>0</sup>F) and provided slightly better protection than that shown by the vapor deposited NiCoCrAlY coating of essentially similar composition. However, the oxidation behavior of the low pressure chamber sprayed CoCrAlY coating was inferior to that of vapor deposited CoCrAlY on the B1900 + Hf alloy.

- Silicon and tantalum additions to the basic NiCoCrAlY chemistry significantly improved the cyclic oxidation resistance of this coating at 1394<sup>0</sup>K (2050<sup>0</sup>F). Low pressure chamber plasma sprayed NiCoCrAlY + Si (1 to 2 w/o) and NiCoCrAlY + 8.5Ta coatings exhibited a twofold life improvement over the baseline vapor deposited NiCoCrAlY coating on the single crystal alloy. The low pressure chamber plasma sprayed NiCoCrAlY + Si system was selected for Task III engine testing based on a good balance of oxidation and corrosion resistance plus tensile ductility.
- Comparative 1394<sup>0</sup>K (2050<sup>0</sup>F) cyclic oxidation burner rig testing of the CoCrAlY based coating systems on B1900 + Hf revealed that only the low pressure chamber plasma sprayed CoCrAlY + Si (1.5 to 2.5 w/o) coating exhibited durability superior to the baseline vapor deposited CoCrAlY coating on the B1900 + Hf alloy. This coating system was therefore selected for Task III engine testing.
- Hot isostatic pressing of the CoCrAlY coating at two temperatures, 1470<sup>0</sup>K (2185<sup>0</sup>F)/3 hours and 1352<sup>0</sup>K (1975<sup>0</sup>F)/4 hours, improved coating density, however, this improvement did not increase the cyclic oxidation resistance of the coating.
- The low pressure chamber sprayed NiCoCrAlY-type and CoCrAlY-type coatings provided the single crystal and B1900 + Hf alloys with satisfactory protection in 500 hour cyclic burner rig hot corrosion tests at 1172<sup>0</sup>K (1650<sup>0</sup>F).
- Ductility tests conducted at 588<sup>0</sup>K (600<sup>0</sup>F) indicated that low pressure chamber sprayed MCrAlY coatings are slightly more ductile than vapor deposited MCrAlY coatings of similar composition. This behavior is believed to be related to the structural differences (grain size and orientation; defect type and shape) between the coatings produced by the two processes.



- Silicon and tantalum additions to NiCoCrAlY and silicon additions to CoCrAlY reduced coating ductility at 588<sup>0</sup>K (600<sup>0</sup>F). However, the low pressure chamber sprayed NiCoCrAlY + Si and CoCrAlY + Si coatings still exhibited fracture strains equivalent to those shown by the baseline vapor deposited NiCoCrAlY and CoCrAlY coatings.

## 6.0 RECOMMENDATIONS

Based on the results and conclusions of this program, the following courses of action are recommended.

- With the identification of the low pressure chamber plasma spray process as a workable method to produce MCrAlY coatings, establishment of production methods, process control techniques, and quality assurance standards for depositing these coatings on a high volume basis is recommended.
- The thermal fatigue behavior of the NiCoCrAlY + Si and CoCrAlY + Si coatings should be determined to ascertain how use of these coatings will impact total fatigue life of coated turbine blades and vanes.
- With the identification of the silicon modified NiCoCrAlY and CoCrAlY coating compositions as prime candidates for protecting airfoils, detailed studies of the effects of silicon on protection mechanisms and the impact of this element on the distribution of aluminum and yttrium in the coatings are recommended.

## References

- (1) Lowell, C.E., and Miner, R.V., "Improvement in Cyclic Oxidation of the Nickel-Base Superalloy B-1900 by Addition of One Percent Silicon", NASA Technical Memorandum X-68191.
- (2) Santoro, G.J., Deadmore, D.L., and Lowell, C.E., "Oxidation of Alloys in Nickel-Aluminum System with Third-Element Additions of Chromium, Silicon, and Titanium at 1100°C", NASA Technical Note D-6414, July 1971.
- (3) Gedwill, M.A., "An Evaluation of Three Oxidation-Resistant Alloy Claddings for IN100 and WI52 Superalloys", NASA Technical Note D-5483, 1969.
- (4) Stringer, J., Allam, I.M., and Whittle, D.P., "The High Temperature Oxidation of Co-Cr-Al Alloy Containing Yttrium and Hafnium" Proceedings of the International Conference on Metallurgical Coatings, San Francisco, CA, March 1977.
- (5) Pettit, F.S., and Tien, J.K., Metallurgical Transaction 3 1587, 1972.
- (6) Hecht, R.J., "Superalloy Base Having a Coating Containing Silicon for Corrosion/Oxidation Protection", U.S. Patent No. 4,034,142, July 5, 1977.
- (7) Grisaffe, S.J., and Merutka, J.P., "Coatings for Aircraft Gas Turbine Engines and Space Shuttle Heat Shields: A Review of Lewis Research Center Programs", NASA Technical Memorandum X-68007.
- (8) Felten, E.J., Unpublished Research, Pratt & Whitney Aircraft.
- (9) Goebel, J.A., "Advanced Coating Development for Industrial/Utility Gas Turbine Engines", Proceedings of the First Conference on Advanced Materials for Alternative Fuel Capable Directly Fired Heat Engines, Castine, Maine, July 1979.

- (10) Vargas, J.R., Ulion, N.E., and Goebel, J.A., "Advanced Coating Development for Industrial/Utility Gas Turbine Engines", Proceeding of Sixth International Conference on Metallurgical Coatings, San Diego, CA, April 1980.
- (11) Baur, R., Grunling, H., and Scheneider, K., "Silicon and Chrome Base Coatings for Stationary Gas Turbines", Proceedings of the First Conference on Advanced Materials for Alternative Fuel Capable Directly Fired Heat Engines, Castine, Maine, July 1979.
- (12) Pettit, F.S., and Giggins, C.S., Unpublished Research, Pratt & Whitney Aircraft.

## DISTRIBUTION LIST

Mr. G. C. Deutsch/RW  
NASA Headquarters  
600 Independence Avenue  
Washington, DC 20546

Library (2) Copies  
MS 60-3  
NASA Lewis Research Center  
21000 Brookpark Road  
Cleveland, OH 44135

Mr. S. J. Grisaffe  
MS 105-1  
NASA Lewis Research Center  
2100 Brookpark Road  
Cleveland, OH 44135

Mr. R. Rudey  
MS 60-4  
NASA Lewis Research Center  
21000 Brookpark Road  
Cleveland, OH 44135

Library  
NASA  
Goddard Space Flight Center  
Greenbelt, MD 20771

Library  
NASA  
Marshall Space Flight  
Center  
Huntsville, Alabama 35812

Applied Technology Lab  
DAVDL-ATP-ATP  
Attn: J. Lane  
Ft. Eustis, VA 23604

Dr. L. Harris/RW  
NASA Headquarters  
60000 Independence Avenue  
Washington, DC 20546

Technology Utilization  
MS 3-19  
NASA Lewis Research Center  
21000 Brookpark Road  
Cleveland, OH 44135

Dr. M. Greenfield/RWM  
NASA Headquarters  
600 Independence Avenue  
Washington, DC 20546

Report Control Office  
MS 5-5  
NASA Lewis Research Center  
21000 Brookpark Road  
Cleveland, OH 44135

Mr. N. T. Saunders  
MS 49-1  
NASA Lewis Research Center  
21000 Brookpark Road  
Cleveland, OH 44135

Mr. Mike Bauccio DRDAV-DS  
Army Av. Res. & Dev. Com.  
4300 Goodfellow  
St. Louis, MO 63120

Library/Acquisitions  
Jet Propulsion Lab.  
4800 Oak Grove Drive  
Pasadena, CA 91103

Mr. J. Fairbanks  
DOE  
Division of FFU  
MSE 178  
Washington, DC 20545

Reports Acquisition  
Aerospace Corporation  
P.O. Box 92957  
Los Angeles, CA 90009

Matls. & Struct. Section  
MS 501-11  
21000 Brookpark Road  
Cleveland, OH 44135

Mr. J. P. Merutka (10) Copies  
MS 49-1  
NASA Lewis Research Center  
21000 Brookpark Road  
Cleveland, OH 44135

DISTRIBUTION LIST (Cont'd)

Dr. H. B. Probst  
MS 49-3  
NASA Lewis Research Center  
21000 Brookpark Road  
Cleveland, OH 44135

Dr. S. R. Levine  
MS 49-1  
NASA Lewis Research Center  
21000 Brookpark Road  
Cleveland, OH 44135

Library M.S. 185  
NASA  
Langley Research Center  
Langley Field, VA 23365

Dr. R. I. Jaffee  
E.P.R.I.  
2412 03 Hillview Avenue  
Palo Alto, CA 94304

Mr. A. L. Baldi V.P. R&D  
Alloy Surfaces Co. Inc.  
100 S. Justison Street  
Wilmington, DE 19899

Dr. S. Shankar  
Howmet Corporation  
699 Benston Road  
Whithall, MI 49461

Dr. Paul Stemers K1,4A21  
General Electric Company  
R&D Center  
P. O. Box 8  
Schenectady, N.Y. 12341

Mr. D. Hanink  
Engineering Operations  
Detroit Diesel Allison  
General Motors Corp.  
Indianapolis, IN 46206

Dr. Owen  
TRW INC-AECR  
1400 N. Cameron Street  
Harrisburg, PA 17105

Materials Division File  
MS 49-1  
NASA Lewis Research Center  
21000 Brookpark Road  
Cleveland, OH 44135

Mr. B. Stein  
MS 188-B  
NASA  
Langley Research Center  
Langley Field VA 23665

Technical Library, Code JM6  
NASA  
Manned Space Craft Center  
Houston, TX 77058

Mr. G. A. Wacker  
Head Metals Division  
Naval Ship R&D Center  
Annapolis, MA 21402

Mr. W. R. Freeman  
Howmet Corporation  
600 Terrace Plaza  
Muskegon, MI 49441

Mr. Charles Ammann  
Tech. Dir., Coated Products  
Chromalloy R&T Div.  
Blaisdell Road  
Orangeburg, NY 10962

Mr. J. R. Rairden K1,  
General Electric Company  
R&D Center  
P. O. Box 8  
Schenectady, NY 12341

Mr. A. R. Stetson  
Solar Turbines Int'l  
2200 Pacific Highway  
P. O. Box 80966  
San Diego, Cal. 92138

Mr. John Kocis  
TRW INC-AECR  
1400 N. Cameron Street  
Harrisburg, PA 17105

DISTRIBUTION LIST (Cont'd)

Technical Reports Library  
Oak Ridge National Lab.  
Oak Ridge, Tenn. 37830

Library  
Research & Delv. Center  
General Electric Company  
P. O. Box 8  
Schenectady, N.Y. 12301

Mr. R. Hecht  
Pratt & Whitney Aircraft  
United Technologies Corp.  
Government Products Division  
West Palm Beach, FL 33402

Mr. George A. Graves  
University of Dayton  
Research Center R 162 KL  
300 College Park Avenue  
Dayton, Ohio 45409

Dr. Donald Wood K1,  
General Electric Company  
R&D Center  
P. O. Box 8  
Schenectady, NY 12341

Ms. Lulu Hsu  
Solar Turbines Int'l  
2200 Pacific Highway  
P. O. Box 80966  
San Diego, CA 92138

Dr. D. K. Gupta  
J. Building (MERL)  
Pratt & Whitney Aircraft  
400 Main Street  
East Hartford, CT 06108

MCIC  
Battelle Memorial Inst.  
505 King Avenue  
Columbus, OH 43201

Library  
AVCO Systems Division  
201 Lowell Street  
Lowell, Mass. 01851

UTC Library, M. Donnelly  
United Technologies Corp.  
400 Main Street  
East Hartford, CT 06108

Mr. N. Geyer  
AFWAL/MLLM  
Wright Patterson AFB  
Ohio 45433

Dr. W. B. Hillig K1, 4A21  
General Electric Company  
R&D Center  
P. O. Box 8  
Schenectady, NY 12341

Mr. S. Rangaswamy  
METCO, Inc.  
1101 Propsect Avenue  
Westbury, L.I., NY 11590

Mr. J. W. Vogan  
Solar Turbines Int'l  
2200 Pacific Highway  
P. O. Box 80966  
San Diego, CA 92138

Dr. T. E. Strangman  
Airesearch Mfg. Company  
111 S. 34th Street  
Phoenix, AZ  
85034

Library  
Cabot Corporation  
Stellite Division  
P. O. Box 746  
Kokomo, Indiana 46901

DISTRIBUTION LIST (Cont'd)

Library  
Pratt & Whitney Aircraft  
United Technologies Corp.  
West Palm Beach, FL 33402

Mr. E. E. Bailey  
AFWAL-NASA  
Wright-Patterson AFB  
Ohio 45433

Dr. N. Lindblad MPTL  
Mail Drop M-85  
General Electric Company  
Cincinnati, OH 45215

Mr. D. K. Ratcliffe  
Corning-Zircoa  
31501 Solon Road  
Solon, OH 44139

Dr. William P. Minnear  
Build K-1, Room 4A45  
General Electric Company  
Corp. R&D Center  
Schenectady, NY 12301

Dr. T. A. Taylor  
Linde Division  
Union Carbide Corporation  
1500 Polco Street  
Indianapolis, IN 46224

Dr. S. C. Singhal  
Ceramic Science  
Westinghouse Res. Labs.  
Beulah Road  
Pittsburgh, PA 15235

Dr. H. Beale  
Battelle Labs.  
505 King Avenue  
Columbus, OH 43201

Dr. Donald H. Boone  
Lawrence Berkeley Lab.  
Bldg. 62, Rm. 351, U. of CA  
Berkeley, CA 94720

Mr. Vern Anderson  
Pratt & Whitney Aircraft  
Government Products Division  
West Palm Beach, FL 33402

Mr. I. Machlin  
Code AIR-52031B  
Department of the Navy  
Naval Air System Command  
Washington DC 20361

Mr. H. Heckler  
Mail Drop D-83  
General Electric Company  
Cincinnati, OH 45215

Mr. John M. Richardson III  
Alloy Surface Company  
100 S. Justison Street  
Wilmington, DE 19899

Dr. G. W. Goward  
Pratt & Whitney Aircraft  
United Technologies Corp.  
400 Main Street  
East Hartford, CT 06108

Mr. L. Hjelm  
AFWAL-MIL  
Wright-Patterson AFB  
OH 45433

Dr. R. F. Bunshah  
Mat'l's Department  
6532 Boelter Hall  
Univ. of California  
Los Angeles, CA 90024

Mr. D. E. Schwab  
Materials Engineer  
Airearch Mfg. Company  
2525 W 190th Street  
Torrance, CA 90509

Dr. David P Whittle  
Lawrence Berkeley Lab.  
Bldg. 62, Rm. 141, U. of CA  
Berkeley, CA 94720



DISTRIBUTION LIST (Cont'd)

Mr. David Rigney  
Mail Drop D 83  
General Electric Company  
Cincinnati, OH 45215

Mr. Donald E. Snedecker  
Corning-Zircoa  
31501 Solon Road  
Solon, OH 44139

Prof. R. A. Rapp  
116 West 19th Avenue  
Ohio State University  
Columbus, OH 43220

Prof. H. Herman  
Dept. of Mat'l's Science  
State University of NY  
Stonybrook, L.I., NY 11794

Mr. H. Doering, Bld 53-316  
Gas Turbine Prod. Div.  
General Electric Company  
1 River Road  
Schenectady, NY 12345

Mr. William G. Barker  
Naval Air Propulsion Center  
P. O. Box 7176  
Trenton, NJ 08628

Mr. L. M. Bianchi VP & GM  
Turbine Coat. Facility  
AIRCO TEMESCAL  
2850 Seventh Street  
Berkeley, CA 94720

Mr. Robert Beck  
Mat. Dev. & Manuf. Engr.  
Teledyne CAE  
1330 Laskey Road  
Toledo, OH 43612

Mr. Lyle B. Spiegel  
AVCO-EVE. Labs  
550 S. Main Street  
Stratford, CT 06497

Mr. Joseph J. Falco  
Army Mat. & Mech. Res. Center  
Arsonel Street  
Watertown, MA 02192

Mr. David M. Thompson  
Corning-Zircoa  
31501 Solon Road  
Solon, OH 44139

Dr. R. C. Tucker, Jr.  
Linde Division  
Union Carbide Corp.  
1500 Polco Street  
Indianapolis, IN 46224

Dr. R. Bratton, Mgr.  
Ceramic Science  
Westinghouse Res. Labs.  
Beulah Road  
Pittsburgh, PA 15235

Dr. M. A. H. Howes  
Metals Division  
ITT Research Inst.  
10 W. 35th Street  
Chicago, IL 60616

Mr. Sylvester Lee  
AFWAL-MLTM  
Wright-Patterson AFB  
OH 45433

Mr. S. Mutialu  
Turbine Coat. Facility  
AIRCO TEMESCAL  
2850 Seventh Street  
Berkeley, CA 94720

Acquisition Dept (25) Copies  
NASA S&T Info. Facility  
P. O. box 8757  
Balt-Wash Internat'l Airport  
Maryland 21240

Curtiss-Wright Corp.  
Attn: Dr. Sam Wolosin  
Mtls. Engrg. Dept.  
One Passaic Street  
Woodridge, NJ 07075

DISTRIBUTION LIST (Cont'd)

Mr. Kenneth Ryan  
GMC-DDA  
P. O. Box 894  
Indianapolis, IN 46806

NASA  
Attn: Library  
AMES Research Center  
Moffett Field, CA 94035

NASA  
Attn: Mr. Gene Cataldo  
Geo. C. Marshall Spec. Center  
Marshall SFC, AL 358121

Dr. William Lee  
Rockwell International  
Energy Systems Group  
8900 Desoto Avenue  
Canoga Park, CA 91304

TRW Equipment TM-2966  
Attn: I. M. Matay  
23355 Euclid Avenue  
Cleveland, OH 44117

Argonne National Lab  
Attn: Harold Herman  
9700 Sought Cass Avenue  
Argonne, IL 60439

Mr. Manohar Asnani  
TRW, Inc.  
1455 E. 185th Street  
Cleveland, OH 44110

Mr. Daniel D. Profant  
AVO-Lycoming  
550 S. Main Street  
Stratford, CT 06497

NASA  
Attn: Dr. S. Stecura  
Lewis Research Center  
21000 Brookpark Road  
Cleveland, OH 44135

Dr. T. S. Piwonka TM-2966  
TRW Equipment  
23355 Euclid Avenue  
Cleveland, OH 44117

NASA  
Attn: Curt Liebert  
Lewis Research Center  
21000 Brookpark Road  
Cleveland, OH 44135

Naval Sea Systems Command  
Attn: S. B. Shepard  
Code 5231  
Washington, DC 20362

TRW Equipment TM-2110  
Attn: J. N. McCarthy  
23355 Euclid Avenue  
Cleveland, OH 44117

Dr. Istvan J. Toth TM-2966  
TRW Equipment  
23355 Euclid Avenue  
Cleveland, OH 44117

AVCO Corporation  
Lycoming Division  
Attn: A. F. Deferrari  
550 S. Main Street  
Stratford, CT 06497

METCO Inc.  
Mr. M. Ortner  
Dir. U. S. Marketing  
1101 Prospect Avenue  
Westbury, L.I., NY 11590

Dr. S. Raghuranim-2966  
TRW Equipment  
23355 Euclid Avenue  
Cleveland, OH 44117

NASA  
Attn: Frank Stepka  
Lewis Research Center  
2100 Brookpark Road  
Cleveland, OH 44135

DISTRIBUTION LIST (Cont'd)

Pratt & Whitney Aircraft  
Attn: D. Scott Duvall  
400 Main Street  
East Hartford, CT 06108

Mr. Tom Sherlock-Lab 101  
Westinghouse Electric  
P. O. Box 251  
Concordville, PA 19331

Westinghouse Electric  
Attn: C. A. Anderson  
Research Laboratory  
1310 Beulah Road  
Pittsburgh, PA 15668

Mr. James Clare  
METCO Inc.  
1101 Prospect Avenue  
Westbury, L.I., NY 11590

Mr. Y. Horada  
ITT Research Inst.  
10 West 35th Street  
Chicago, IL 60616

Mr. George A. Grave, Jr.  
Univ. of Dayton  
Dayton, Ohio  
45409

Mr. John Klein  
METCO Inc.  
1101 Prospect Avenue  
Westbury, L.I., NY 11590

Dr. Sherman D. Brown  
Ceramic Eng. Dept.  
Univ. of Illinois  
Urbana, IL 61801

Mr. Tom Derkacs  
TRW Inc.  
23355 Euclid Avenue  
Cleveland, OH 44117

Rockwell International  
Attn: G. E. William  
Rocketdyne Division  
6633 Canoga Avenue  
Canoga Park, CA 91304

Mr. S. T. Scheirer  
Westinghouse Electric  
Combustion Turbines Systems  
P. O. Box 251 (M-CODE 210)  
Concordville, PA 19331

Dr. R. G. Carlson MPTL  
Mail Drop M-85  
General Electric Company  
Cincinnati, OH 45215

Mr. Ram Darolia MPTL  
Mail Drop M-85  
General Electric Company  
Cincinnati, OH 45215

Mr. Shiro-Fujishiro  
AFWAL/  
Wright-Patterson AFB  
Ohio 45433

Mr. R. Jackson K1  
General Electric Company  
R&D Center, P. O. Box 8  
Schenectady, NY 46206

Mr. Frank N. Longo  
METCO Inc.  
1101 Prospect Avenue  
Westbury, L.I., NY 11590

Mr. Charles E. Fetheroff  
TRW Equipment TM-2966  
23355 Euclid Avenue  
Cleveland, OH 44117

DISTRIBUTION LIST (Cont'd)

Mr. Merle Funkhouser  
Pratt & Whitney Aircraft Group  
Government Products Division  
P. O. Box 2691  
West Palm Beach, FL 33402

Mr. Don Kearns, Suite 422  
Solar Turbines Inter.  
499 South Capital Street. SW  
Washington, DC 20003

Mr. Robert Benden  
TRW Inc.  
23355 Euclid Avenue  
Cleveland, OH 44117

Prof. L.L. Siegle  
Dept. of Materials Sc.  
State Univ. of NY  
Stony Brook, L.I. , NY 11794

Mr. L.E. Dardi  
Howmet Corporation  
Technical Center  
699 Benston Road  
Whitehall, MI. 49461

Mr. R. L. Shamakian  
Pratt & Whitney Aircraft Group  
Government Products Division  
P. O. Box 2691  
West Palm Beach, FL 33402

Mr. E. Kerzicnik MPTL  
Mail Drop M-85  
General Electric Company  
Cincinnati, OH 45215

Mr. Stanley L. Bost  
Corning/Zircoa  
31501 Solon Road  
Solon, OH 44139

Mr. R. Stueber  
Chromalloy R&T  
Blaisdell Road  
Orangeburg, NY 10962